Enhancing Transportation Resilience under Multi-Hazard Conditions: A Tool for the Mid-Term Recovery Phase in Earthquake-Affected Regions

A Case Study of Earthquake and Flood Disruptions in Antakya, Türkiye

Thesis MSc Engineering and Policy Analysis

M.R.J. van der Jagt

Delft University of Technology

TU Delft

Enhancing Transportation Resilience under Multi-Hazard Conditions: A Tool for the Mid-Term Recovery Phase in Earthquake-Affected Regions

A Case Study of Earthquake and Flood Disruptions in Antakya, Türkiye

by

M.R.J. van der Jagt

To obtain the degree of Master of Science at the Delft University of Technology,
The public defence will take place on Thursday, June 12, 2025 at 14:30.

Student number:	4499697
Project Duration:	October 2024 - June 2025
Thesis committee:	Dr. J.A. Annema
	Dr. N.Y. Aydin
	Dr. S. Balakrishnan

Cover: H. L. Smith (2023)

An electronic version of this thesis is available at:
http://repository.tudelft.nl/.

The code used in this thesis is available at:
github.com/matthijsjagt/multi-hazard-intermediate-recovery

TU Delft

Preface

Dear reader,

This thesis marks the final step in completing the Master of Science in Engineering and Policy Analysis at Delft University of Technology. It reflects not only months of research into the challenges of intermediate, multi-hazard transport recovery after earthquakes, but also everything I've learned, experienced, and come to appreciate throughout my time as a student.

It wouldn't have come together without the support and encouragement of many people. I'm especially grateful to my supervisors at TU Delft for their thoughtful feedback, patience, and guidance throughout the process. I also want to thank my friends and family for the coffee breaks, the welcome distractions, and the smiles that helped me through the tougher moments of coding, writing, and reading, whether it was at EWI, Civil, TPM, or deep into the evening in the library.

Right now, it still feels a little surreal to be closing this chapter, both the research and this unforgettable period of being a student. But with that, I look forward to what's next, curious and excited to see where the path from here will lead.

Time to turn the page, enjoy the read!

M.R.J. van der Jagt
Delft, May 2025

Executive Summary

The recovery of transport infrastructure is crucial for earthquake-affected areas, yet these systems remain vulnerable during the intermediate recovery phase, particularly when additional hazards strike. This research investigates how the interaction between earthquakes and floods affects the resilience and recovery of transportation networks. Although awareness of multi-hazard risks is growing, little is known about how multi-hazards disrupt mid-term recovery.

Through an illustrative case study of Antakya, Türkiye, severely affected by the February 2023 earthquake and subsequent flooding, a modeling framework is developed that overlays flood simulations onto an earthquake-damaged network. This integrated approach combines flood hazard mapping with network performance analysis, capturing how inundation fragments connectivity and reduces access to essential services. Such disruptions are particularly damaging during the intermediate recovery phase, when infrastructure remains only partially functional and communities are highly sensitive to further disruption.

The analysis adopts three performance metrics to assess different dimensions of network resilience. Network centrality identifies structurally critical road segments for maintaining connectivity. Accessibility to critical services evaluates whether shelters retain access to essential facilities such as hospitals and markets. Disruption-adjusted shelter flows estimate how many potential trips are affected by flooded roads, linking structural exposure to functional loss. These indicators are assessed across both single-hazard and multi-hazard scenarios, with flood intensities corresponding to 25-, 50-, and 100-year return periods.

Results show that flooding worsens network performance in a system already weakened by earthquake damage. Accessibility to critical amenities deteriorates, particularly in communities reliant on a limited number of corridors. These disruptions reroute shelter-related travel flows onto secondary roads, increasing travel distances and reducing accessibility, particularly in areas with low network connectivity. Spatial analysis highlights that targeted recovery of a few key corridors could improve mobility and prevent further disruptions affecting already displaced communities during multi-hazard events.

From a policy perspective, the findings emphasize the importance of adopting a multi-hazard approach in mid-term recovery planning. Strategies designed for a single hazard often lack robustness when additional threats emerge. Incorporating multi-hazard risk perspectives enables an improved understanding of vulnerabilities and supports more effective recovery planning. Doing so requires the integration of data on flood risks, transport infrastructure, and population movements into the recovery process.

Contents

Preface i

Executive Summary ii

1 Introduction 1
- 1.1 Problem Introduction . . . 1
- 1.2 Research Approach . . . 3

2 Methodology 5
- 2.1 Research Approach & Methods . . . 5
- 2.2 Modeling Framework . . . 7
- 2.3 Network Model . . . 9
- 2.4 Flood Modeling Using Arc-Malstrøm . . . 12
- 2.5 Model Parameters and Assumptions . . . 14
- 2.6 Scenario Implementation . . . 15
- 2.7 Selection and Specification of Performance Metrics . . . 17

3 Theoretical Framework 20
- 3.1 Disaster Resilience . . . 20
- 3.2 Defining Post-Disaster Recovery . . . 22
- 3.3 Identifying Recovery Activities . . . 24
- 3.4 Defining Intermediate Recovery . . . 29
- 3.5 Multi-Hazard Events in Recovery Contexts . . . 30

4 Intermediate Recovery under Multi-Hazard Conditions: The Case of Antakya 31
- 4.1 Case Introduction . . . 31
- 4.2 Area of Interest . . . 32
- 4.3 Localizing critical intermediate Infrastructure . . . 34
- 4.4 Flooding risks . . . 35
- 4.5 Data availability . . . 36
- 4.6 Model Output . . . 37

5 Results on Multi-Hazard Network Performance 40
- 5.1 Impact of Pluvial Flooding on Road Infrastructure . . . 40
- 5.2 Edge Betweenness Centrality under Multi-Hazard Scenarios . . . 42
- 5.3 Access to Critical Services from Temporary Shelters . . . 52
- 5.4 Disruption of Shelter Flows under Multi-Hazard Conditions . . . 59
- 5.5 Summary of the Results . . . 66

6 Discussion and Limitations **67**
6.1 Discussion 67
6.2 Limitations 68

7 Conclusion & Policy Recommendations **70**
7.1 Policy Recommendations 72
7.2 Scientific Contribution 73
7.3 Future Research 74

References **75**

A Mapping Shelter and Amenity Locations **82**
A.1 Mapping Shelter locations 82
A.2 Georeferencing and Mapping Amenity locations 83

B Results Q25 and Q50 Flooding Scenario **85**

1

Introduction

1.1. Problem Introduction

Earthquakes are among the most devastating natural disasters worldwide, with certain regions particularly vulnerable due to their geographical location (Pal et al., 2022). Following an earthquake, consequences can be severe and recovery processes often extend over several years (Platt et al., 2020). In addition to human casualties, critical infrastructure such as housing, transportation networks, and the production and distribution of essential services like water and food are frequently damaged. These disruptions leave affected and displaced communities highly vulnerable, particularly during the recovery phase when additional hazards may strike. As critical infrastructure and essential services are not yet fully restored, the system operates in a weakened state, making it more susceptible to further disruption. When a subsequent hazard strikes during this vulnerable phase, it can significantly worsen the existing damage, delay recovery efforts, and further weaken societal and economic vulnerabilities.
In addition, climate change increases the likelihood of climate-related hazards, such as floods and droughts, further amplifying vulnerabilities and risks to infrastructure and communities during the vulnerable recovery phase (De Ruiter et al., 2020). When hazards occur simultaneously, in a cascading sequence, or as cumulative events, collectively referred to as a multi-hazard phenomenon, the situation becomes significantly more complex, severely challenging recovery efforts and amplifying societal and economic losses (Lee et al., 2023).

To better understand how affected areas recover and remain vulnerable to additional hazards, it is important to consider the different phases of the post-earthquake recovery process. Recovery generally unfolds over several phases. In the immediate aftermath, typically spanning the first few days, efforts focus on emergency response activities, such as restoring basic access, clearing debris, and providing urgent relief (Boyd et al., 2014; Wu & Chen, 2023). Road infrastructure networks serve as lifelines during this period by enabling the delivery of critical goods, such as food, water, and medicine, and by ensuring that aid workers can reach impacted communities. The first 72 hours, often referred to as the "Golden Hours," are critical for minimizing mortality

through timely interventions (Nain et al., 2023; Rezapour et al., 2018).
In the weeks following the disaster, recovery transitions into the mid-term phase, centered on restoring basic services, repairing essential infrastructure, and enabling the gradual resumption of economic and social activities. Maintaining the functionality of road networks during this phase remains essential for supporting economic recovery and the rebuilding of communities. Finally, months to years after the event, recovery efforts shift toward long-term reconstruction, aiming to structurally rebuild and enhance the resilience of affected areas, often surpassing pre-disaster conditions (Boyd et al., 2014; Di Ludovico et al., 2019).

Despite the critical role of the mid-term recovery phase in stabilizing affected areas and facilitating the transition toward sustainable reconstruction, this phase remains underexplored in the literature (Almeida et al., 2022). Research has primarily focused on immediate disaster response and long-term rebuilding, while the intermediate period, when recovery has started but systems remain vulnerable, receives little attention. This gap is particularly significant given that essential services and infrastructure, such as transportation networks, often operate at reduced capacity during mid-term recovery, making affected areas highly vulnerable to further disruption.
The area's vulnerability becomes even more critical when considering the potential impact of multi-hazard events, which remain largely overlooked in existing research (Ward et al., 2022). Although multi-hazard events account for a significant share of disaster-related economic losses, recovery strategies predominantly address single hazards (Zscheischler et al., 2020). This under-representation of multi-hazard risks during the vulnerable mid-term phase forms a critical gap in the literature, underscoring the need for more comprehensive approaches to enhance resilience.

This knowledge gap forms the foundation of this research, which aims to contribute to a better understanding of the impact of multi-hazard conditions on transportation network resilience during mid-term recovery. By addressing this underexplored phase, the study aims to contribute to the improvement of recovery strategies that not only enhance resilience and reduce vulnerability in earthquake-affected communities, but also address the compounded risks posed by multi-hazard events during the recovery process.

A recent event that highlights the relevance of this topic is the earthquake that struck Türkiye on February 6, 2023. The earthquake and subsequent aftershocks caused widespread damage, with over 50,000 deaths and the destruction of thousands of buildings (United Nations Development Programme (UNDP), 2023). A few months after, heavy rainfall and subsequent flooding further exacerbated the situation, rendering key roads impassable and submerging tent camps where displaced people had sought shelter (OCHA, 2023b). The inaccessibility of the transport network not only hindered immediate relief efforts but also delayed the recovery of essential infrastructure. Therefore, this case serves as an illustrative example to better understand the vulnerabilities and resilience challenges of transportation networks during the mid-term recovery phase under multi-hazard conditions.

1.2. Research Approach

The aim of this research is to enhance the resilience of transportation networks in earthquake-affected communities by improving mid-term recovery strategies. This is achieved by setting up a modeling tool that simulates the performance of transportation networks during the mid-term recovery phase under multi-hazard conditions. The tool identifies critical vulnerabilities, quantifies performance dynamics, and supports the formulation of targeted policy recommendations. The research focuses on bridging the knowledge gap that exists between the widely studied short-term emergency response and long-term reconstruction phases, ensuring that mid-term recovery contributes to enhancing the long-term resilience of transportation networks in earthquake-affected communities.

To support this objective, a network model of the area affected by the February 2023 earthquake in Türkiye is developed as an illustrative case study. Graph theory is applied to simulate and analyze the performance and connectivity of the transportation network under scenarios involving both earthquake and flooding events. The model identifies vulnerabilities that could limit transport accessibility and thereby hinder the recovery of earthquake-affected communities under multi-hazard conditions.
The application of graph theory to transportation system analysis is an established approach. Pan et al. (2021) reviewed approximately 140 studies and identified graph theory, alongside complex network theory, as key methods for analyzing transportation systems. An example is the work by Testa et al. (2015), who used graph theory to model the New York City metropolitan highway system and assess its resilience to extreme events.

Finally, the research aligns with the objectives of the TU Delft Master's programme in Engineering and Policy Analysis, which emphasizes addressing complex societal and technical challenges through modeling, simulation, and policy analysis (TU Delft, n.d.). It also supports several United Nations Sustainable Development Goals (SDGs), notably SDG 3 ("Good Health and Well-Being"), SDG 9 ("Industry, Innovation, and Infrastructure"), and SDG 11 ("Sustainable Cities and Communities") by promoting resilient infrastructure and sustainable recovery practices (United Nations, 2015).

1.2.1. Research Questions

Despite the increasing attention to disaster recovery, the literature provides limited insights into how mid-term recovery strategies for transportation networks can be evaluated and improved under multi-hazard conditions. To address this gap, the following main research question is formulated:

Research Question

How can mid-term recovery be modeled to evaluate and enhance transportation network resilience under multi-hazard conditions in earthquake-affected communities?

To structure the research and guide the methodological approach, the main question is divided into five sub-questions:

Sub-question 1: How can a methodological approach be designed to model and integrate earthquake and flood hazards within a network-based recovery framework?

Sub-question 2: How is the mid-term recovery phase defined within the broader disaster recovery timeline and what factors are relevant for transportation networks during this phase?

Sub-question 3: How can the February 2023 earthquake in Türkiye be used as a case study to illustrate vulnerabilities in mid-term recovery of transportation networks under multi-hazard conditions?

Sub-question 4: How can the impact of multi-hazard events on mid-term recovery be operationalized and evaluated using network models?

Sub-question 5: How do multi-hazard events impact the transportation network performance following the February 2023 earthquake in Türkiye?

1.2.2. Thesis Outline

This thesis is structured into seven chapters. First, Chapter 2 describes the research approach, the conceptualization of the network and flooding models, and the selection of the illustrative case study. Next, Chapter 3 presents the theoretical framework, introducing concepts such as disaster resilience, recovery phases, and multi-hazard phenomena forming the theoretical basis for the subsequent analysis. Subsequently, Chapter 4 applies this framework to the case of Antakya, Türkiye, explaining the local context, the operationalization of the models, and the definition of performance metrics. Chapter 5 then presents the results of the network modeling, assessing the impacts of multi-hazard events on accessibility, network structure, and transport performance. Building on the results, Chapter 6 presents key conclusions, formulates policy recommendations to strengthen mid-term recovery strategies and enhance community resilience, and identifies opportunities for future research. Chapter 7 concludes the research by reflecting on its limitations.

2

Methodology

This chapter presents the methodology developed for assessing transportation recovery under multi-hazard conditions. It introduces the overall research design, followed by an explanation of the multi-method approach, which combines a literature review with quantitative modeling. The modeling framework integrates network and flood models to simulate the accessibility of critical services during the intermediate recovery phase. The second part of the chapter details the operationalization of the models, including network construction, hazard integration, and scenario design. Finally, the chapter outlines the performance metrics used to evaluate network functionality under varying hazard conditions. In doing so, this chapter contributes to answering Sub-question 1, by designing a framework that integrates earthquake and flood hazards into a network-based model, and Sub-question 4, by translating multi-hazard impacts into evaluable network performance metrics.

2.1. Research Approach & Methods

To provide an overview of how the research is structured and how each method contributes to answering the sub-questions, the conceptual flow of the research is presented in Figure 2.1. This diagram outlines the sequential logic of the research, showing how the literature study, modeling framework, and case study application collectively inform the overall methodology.

Literature study

To start, a theoretical foundation is established to analyze and illustrate the multi-hazard dynamics in post-earthquake recovery. This literature study draws on relevant qualitative academic literature on post-disaster recovery and related topics, such as disaster resilience, in order to provide insights into definitions and key concepts. The literature was accessed through databases like Scopus and Google Scholar. The literature study also aims to define and contextualize the mid-term recovery phase by analyzing recovery activities on the broader recovery timeline. Therefore, both qualitative and quantitative academic sources are considered, alongside relevant 'grey' literature such as news articles for current and practical information.

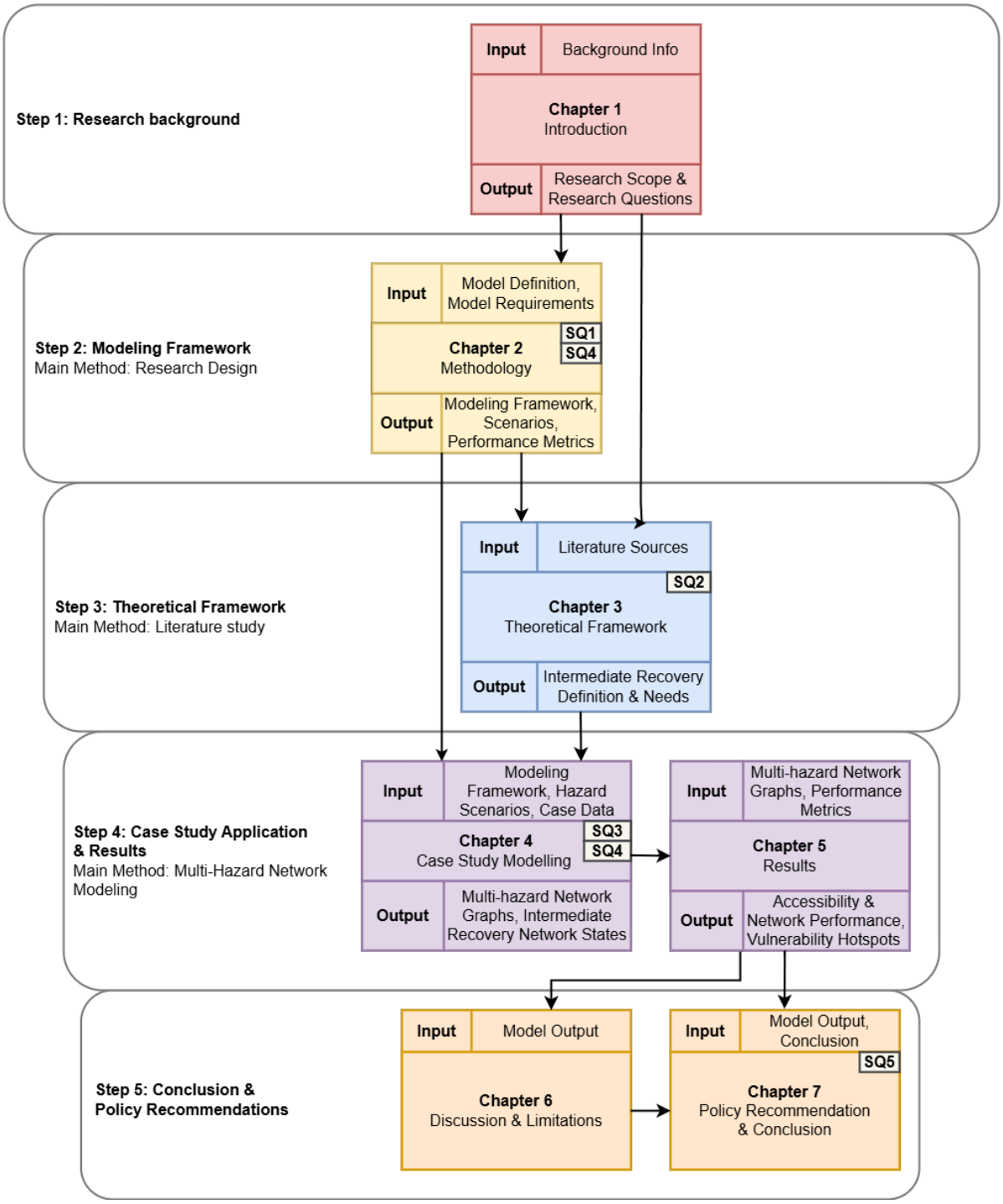

Figure 2.1: Conceptual flow of the research structure.

The academic articles used in the literature study are based on the context of post-disaster recovery, with a preference for English-language, cited and published in the last 10 to 15 years. The theoretical foundation developed from this literature will serve as the framework for both the application of the case study, and modeling of the road network and flood risks during the mid-term recovery period. While the literature study is intended to provide a theoretical foundation, certain limitations must be acknowledged. For instance, the focus

on English-language literature may result in the exclusion of region-specific information available only in the language of the case study: Turkish. Furthermore, caution is needed when generalizing findings to the Turkish context, as studies are context-specific and may be conducted in different geographic or socio-political settings.

Quantitative Modeling

The second method used in this research, is the quantitative modeling component, consisting of the network and flooding model. The network modeling represents the structure and connectivity of the road infrastructure, while the flood model identifies infrastructure vulnerable during different rainfall intensities. This method complements the literature study and illustrative case study by enabling the analysis of multi-hazard disruptions and their impact on road network accessibility during the mid-term recovery phase. Accordingly, these models simulate how earthquake-induced damage and subsequent flooding affect the accessibility of the affected community. The integration of both models is further detailed in the following section, which outlines the modeling framework used to simulate network performance under earthquake and flooding conditions.

2.2. Modeling Framework

To assess the impact of multi-hazard events on road network accessibility during the mid-term recovery phase, this research applies an integrated modeling framework. The framework is designed to combine the structural characteristics of road infrastructure with the spatial extent of flooding, enabling the evaluation of network performance under both earthquake and flood conditions. The approach reflects the temporal and spatial vulnerability of transportation systems during recovery, when infrastructure remains partially functional and susceptible to additional hazards.

The framework consists of five key steps as can seen in Figure 2.2, each representing a critical phase in the operationalization of the model:

1. **Construction of the base network:** A graph-based representation of the road infrastructure is created using OpenStreetMap data. This base network reflects the topology and connectivity of the road system.
2. **Integration of critical facilities and earthquake damage:** Nodes and edges are enriched with attributes representing shelters, amenities, and physical damage. This step incorporates key spatial and functional elements that are relevant for evaluating network performance during the mid-term recovery phase, as further discussed in Chapter 3.
3. **Simulation of flood exposure:** Rainfall scenarios are applied using Arc-Malstrøm to simulate pluvial flooding based on topographic characteristics. The model produces flood exposure maps that identify areas of surface water accumulation and the corresponding road segments at risk of flooding. Specific inputs are defined in the case study presented in Chapter 4.

4. **Overlay of flood data on the disrupted network:** The flood exposure maps are integrated with the earthquake-affected network to construct a multi-hazard model. This combined model enables scenario-based analysis of network performance and accessibility during the mid-term recovery phase.

5. **Scenario analysis and performance evaluation:** The multi-hazard network model is used to assess how different disruption scenarios affect network performance. Performance metrics are applied to identify vulnerable or high-impact segments within the network.

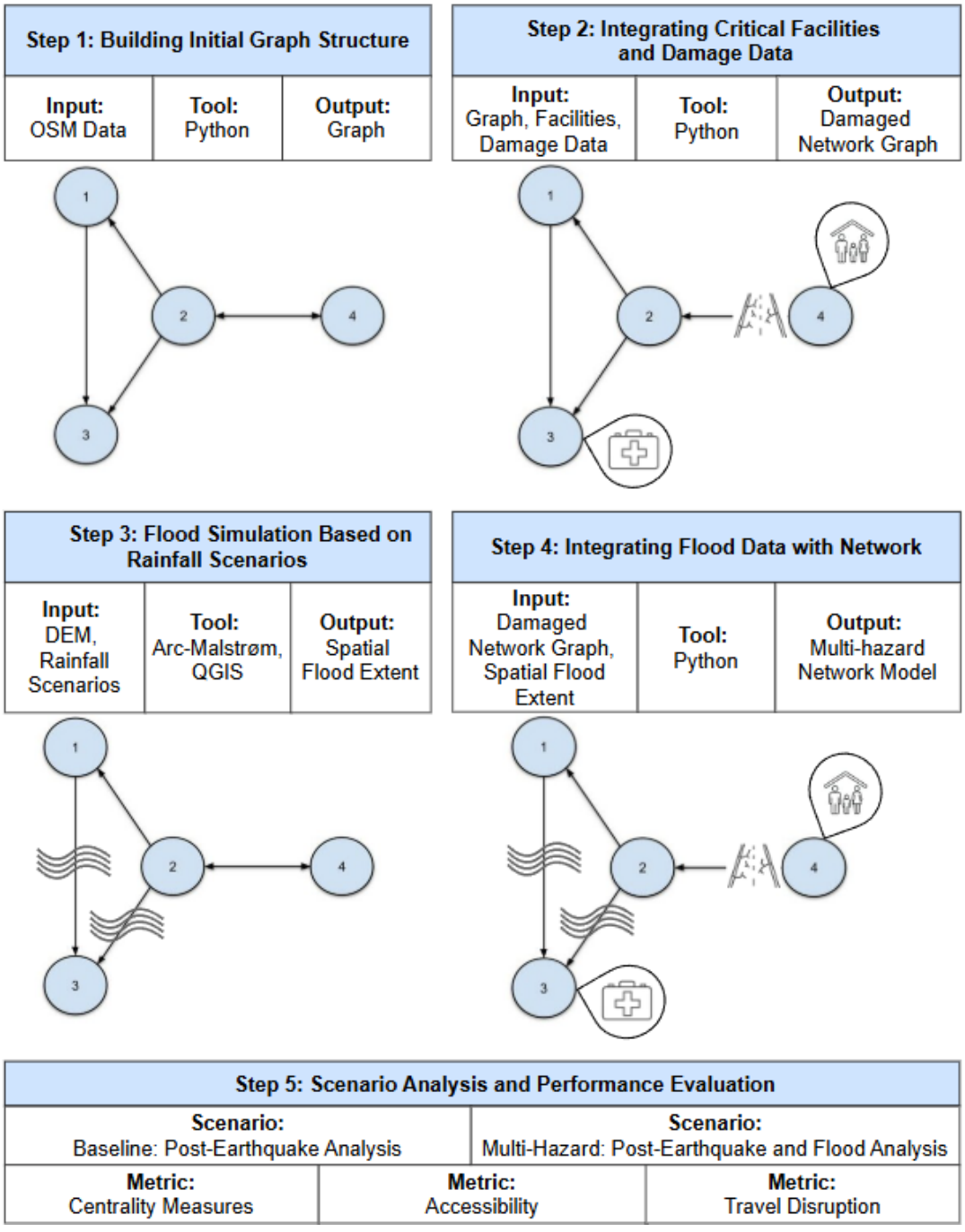

Figure 2.2: Conceptual workflow for constructing the multi-hazard network model.

The modeling framework enables the transition from scenario-based hazard inputs to a functional network model capable of simulating performance under multi-hazard disaster conditions. It links physical disruption to accessibility outcomes and supports the evaluation of transport resilience throughout the mid-term recovery process.

2.3. Network Model

2.3.1. Introduction to the Network Model

The network model developed and applied in this research forms the analytical foundation for evaluating the impact of multi-hazard conditions on urban road infrastructure during the mid-term recovery phase. It is operationalized through a sequence of modular Python scripts, each corresponding to a functional step in the modeling process. As outlined in Section 2.2, the network model addresses Steps 1, 2, 4 and 5 of the conceptual framework: the construction of a base graph structure, the integration of critical facilities and earthquake-related damage, and the overlay of flooding data on the disrupted network.

This section outlines the step-by-step implementation of the network model, developed in line with the proposed framework and applied in this research to support scenario-based performance analysis. The model supports the analysis of metrics such as accessibility, centrality, and travel disruption. An overview of the model structure is provided in Figure 2.3, and the following subsections detail each step in the process.

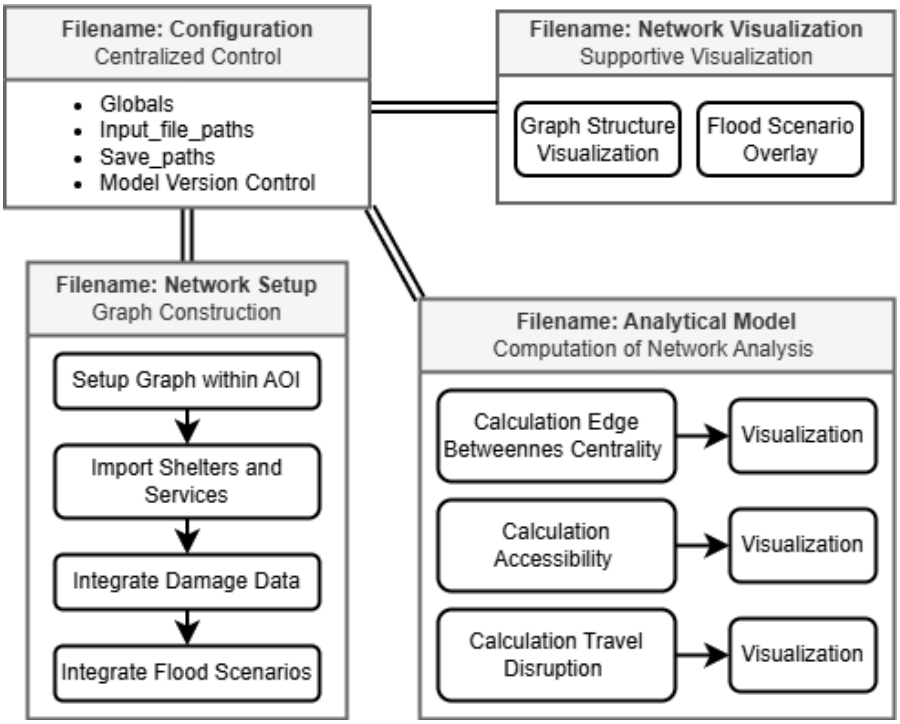

Figure 2.3: Structure of the Network Model Scripts.

2.3.2. Theoretical Background: Network Theory

Network Theory provides the foundation for modeling transportation infrastructure in this research. It allows for the representation of physical systems as graphs, where intersections (nodes) are connected via road segments (edges) Newman (2003). Graphs may be either directed or undirected, depending on whether flow is unidirectional or bidirectional. In this research, directed graphs are used to reflect the one-way nature of certain roads. A directed edge is shown using an arrow to indicate directionality, while undirected edges lack such indication. The mathematical representation of a graph is defined as $G = (V, E)$, where V is the set of nodes and E is the set of edges that connect them.

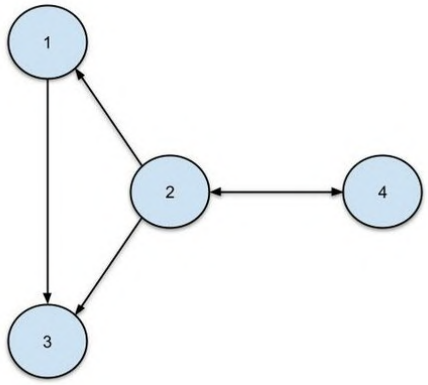

Figure 2.4: Example of a directed graph (Dahiphale, 2023).

2.3.3. Data Collection and Preprocessing

The application of the network model requires a set of geospatial datasets that describe the physical and functional characteristics of road infrastructure within a selected study area. In this research, the road network was retrieved from OpenStreetMap and clipped to a custom-defined Area of Interest (AOI) using a shapefile, in order to ensure spatial consistency across all model components.

To incorporate the network with attributes relevant to mid-term recovery, additional datasets were collected and processed. These include the locations of critical facilities for which access is essential during the recovery phase. GeoPackages containing these locations were prepared and spatially aligned for integration into the base network. Earthquake-related damage was incorporated using separate shapefiles for road and building damage. Finally, flood exposure layers were derived from Arc-Malstrøm model outputs, with each rainfall scenario stored as a GeoPackage file identifying inundated zones.

To ensure compatibility with the modeling workflow, all datasets were cleaned and harmonized. This included aligning coordinate reference systems and confirming that the spatial coverage matched the defined AOI. Data preprocessing was carried out using a combination of Python scripts and GIS tools such as QGIS. Further details on the specific data preparation procedures followed in this research are provided in Appendix A.

2.3.4. Graph Construction and Hazard Integration

The network model is constructed in Python 3.12 using the OSMnx package (version 2024.2.4), which converts OpenStreetMap (OSM) road data into a directed multigraph. OSMnx builds upon the NetworkX and GeoPandas libraries to structure and analyze road networks and handle geospatial data. In the resulting graph, intersections are represented as nodes and road segments as directed edges, with two-way streets modeled as paired edges in opposite directions.

Following the construction of the base graph, critical facilities relevant during mid-term recovery are added as nodes to the network. These locations are connected to the nearest road segment through proximity-based edges, allowing them to be included in accessibility analyses. Earthquake-induced disruptions are incorporated by linking damage data for roads and buildings to specific edges in the network using spatial joins. Affected segments are flagged to reflect impaired accessibility, capturing the lingering effects of debris clearance and repair operations typical of the mid-term recovery phase. Spatial joins between damage layers and the network graph can be used to dynamically assign accessibility constraints.

In the final layer, flood exposure is similarly integrated by overlaying spatial outputs from Arc-Malstrøm, described in Section 2.4. For each rainfall scenario, road segments intersecting flooded areas are tagged with boolean attributes to indicate inundation status under specific conditions. The integrated network serves as input for the scenario-based performance analyses discussed in the next section.

2.3.5. Scenario Analysis and Performance Evaluation

The model evaluates three core performance metrics: edge betweenness centrality, accessibility, and travel disruption. These metrics quantify the structural importance of road segments for overall network connectivity, the accessibility of essential services from shelters under disrupted conditions, and the functional impact of flooded road closures on service access for displaced populations.

By comparing a baseline (earthquake-only) scenario with a multi-hazard scenario that includes both earthquake and flood impacts, the model enables an assessment of how compounding disruptions affect network performance. The scenarios and associated metrics are further defined in Section 2.6 and Section 2.7. This final step in the modeling framework builds on the integrated network and enables comparative analysis across disruption conditions. It also supports the identification of vulnerable or high-priority segments that may hinder recovery efforts.

2.3.6. Configuration and Visualization Tools

A centralized configuration script is used to manage global model parameters, including file paths, input variables, and version control settings. This centralized structure ensures consistency across all scripts and facilitates efficient switching between model versions. A standalone visualization script can be used to generate spatial plots and network diagrams.

Although these visual outputs are not part of the quantitative evaluation, they help to contextualize results and support interpretation of scenario outcomes.

Concluding Remarks

This section has described the network model developed to represent multi-hazard impacts on urban road infrastructure during the mid-term recovery phase. The multi-hazard network model developed in this research enables performance assessment of road infrastructure during mid-term recovery. Following its construction, a range of scenario-based analyses is performed to evaluate accessibility, centrality, and travel disruption.
Flood exposure data constitute one of the key hazard inputs in this modeling process. The next section describes the flood modeling, which produces the rainfall-based inundation layers used as spatial inputs in the network analysis.

2.4. Flood Modeling Using Arc-Malstrøm

2.4.1. Model Background

This research uses Arc-Malstrøm, a 1D hydrologic screening tool designed to simulate surface water accumulation based on topographic depressions Balstrøm and Crawford (2018). It operates within a GIS environment and is particularly suited for urban flood risk assessments using digital elevation data. In the modeling workflow, Arc-Malstrøm serves as the primary model for identifying potential flood zones under pluvial conditions. The model works by detecting terrain sinks, known as "bluespots", in a Digital Elevation Model (DEM). Each sink is analyzed to determine its storage capacity, associated pour point, and local contributing catchment. These units are the basis for simulating rainfall accumulation. Rainfall inputs are converted to runoff using Hortonian flow assumptions, which means infiltration is considered negligible.

Once rainfall volumes exceed a sink's storage capacity, excess water spills over at the pour point and is routed downstream using a geometric network. This network consists of junctions (sinks) and edges (flow paths), enabling efficient spillover tracing through downstream catchments. The accumulated spillover volumes are computed using a custom trace tool based on ArcGIS geometric network structures, allowing rapid analysis of interconnected flood risks.
The outputs include spatial polygons of flooded areas, pour point attributes, and downstream flow paths. These results provide a rapid, first-order approximation of urban flood exposure under different rainfall scenarios. Although the model is simplified compared to full hydrodynamic simulations, its low data and computational requirements make it highly effective for screening applications in multi-hazard contexts.

2.4.2. Data Preparation and Scenario Definition

The flood model requires a DEM and rainfall intensity values as primary inputs. The DEM used in this study was sourced from Copernicus Copernicus (2024), with an original resolution of 30×30 meters. To enable integration with finer-scale building footprint data, the DEM

was resampled to a 1×1 meter grid using QGIS. This process increases spatial resolution for analytical purposes but does not enhance the vertical accuracy of the elevation data.

Building footprints from OpenStreetMap were incorporated by treating them as impermeable surfaces. This was achieved by increasing the elevation values of building footprints by 30 meters. Based on characteristics of the city center in the case study area, where mid-rise buildings are predominant, this assumption ensures that simulated surface water is diverted realistically around built structures.

The model was run for three different rainfall scenarios, representing 25-year, 50-year, and 100-year return periods. These intensities were applied as uniform rainfall inputs over a six-hour period.

2.4.3. Model Application and Parameters

To simulate flood exposure in the study area, Arc-Malstrøm was executed in bundled mode via a single command-line operation. This approach automatically performs all key hydrological steps: bluespot detection, depression filling, watershed delineation, and spillover routing, based on the preprocessed DEM. The simulation assumes zero infiltration, reflecting post-earthquake conditions where debris and soil compaction reduce surface permeability.

The simulation is executed using the `malstroem complete` command, which chains all hydrological operations into one streamlined process. This command initiates the entire modeling workflow, from processing elevation inputs to generating flood exposure outputs, and served as the standard routine for all three rainfall scenarios. The core command used is:

```
malstroem complete -r "RAINFALL INPUT" -dem "DEMFILE" -outdir "OUTPUTMAP"
    -accum -filter "maxdepth > 0.5"
```

Where:

- `"RAINFALL INPUT"` defines the rainfall amount in millimeters used for the simulation. This input can be repeated to run multiple scenarios simultaneously (e.g., `-r 30.5` for a 25-year return period event);
- `"DEMFILE"` specifies the file path to the input DEM, which must be in meters and may include artificial building elevations to represent impermeable surfaces;
- `"OUTPUTMAP"` designates the target directory for storing model outputs. This directory must exist prior to execution and should be empty;
- The `-accum` flag activates upstream accumulation analysis across connected bluespots, enabling spillover volume tracing throughout the flow network;
- The `-filter` flag applies a conditional expression (e.g., `maxdepth > 0.5`) to exclude bluespots below a specified threshold. This filtering step supports risk-based screening, such as excluding areas where water depth is unlikely to impact road accessibility.

2.4.4. Postprocessing and Integration with the Network Model

The raw model outputs consist of spatial layers representing flooded areas. To filter for significant flood risks, only bluespots with an average water depth greater than 0.5 meters are retained, based on road safety guidance Kramer et al. (2016). The average depth is calculated as the total stored volume divided by the surface area of each depression.

The filtered results are imported into QGIS and converted into GeoPackage format. During this process, adjacent cells belonging to the same depression are merged into unified bluespot polygons, representing continuous flood zones rather than individual raster cells. These layers are then spatially overlaid with the network model. Road segments intersecting filtered bluespots are flagged with binary inundation attributes, enabling their inclusion in the multi-hazard network analysis as described in Section 2.3.4.

2.5. Model Parameters and Assumptions

2.5.1. Flooding model

Flood classification threshold. To determine whether an area is considered flooded, a threshold depth of 0.5 meters was applied. Given the lack of detailed information about internal water distribution within each bluespot, a uniform depth is assumed across the entire area. As a result, if the average depth within a bluespot exceeds 0.5 meters, the entire area is classified as flooded, even though local depth variations may exist.

Flooded road identification. Building on this classification, flooded roads are identified through a spatial overlay analysis between the bluespots and the road network. In this approach, a road segment is marked as flooded if it intersects with any part of a flooded bluespot, regardless of the extent of the overlap. This assumption implies that even minimal contact with floodwater the entire segment is treated as inaccessible in the model.

Exception for bridges. An exception to this rule is made for bridges. Although they may be flagged as flooded due to overlapping with bluespots, they are retained in the network model. This decision is based on the assumption that bridges remain passable as long as their connecting road segments are accessible. Even when water depths beneath bridges exceed the 0.5-meter threshold, it is presumed that the water flows beneath the structure without necessarily compromising its usability.

2.5.2. Network model

Model extent and spatial coverage. The network is constructed based on a defined Area of Interest (AOI), which is extended with a 500-meter buffer zone. This buffer ensures that roads near the AOI boundary are fully captured, thereby preventing unintended disconnections at the network's edges. Within this buffered area, shelters and amenities are included in the model. However, those located outside the AOI are generally excluded, except for hospitals, which are retained regardless of location due to their critical regional role in emergency response.

Connecting unmapped facilities. To integrate unmapped shelters and amenities into the network, a nearest node connection method is applied. This approach accounts for the fact that such facilities, particularly shelters and markets, are often located in open spaces without explicitly mapped access roads. Consequently, temporary infrastructure is assumed, and a direct link is created to the nearest node in the road network to establish connectivity.

Modeling road blockages due to debris. A key component of the network model is the simulation of road blockages caused by building debris. These are identified through spatial matching between damaged buildings and nearby roads. Drawing on the debris spread estimations proposed by Nishino et al. (2012), which suggest a range between H/8 and H/2 of a building's height (H), the model adopts the upper limit of H/2 to represent a worst-case disruption scenario. Based on the characteristics of the case study's city center, Antakya, where mid-rise buildings are predominant, a maximum building height of 30 meters is assumed. This leads to a 15-meter buffer zone around damaged structures, within which roads are flagged as potentially disrupted by debris. In contexts where building typologies differ, for instance in low-rise or high-rise urban areas, alternative buffer values may be more appropriate to more accurately reflect expected debris dispersal patterns.

Accessibility scoring system. To further refine the impact assessment of debris on road accessibility, an accessibility scoring system is applied. This method builds on the structural damage-to-debris relationships identified by Iskandar et al. (2023), allowing for a probabilistic estimation of disruption severity. Assuming partial clearance efforts in the short term, roads are assigned an accessibility score based on the damage state of adjacent buildings: 1.0 for no disruption, 0.75 for minor, 0.5 for moderate, and 0.25 for severe disruption. This scoring approach enables the model to reflect accessibility loss providing a structured, evidence-informed approach to representing access limitations in the absence of detailed field data.

2.6. Scenario Implementation

To assess the network's performance under multi-hazard conditions during the intermediate recovery phase, the three selected performance metrics are applied at two representative points along the recovery timeline. These moments represent distinct stages of post-disaster conditions, allowing for a comparative analysis of accessibility and vulnerability under evolving hazard impacts. The implementation of the scenarios and their position within the recovery phase is illustrated in Figure 2.5.

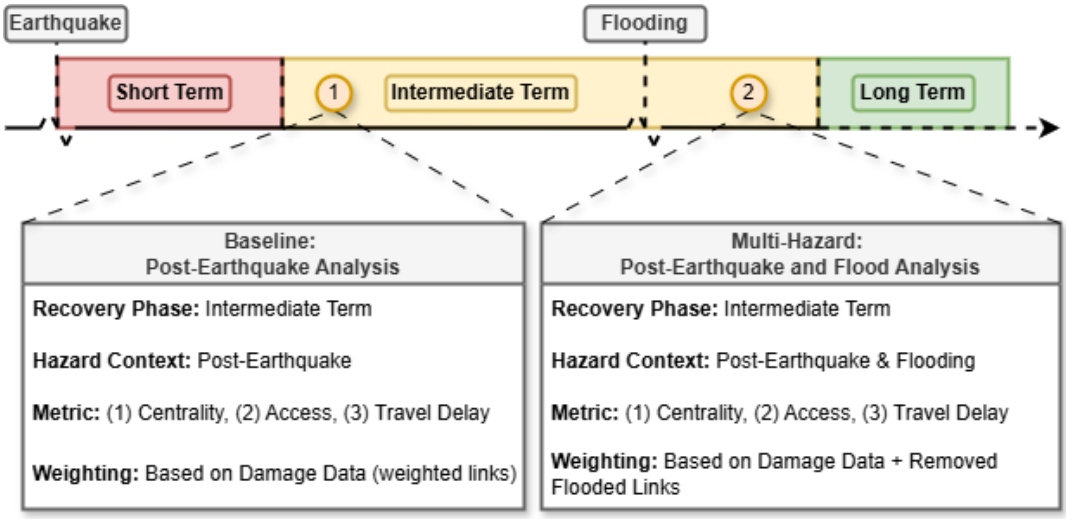

Figure 2.5: Recovery Timeline and Scenario Application for Intermediate Recovery Analysis

Baseline: Post-Earthquake Analysis

The Baseline scenario reflects the condition of the road network during the intermediate recovery phase following an earthquake. While parts of the network have regained some level of operability, disruption remains due to structural damage and ongoing recovery efforts. This disrupted state forms the starting point for the analysis.

Earthquakes often lead to lasting changes in the built environment, both physically and functionally. As damaged areas are gradually rebuilt, the resulting spatial configuration is unlikely to mirror pre-disaster conditions. Instead, the disrupted system becomes the new operational context for an extended period. This baseline therefore reflects the altered state in which recovery activities take place and future hazards may occur.

To assess network performance under these conditions, the links in the graph-based network model are assigned weights based on the severity of nearby building damage. These weights represent varying levels of disruption, with lower weights indicating greater impediments to travel. No links are fully removed. Instead, reduced weights simulate decreased accessibility due to surrounding destruction. Network functionality is evaluated using three performance metrics: centrality, access to critical services, and flow disruption between shelters and essential midterm-recovery amenities.

Multi-Hazard: Post-Earthquake and Flood Analysis

In the multi-hazard scenario, the analysis builds upon the disrupted post-earthquake network but incorporates additional impacts caused by rainfall-induced flooding. Based on the flood model results, roads intersecting with inundated areas are identified and removed from the network if flagged as *flooded* = *True*, representing functional loss. This simulates the compounded effects of a multi-hazard environment during the intermediate recovery phase, where existing road disruptions from earthquake damage are intensified by flooding-related link failures.

Three flood intensity scenarios are evaluated, corresponding to return periods of 25, 50, and 100 years. The damage-based link weights from the baseline scenario remain unchanged, and no additional recovery progress is assumed. Flood-affected links are excluded from the graph to reflect complete inaccessibility, allowing a focused assessment of how flooding exacerbates existing vulnerabilities and further impairs access to critical services under static recovery conditions.

2.7. Selection and Specification of Performance Metrics

To assess how multi-hazard disruptions affect community recovery and access to critical services during the intermediate recovery phase, this section defines the decision attributes used to evaluate the network model. In the literature, various attributes have been proposed to guide disaster recovery planning (Faturechi & Miller-Hooks, 2014). Zamanifar and Hartmann (2021) synthesized these by systematically ranking 57 attributes and identifying six core metrics specifically tailored to evaluating post-disaster transportation network recovery. From this set, three were selected for inclusion in this methodological framework based on their conceptual relevance and practical applicability.

The selected attributes, centrality, accessibility, and flow disruption, capture essential structural and functional aspects of transportation networks. These indicators are suitable for static, spatially based modeling and align with the goal of enabling generalized, scalable analysis under data-limited conditions. According to Zamanifar and Hartmann (2021), they are particularly valuable in contexts where detailed operational information is unavailable but timely decision support is needed.

The three remaining attributes from the original set, which focus on travel time improvements, link capacity, and recovery duration, require more dynamic input data. Their application depends on access to temporal datasets such as real-time travel flows, recovery timelines, or resource allocation rates. While important in broader recovery assessments, they are not included here due to the framework's emphasis on static modeling and its focus on the intermediate recovery phase, where such detailed operational data may not yet be available.

2.7.1. Centrality Measures

To evaluate the structural importance of road segments in maintaining overall network connectivity, the centrality indicator edge betweenness centrality is employed. This measure, implemented using the `edge_betweenness_centrality` and `edge_betweenness_centrality_subset` functions from the NetworkX library in Python, quantifies how frequently a given edge lies on the shortest paths between node pairs, based on edge weights representing travel distance.

The first metric, calculated with `edge_betweenness_centrality`, considers all possible node pairs in the network. It helps identify segments that serve as critical structural connectors, links whose failure would fragment the network. The failure of high-betweenness edges can

cause fragmentation of the network, a vulnerability that becomes more pronounced under multi hazard conditions, where disruptions may accumulate over time.

A more targeted analysis is conducted using `edge_betweenness_centrality_subset`, which restricts the analysis to a subset of origin-destination pairs, specifically, routes connecting shelter locations to critical service providing nodes such as hospitals and markets. This approach highlights links that are not only structurally important but also functionally essential for maintaining access to key services by displaced populations during the intermediate recovery phase.

Together, these complementary measures reveal both general and socially critical vulnerabilities within the transportation network. Segments that are central in both the structural and functional sense represent high-priority corridors for protection, monitoring, or early restoration, as their disruption would affect network connectivity as well as the mobility and well-being of vulnerable communities.

2.7.2. Access to Service-Providing Nodes

This attribute measures whether essential facilities remain reachable from shelters within the damaged transportation network. Service-providing nodes include locations such as hospitals and markets that are crucial for survival and recovery in the aftermath of a disaster.

The associated performance metric calculates the shortest path distances between shelter nodes and these facilities using the `shortest_path` function from the NetworkX library in Python. This function identifies the sequence of nodes that form the shortest route, while the total travel distance is subsequently computed using `path_weight`, which sums the edge weights representing travel distance. Flood-related disruptions can increase travel distances between shelters and essential services, thereby reducing effective accessibility for affected communities.

The metric thus captures the continuity (or loss thereof) in functional access to key services during the recovery phase. Locations where travel distances increase substantially may indicate communities at risk of extended isolation or reduced access to essential services, helping to prioritize interventions where mobility is most critical.

2.7.3. Travel Disruption Adjusted by Shelter Flows

To assess the impact of flood-related road closures on community mobility, this attribute integrates shelter-level movement demand with spatial exposure to flooding. The model uses the number of container units available per shelter location as a proxy for potential movement volume, under the assumption that these containers reflect the concentration of displaced populations and their likely need to access services.

The performance metric identifies road segments that are rendered inaccessible by flooding and calculates the associated loss of flow by estimating how many potential trips (from shelters to

essential services) would have used those segments. These shortest path routes are computed using the `shortest_path` function from the NetworkX library in Python, with edge weights representing travel distance.

This flow-weighted assessment provides a more nuanced perspective on flood impacts: not all flooded roads are equally critical. By weighting path calculations with shelter-level demand and edge-level accessibility, the metric helps distinguish those closures that lead to the most substantial losses in service access. The results guide recovery prioritization by highlighting corridors where restoration would yield the highest gains in accessibility for displaced populations.

3

Theoretical Framework

Resilience has become an important concept in disaster management, commonly used to analyze and enhance how systems function and adapt under disruptive conditions (Demiroz & Haase, 2018; Huq et al., 2021). The concept is key to understanding how transportation networks can maintain functionality during disruptive events and adapt to future risks. Therefore, Section 3.1 starts by presenting the resilience terminology used in this report, establishing a foundation for the analysis of the recovery timeline of transportation infrastructures and contributing factors discussed in Section 3.2. Finally, in Section 3.4 the Intermediate recovery phase is defined including relevant recovery strategies. Altogether, this chapter aims to answer the second Sub-question

3.1. Disaster Resilience

The literature presents various definitions of the term *resilience*, applied to organizational, social, economic, and engineering systems (Hosseini et al., 2015). In general, the definition refers to the systems ability to *bounce back* to the the pre-disaster state, and also to *build back better*, and even to *bounce forward*, meaning to anticipate for future disruptions (Platt et al., 2016). Actions include the prevention, preparation, absorption and recovery to return or improve the systems functionality beyond its pre-disaster state (Graveline & Germain, 2022).

Resilience characteristics

The concept of disaster resilience in this research follows the definition by The National Academy of Sciences (2012), which describes it as the ability "*to prepare and plan for, absorb, recover from, or more successfully adapt to actual or potential adverse events*". To quantitatively assess the concept of resilience, Bruneau et al. (2003) presented four characteristics consisting of the following elements: *Redundancy* – The degree to which a system contains substitutable or backup components. *Resourcefulness* – The ability to recognize challenges and effectively mobilize the necessary resources to address them. *Robustness* – The capacity of a system to endure stress or disruption without significant loss of function. *Rapidity* – The ability to swiftly

prioritize actions and achieve objectives within a timely manner. Together, these characteristics provide a comprehensive framework for evaluating the resilience of adverse events.

Building on these general resilience characteristics, the following section considers how they relate specifically to transportation systems. Following the transport resilience framework by Leobons et al. (2019), robustness and redundancy are emphasized as intrinsic system properties essential for maintaining an acceptable level of service during disruptions. Robustness allows networks to sustain functionality under stress, while redundancy provides alternative routes to preserve accessibility. In contrast, resourcefulness and rapidity are linked to the system's management and operational capacities, reflecting the ability to mobilize resources and implement recovery actions efficiently. These resilience characteristics provide the foundation for evaluating the structural and functional performance of the transport network under multi-hazard conditions.

Resilience curve

One of the key phases of resilience is the recovery phase, which is the focus of this research. According to the resilience definition, four key disaster phases can be identified: *Preparedness* - pre-event measures to enhance the capacity of the systems to withstand potential disruptions, *Absorption* - the ability of the systems to minimize the impact of a disruption, *Recovery* - restoration of functionality to pre-disaster levels through repairing, rebuilding, and re-establishing operations, and lastly *Adaptation* - enhancing resilience by implementing lessons learned to better withstand future disruptions (Alizadeh et al., 2024). The systems functionality can be visualized as a curve, Figure 3.1, adapted from Linkov and Kott (2018), visualizes this concept know as the resilience curve, where a disruptions causes a loss of the systems functionality, which is subsequently restored or even enhanced over time.

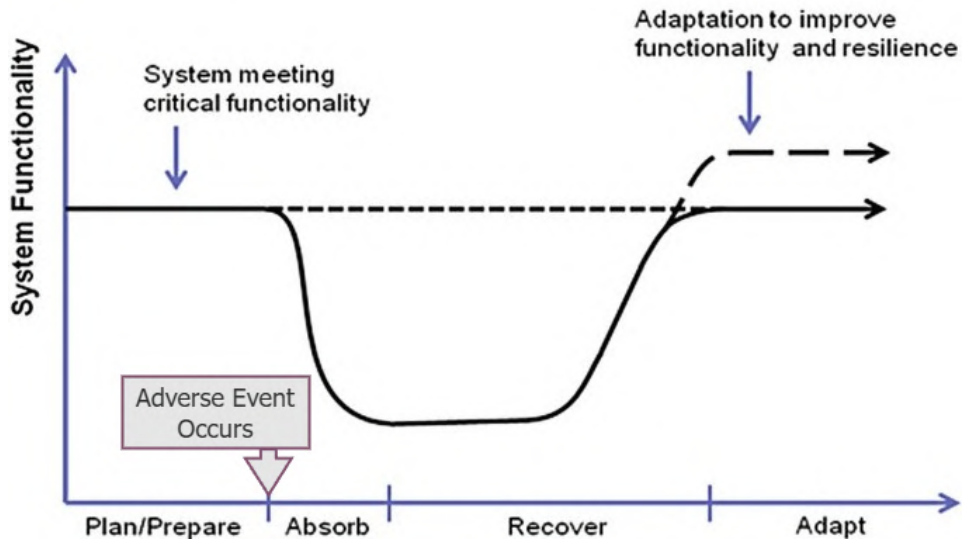

Figure 3.1: Resilience Curve (adapted from Linkov and Kott (2018)).

3.2. Defining Post-Disaster Recovery

3.2.1. Definition & Concept

In the context of disaster resilience, disruptive events, such as earthquakes, are causing a reduction in system functionality across sectors within the affected area. The immediate impacts are often manifested as infrastructure closure, loss of housing, healthcare system overloads or interruptions in the education system. Beyond this visible damage, such events may destabilizes the area in their economic, social, and environmental structures (Arcaya et al., 2020). Smith and Wenger (2007) described disaster recovery as "the differential process of restoring, rebuilding, and reshaping the physical, social, economic, and natural environment through pre-event planning and post-event actions."

Transportation networks, as the backbone of critical infrastructure, play an important role in the functionality of other systems within a community (Boakye et al., 2021). Functional transportation networks allow the movement of goods, services and people, serving a critical link between sectors such as healthcare, economic activity, and other services. Federal Emergency Management Agency (FEMA) (2023) include this function of the infrastructure systems in their *National Disaster Recovery Framework*, highlighting the goal of the recovery process to align post-disaster infrastructure with the community's anticipated needs for its "built and virtual environment".

Many studies emphasize a comprehensive approach to post-disaster recovery, recognizing it as a multi-dimensional concept (Khazai et al., 2018; Zeil, 2014). Following this perspective, Boyd et al. (2014) developed a framework built around six interrelated policy areas for addressing community recovery: (1) Land-Use and Reconstruction Standards, (2) Infrastructure and Transportation Restoration, (3) Housing Recovery, (4) Economic Redevelopment, (5) Environmental Restoration, and (6) Health and Social Recovery.
Similar areas are identified in other frameworks in the literature, such as the framework by MacDonald et al. (2015), based on New Zealand's Ministry of Civil Defence & Emergency Management (2005) and the Canterbury Earthquake Recovery Authority (2012). This framework conceptualizes five community components, namely the *Economic, Psycho-social, Cultural, Built-, and Natural Environment* dimensions.
Boyd et al. (2014) describes these areas as interconnected, as each area influences and supports the others. This interdependence is also emphasized is also emphasized in other frameworks, such as MacDonald et al. (2015), highlighting that recovery processes are multi-dimensional and mutually reinforcing. For example, effective housing recovery requires more than just rebuilding homes; it also depends on restoring transportation networks for access to jobs and services, revitalizing the economy to provide financial stability, and ensuring access to health and social services to support overall community well-being (Boyd et al., 2014).

The focus areas and policy approach outlined in Boyd et al. (2014) serve as the foundation for analyzing post-disaster recovery activities in this research. Within this framework, a socio-economic recovery perspective is adopted, concentrating on the restoration of infrastructure,

housing, economic activity, and health and social services. The selected areas are illustrated in Figure 3.2 and are further elaborated in Section 3.3.

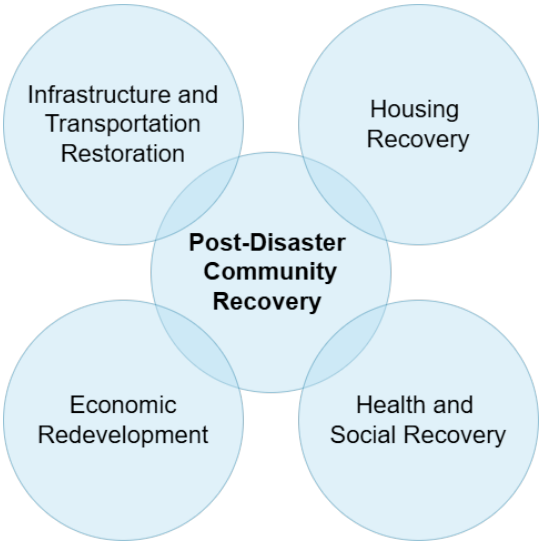

Figure 3.2: Policy areas for post-disaster community recovery.

3.2.2. Recovery Progress Approach

The progress of post-disaster recovery actions can be analyzed through different frameworks, most notably the *Time-Based* and *Activity-Based* approaches. Both approaches organize recovery into distinct phases, often incorporating the adaptation phase as illustrated in Figure 3.1. This section elaborates on both approaches to provide a structured understanding of the recovery process.

Time-Based Approach

In the time-based approach, each recovery phase is associated with a specific time frame (Hernantes et al., 2013). Across the literature, this timeline is commonly divided into three phases: Short-term, Intermediate (or Medium-term), and Long-term recovery. Although these phases lack strict time boundaries, since recovery efforts can vary depending on the severity of the event, a general timeframe can be assigned. According to Federal Emergency Management Agency (FEMA) (2023), Short-term recovery typically lasts from days to weeks, Intermediate recovery spans weeks to months, and Long-term recovery can extend from months up to several years.

The Short-term recovery phase focuses on rapid emergency response, including providing first aid, shelter, restoring basic accessibility, and stabilizing the situation (Ingram et al., 2006). Intermediate recovery focuses on the functional restoration necessary to restart daily life within the affected area, while Long-term recovery addresses broader adaptation processes, offering opportunities to rebuild improved and more resilient systems (Ingram et al., 2006). Figure 3.3 illustrates how the short-term, intermediate, and long-term recovery phases evolve over time, with overlapping periods reflecting the lacking strict time boundaries and the dynamic process of post-disaster recovery.

Activity-Based Approach

An alternative way to conceptualize the recovery process is through the classification of activities, identified as the activity-based approach. In this framework, recovery progress is structured around types of activities rather than fixed timeframes. As noted by Hernantes et al. (2013), terminology and classification vary across authors. Contreras (2016) reviewed multiple studies and concluded that most frameworks, including those from the United Nations Development Programme (UNDP) (2008), identify four phases: (1) Relief, (2) Early Recovery, (3) Recovery, and (4) Development. The (1) Relief phase prioritizes life-saving measures, addressing immediate secondary impacts of the disaster, and restoring essential services. The (2) Early Recovery phase aims to re-establish 'normal life', while the (3) Recovery phase focuses on restoring the affected area's functionality. Finally, (4) Development seeks to enhance the area beyond its pre-disaster state (Contreras, 2016).

Rather than being strictly time-bound, these phases are intended to reflect the progress achieved in recovery efforts. As highlighted by Contreras (2016), the transition between recovery phases is often unclear and should be determined by measurable progress rather than by the passage of time. Consequently, recovery follows a non-linear progression, where different groups and affected areas may be at different stages simultaneously, and progression can shift back and forth depending on evolving recovery dynamics (Contreras, 2016; Smith & Wenger, 2007; United Nations Development Programme (UNDP), 2008).

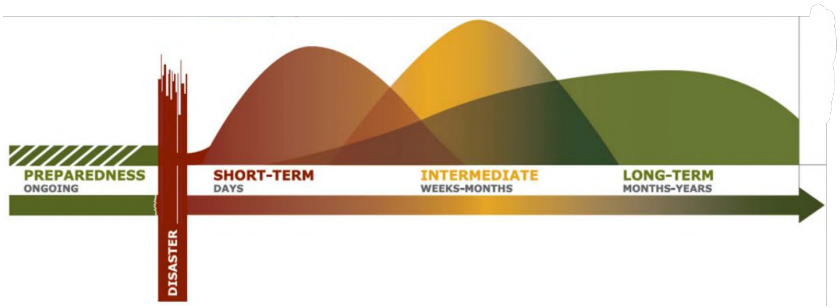

Figure 3.3: Recovery Continuum.

3.3. Identifying Recovery Activities

Building on the selected focus areas presented in the recovery framework, Figure 3.2, this section identifies key recovery activities related to Infrastructure and Transportation Restoration, Housing Recovery, Economic Redevelopment, and Health and Social Recovery. These areas reflect the socio-economic recovery perspective adopted in this research, focusing on the restoration of essential physical, economic, and social systems.

Recovery activities are analyzed using the *Time-Based Approach*, aligning short-, intermediate-, and long-term needs with the evolving priorities of the community throughout the recovery process. While this analysis is not exhaustive within each policy area, it provides a framework for assessing and prioritizing post-disaster recovery strategies, offering insights into the multi-dimensional dynamics of recovery.

3.3.1. Infrastructure and Transportation Restoration

The first policy area to be analyzed is the *Infrastructure and Transportation Restoration*, which, in this research, is scoped to the road network. Restoring the accessibility to and within the affected area immediately after a disruptive event, like an earthquake, is of critical importance (Boyd et al., 2014). Rapid temporary repairs and the establishment of provisional infrastructure are often necessary, as roads may crack open due to the direct impact of seismic activity (MacDonald et al., 2015). More commonly, however, roads are obstructed by landslides or debris, with the collapse of roadside buildings being a major cause of urban road network blockage, necessitating extensive debris removal (Yu & Gardoni, 2021). Other research prioritizes the road repair based on the road type and function, available repair crew and materials, or repair time (Aydin et al., 2018; Li et al., 2020). Hakami et al. (2013) emphasizes that achieving minimal accessibility within the first 72 hours is critical for saving lives and addressing the most urgent needs, such as providing first aid and ensuring the distribution of essential goods and services in the affected area. The critical importance of rapid accessibility is illustrated by the 2025 Tibet earthquake, where all major roads were reopened, and essential goods and services reached the affected area within the same day (Davidson, 2025).

After the first 72 hours, the focus shifts towards further clearing and repairing roads to restore operational capacity. Due to time constraints, debris is often initially pushed to the sides of roads and must later be collected and processed (Çelik et al., 2015; MacDonald et al., 2015). Additionally, provisional road repairs require replacement with more durable and permanent solutions, as highlighted by the spokesperson of the Alaska Department of Transportation in McGee (2018). Depending on the severity of the event, these repair activities can take from several weeks to months. For instance, Joyal (2019) observed that most roads appeared normal again within a week after the 2018 Alaska 7.1 magnitude earthquake. Similarly, the recovery and reconstruction assessment a year after the 7.8 and 7.7 magnitude earthquakes in Türkiye noted that all emergency damages had been repaired during the 'early stage' of recovery (OCHA, 2023a). Restoring the operability of the road network is crucial not only for immediate recovery operations, such as debris removal and material delivery, but also for reestablishing daily life activities, including access to jobs and essential services (Jha, 2010).

Once basic operational capacity has been restored, attention can gradually shift from emergency repairs to longer-term improvements. Post-disaster assessments provide an opportunity to identify vulnerabilities within the road network that were exposed during the disaster. These insights offer valuable lessons for improving building codes and design standards, which can be applied to strengthen network segments and enhance overall functionality beyond pre-event levels (MacDonald et al., 2015). Segments prioritized for improvement may include roads or bridges located in multi-hazard-prone areas, such as landslides or flooding, or aging infrastructure requiring replacement or reinforcement to better withstand future events.
Table 3.1 provides an overview of the key activities and corresponding timeframes involved in restoring road network functionality after a disaster.

Table 3.1: Road recovery activities and their corresponding recovery phases

Road Recovery Activities	Recovery Phase
Temporary Repairs	Short Term
Debris Removal	Short Term
Clearing Roads	Intermediate Term
Road Repair	Intermediate Term
Enhance Infrastructure	Long Term

3.3.2. Housing Recovery

The next policy area to be addressed is *Housing Recovery*, which plays a central role in restoring stability and rebuilding communities after a disaster. Housing recovery can take several years after a disaster, making different forms of temporary housing crucial in bridging the gap between displacement and permanent resettlement (Jha, 2010). Temporary housing solutions offer survivors a gradual pathway back to stable living conditions (Perrucci & Baroud, 2020). While housing recovery often refers to the physical reconstruction of homes, it also encompasses the reconstruction of the "social, economic, natural and cultural environment," as emphasized by Jha (2010), underscoring the need for a multi-dimensional recovery approach.

Perrucci and Baroud (2020) reviewed temporary housing models and identified distinct phases of temporary shelter throughout the recovery timeline. Immediately after an earthquake, ensuring safety and providing emergency shelter is essential for survivors (Arcaya et al., 2020; Boyd et al., 2014). Emergency shelters, such as public buildings or lightweight, portable tents, offer dry and safe conditions but are typically suitable only for a few days. Subsequently, survivors transition into temporary shelters that offer greater comfort and security for several weeks, allowing time to plan longer-term solutions (Perrucci & Baroud, 2020). The next step involves temporary housing, which provides livable conditions with essential utilities and enables the resumption of daily activities. This stage typically includes the use of prefabricated homes or modular units, designed to accommodate people for extended periods, often up to several years. During this time, efforts are directed towards establishing permanent housing solutions to facilitate a full return to normalcy (MacDonald et al., 2015).

A similar timeline for housing recovery can be observed in the shelter project overview by Cluster (2021) following the 2021 Indonesia earthquake. In this case, debris clearing for temporary shelter sites commenced within ten days after the disaster, and within three months, durable shelter solutions were underway.
Temporary housing solutions, however, bring forward a set of challenges. Inexpensive tents are easy to deploy but may raise concerns regarding safety, durability, and the well-being of occupants. Furthermore, placing temporary shelter sites close to original homes is often most effective for maintaining social ties, but can expose residents to residual risks if the area remains hazard-prone. Mismanagement of temporary housing, particularly when it fails to meet the needs of affected populations, can also have significant negative impacts on mental health (Perrucci & Baroud, 2020) Thus, effective planning and management of temporary housing

are crucial not only for supporting physical recovery, but also for safeguarding the social and psychological well-being of affected communities.
Table 3.2 summarizes the main housing recovery activities and their respective timeframes, reflecting the gradual transition from emergency shelter to permanent resettlement.

Table 3.2: Housing recovery activities and their corresponding recovery phases

Housing Recovery Activities	Recovery Phase
Emergency Shelter	Short Term
Temporary Shelter	Short Term – Intermediate Term
Temporary Housing	Intermediate Term
Permanent Housing	Intermediate Term – Long Term

3.3.3. Economic Redevelopment

The third policy area to be addressed is Economic Redevelopment, focusing on reestablishing the physical foundations for economic activity and facilitating the return of income-generating opportunities within the affected community. Disasters can severely disrupt local economies by damaging or destroying business premises, cutting off supply chains, and causing widespread job losses.
Immediately following a disaster, the priority is to enable the flow of essential goods and materials into the affected area. This process is dependent on the restoration of critical infrastructure, such as road networks, ports, and airports, which are essential for sustaining relief operations and supporting early economic activity. Access to warehouses, building materials, and logistics facilities becomes vital for both economic redevelopment and the broader recovery process, including search and rescue operations and the reestablishment of health and social services. Maintaining connectivity with local and regional production centers is equally important to ensure that basic economic activities, such as the distribution of goods and construction services, can resume (Cluster, 2021).

In the intermediate phase, reopening businesses and facilitating commercial activities becomes a key part of the recovery effort (Boyd et al., 2014). To limit prolonged economic disruption, it is crucial to rapidly invest in temporary facilities and restore basic market functions, enabling businesses to resume operations and stabilize local economic activity. However, restoring income-generating activities also depends on progress in infrastructure and housing recovery, as accessible transport networks are needed for the movement of goods and employees, and safe housing supports the return of the workforce (Xie et al., 2018).
Over the longer term, economic redevelopment efforts concentrate on the reconstruction of permanent business infrastructure and the revitalization of broader economic systems (Arcaya et al., 2020; MacDonald et al., 2015). Strengthening supply chains and improving regional connectivity are critical to support sustained economic activity (Xie et al., 2018). As shown by Bodenstein and Scaramucci (2025), severe disasters can cause persistent economic losses, with national GDP remaining notably lower even several years after the event, underscoring the need for an integrated, multi-dimensional recovery process.

A summary of key activities supporting economic redevelopment across different phases of recovery is presented in Table 3.3.

Table 3.3: Economic redevelopment activities and their corresponding recovery phases

Economic Redevelopment Activities	Recovery Phase
Restore Access to Essential Goods and Materials	Short Term
Establish Business and Production Sites	Intermediate Term
Rebuild Permanent Business Infrastructure	Intermediate – Long Term
Strengthen Supply Chains and Regional Connectivity	Long Term

3.3.4. Health and Social Recovery

The final policy area to be addressed is Health and Social Recovery, focusing on restoring critical health services and supporting the psychological well-being of affected communities. Immediately following a disaster, search and rescue operations, first aid, and the provision of basic human needs are of paramount importance (MacDonald et al., 2015). Rapid access to affected areas is critical during this stage, as survival rates remain high within the first 24 hours, at approximately 90%, but decrease significantly to around 20% after 72 hours (Hakami et al., 2013). Ensuring that road networks and key transport routes are cleared and operational is therefore essential for enabling rescue teams, medical services, and relief supplies to reach those in need. Search and rescue operations typically conclude after about a week, particularly when no survivors have been found in the preceding days (Chowdhury et al., 2023; Kovacevic, n.d.).

In the weeks and months following the disaster, maintaining access to essential healthcare services becomes a critical priority for both injured and non-injured populations (Arcaya et al., 2020). This includes not only emergency medical care, but also the provision of mental health support, as earthquakes significantly increase the prevalence of psychiatric illnesses (Akram et al., 2024). It is estimated that one in five people affected by the 2023 Türkiye earthquake will experience psychological impacts (World Health Organisation, 2024). However, the continuity of health services can be challenging, as healthcare facilities are often overwhelmed or may suffer reduced functionality due to infrastructure damage (Hassan & Mahmoud, 2020). For example, following the 2023 Türkiye earthquake, the healthcare system was still struggling two months after the event (Borzenkova, 2023).

Depending on the extent of damage and available resources, temporary healthcare facilities can be established using modular tents and medical camp kits, bridging the intermediate period until permanent structures are repaired or rebuilt (MacDonald et al., 2015; World Health Organization, 2024). In the longer term, spanning several years, the reconstruction of healthcare infrastructure progresses from temporary solutions toward permanent facilities. While initial recovery efforts focus on emergency care and temporary healthcare provision, planning and rebuilding permanent structures gradually become increasingly important as the recovery advances. After the 2018 Indonesia earthquake, for instance, damaged hospitals

were rebuilt three years after the event (Alisjahbana et al., 2022; Meyers, 2021). Alongside the physical rebuilding of facilities, it is essential to maintain long-term psychological support services to address the ongoing mental health needs of affected populations (Brake et al., 2009; MacDonald et al., 2015).
Table 3.4 outlines the primary health and social recovery activities across different stages of the post-disaster recovery process.

Table 3.4: Health and social recovery activities and their corresponding recovery phases

Health and Social Recovery Activities	Recovery Phase
Search and Rescue	Short Term
First Aid	Short Term
Temporary Health Facilities	Short Term – Intermediate Term
Reconstruct Health Facilities	Intermediate Term – Long Term

3.4. Defining Intermediate Recovery

The intermediate recovery phase plays an important role in the overall recovery timeline. While the short-term phase focuses on emergency response and stabilization, the intermediate phase aims to restore essential services and enable the resumption of daily life. This period is typically defined as lasting from several weeks to a few months after the disaster, although timelines may vary depending on the severity and context of the disruption. An overview of the key recovery activities across the short-, intermediate-, and long-term phases, structured around the four focus areas, is illustrated in Figure 3.4.
A recurring theme in the literature is the temporary nature of recovery activities during this phase. As full reconstruction of the affected area is often a long-term process, temporary measures are implemented to bridge the gap between emergency response and permanent rebuilding. These measures focus on restoring basic functionality across the domains; infrastructure, housing, economic activity, and health services, and are essential to supporting the gradual return of normal social and economic life.

Looking specifically at transportation systems, the intermediate phase goes beyond restoring emergency access and focuses on clearing, repairing, and stabilizing networks to support regular traffic flow. Accessibility may still be constrained by ongoing recovery activities such as debris removal and building repairs, affecting mobility across the community.
More broadly, the intermediate phase marks a period of spatial and functional transformation within the living environment. Existing access patterns are disrupted and reshaped, temporary facilities emerge, and essential services such as healthcare, local markets, and community support centers gradually begin to be reestablished. Recovery during this phase requires an integrated approach across all sectors, recognizing that infrastructure, housing, economic activity, and health services are interdependent elements of a functioning community. Rather than focusing solely on physical reconstruction, recovery rebuilds the social infrastructure, allowing communities to reconnect, restore access to key services, and resume daily life.

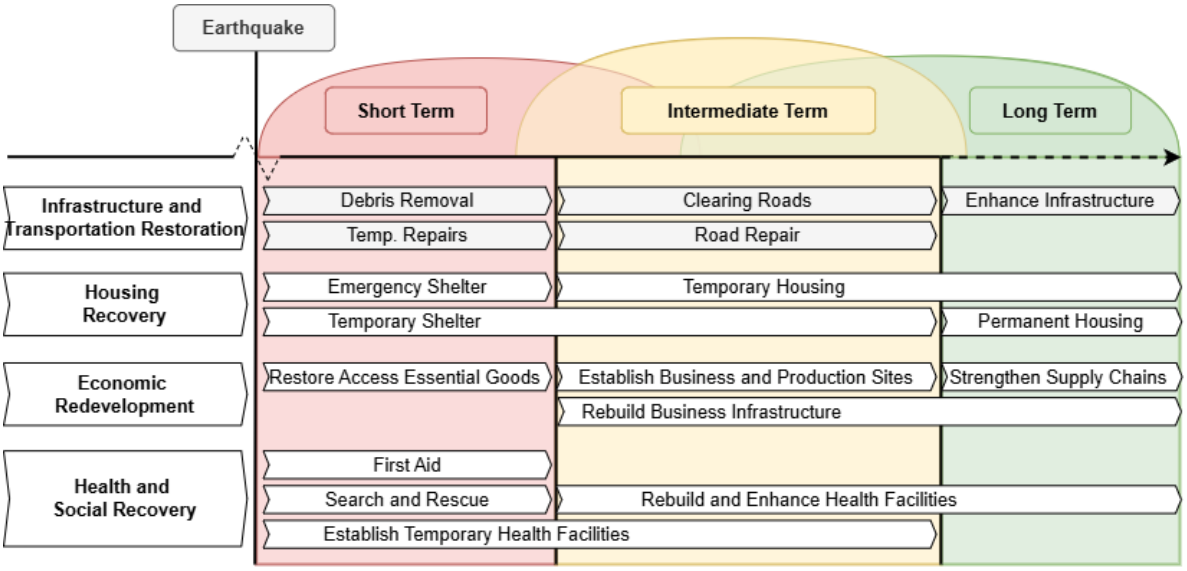

Figure 3.4: Recovery Activities on the Recovery Timeline.

3.5. Multi-Hazard Events in Recovery Contexts

As discussed in Section 3.4, the intermediate recovery phase marks a period in which daily life begins to stabilize, supported by temporary infrastructure and services. This temporary setup allows communities to resume daily routines, but remains vulnerable to additional hazard events that can disrupt these fragile systems and delay recovery. Such hazards may occur in close succession, simultaneously, or as a consequence of the initial hazard. Although approximately 19% of the hazards may be classified as multi-hazard, they cause 59% of the global economic losses (Lee et al., 2023). Nevertheless, hazards are still commonly assessed and managed as separate events (Laino & Iglesias, 2024; Ward et al., 2022). This underscores the importance of applying a multi-hazard perspective, which is likely to be more effective than managing each hazard separately.

In order to better understand the multi-hazard events, different classification of the multi-hazard events can be found in the literature. In this research, the classification described by Drakes and Tate (2022) is used to distinguish between aggregate, cascading, and compound hazards. These classifications with its definitions and examples are summarized in Table 3.5.

Table 3.5: Three classifications of multi-hazard events (Based on Drakes and Tate, 2022)

Classification	Definition	Example
Aggregate hazards	Combined impact of separate events, either sequential or simultaneous.	Several storms in short succession affecting the same area.
Cascading hazards	One event triggers another.	Flooding caused by damaged drainage after an earthquake.
Compound hazards	Different events occur at the same time and affect the same system.	Heavy rainfall and high tides occurring simultaneously, causing flood.

4

Intermediate Recovery under Multi-Hazard Conditions: The Case of Antakya

This chapter applies the modeling framework to the case of Antakya and Defne, focusing on the intermediate recovery phase under multi-hazard conditions. It introduces the case, defines the Area of Interest, maps key temporary infrastructure, and prepares the network and flood models used to assess accessibility. The outputs generated here serve as inputs for the analysis in Chapter 5, where accessibility and system vulnerabilities are examined in detail. In doing so, this chapter contributes to answering Sub-question 3, by illustrating how the February 2023 earthquake reveals vulnerabilities in transportation recovery; and Sub-question 4, by operationalizing multi-hazard impacts through network-based modeling.

4.1. Case Introduction

The February 6, 2023 earthquake in Türkiye serves as a case study in this research. This 7.8 magnitude earthquake struck southern and central parts of the country, causing widespread devastation. According to the Modified Mercalli Intensity (MMI) scale, which measures the perceived shaking and surface impact, the earthquake reached a maximum intensity of "Extreme" near the epicenter and in the Antakya district. A second earthquake of 7.7 magnitude occurred shortly afterward, and was followed by more than 30,000 aftershocks over the subsequent three months, compounding the disruption across the region.

Figure 4.1 illustrates the distribution of seismic activity across the affected region, including the main fault lines in blue, and earthquake epicenters and aftershocks as colored dots. One of the major fault lines runs directly through Hatay province and passes by the city of Antakya. In total, the disaster directly affected 11 provinces, impacting over 14 million people, approximately 16 percent of Türkiye's population. Over 53,000 people lost their lives, making

it one of the deadliest natural disasters in recent history worldwide. The estimated economic damage exceeds US$150 billion. According to the Food and Agriculture Organization (FAO), more than 4 million buildings and over 20 percent of the country's food production were affected.

To better understand how this disaster unfolds in a complex, multi-hazard environment, the remainder of this section explores the context of the disaster in more detail. By defining the Area of Interest, mapping critical amenities, and examining the impact of flooding as secondary hazard, this section lays the foundation for identifying vulnerabilities and analyzing key recovery needs within the urban system during the intermediate recovery phase.

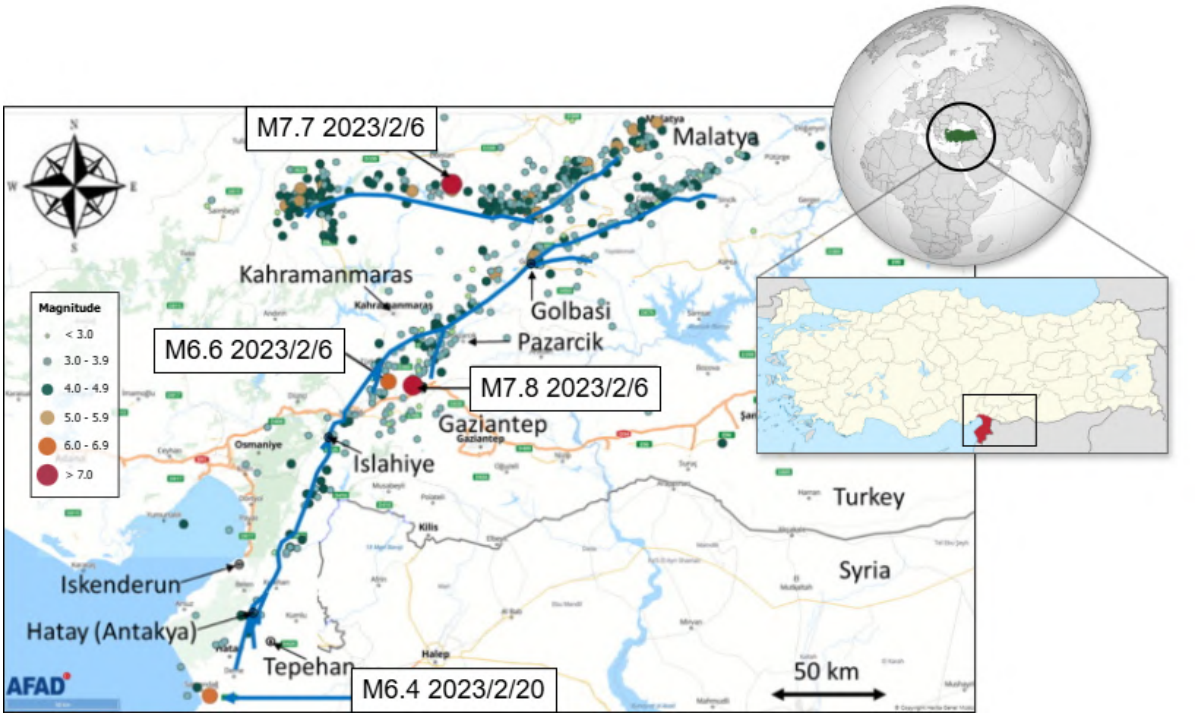

Figure 4.1: Map of the seismic activity in the affected provinces, highlighting the Hatay province in red (Edited and adapted from AFAD (2023))

4.2. Area of Interest

This research focuses on the urban area comprising the districts of Antakya and Defne, which together form the defined Area of Interest (AOI). Although administratively distinct, with Defne covering the southwestern part of the Antakya agglomeration and its surrounding countryside, the two are treated here as a single urban unit and collectively referred to as Antakya for simplicity. Located in the province of Hatay, highlighted in red in Figure 4.1, these adjacent districts were among the most severely affected by the February 2023 earthquakes. Hatay province accounted for over 23,000 deaths, nearly 50% of the national total, with Antakya experiencing the highest level of destruction. Within Antakya, approximately 90% of the buildings and 70% of the homes were either destroyed or rendered unusable, erasing entire

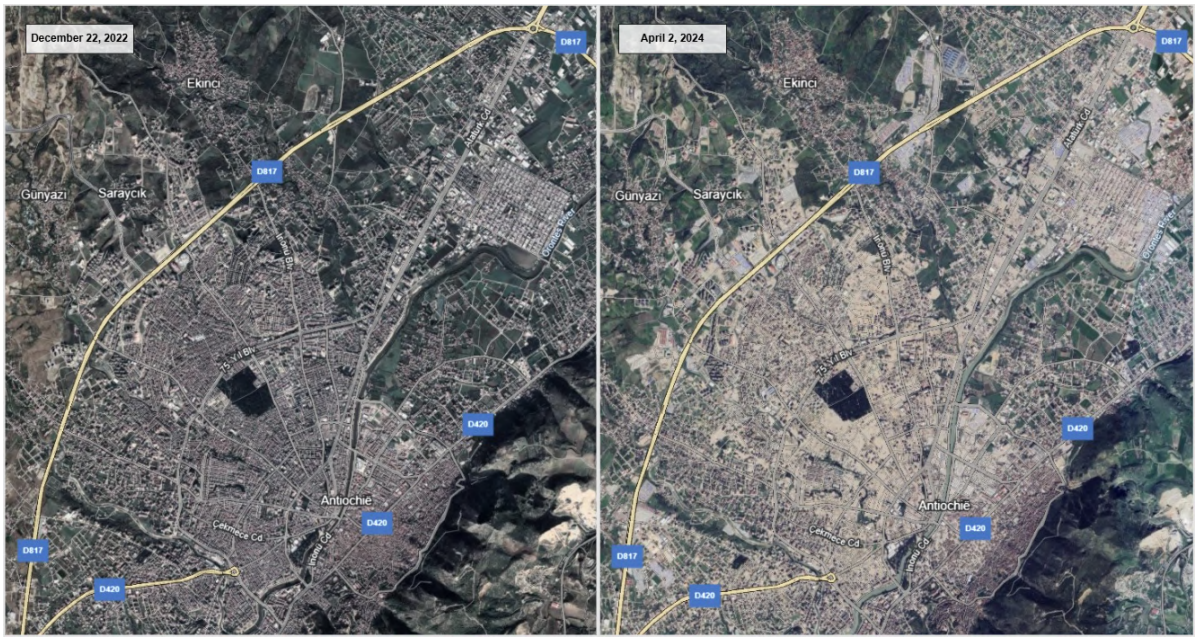

Figure 4.2: Satellite images of the city of Antakya before and after the 2023 earthquake, obtained from Google Earth

neighborhoods, including the historic city center.

The earthquake's devastation is visible in Figure 4.2, which compares satellite images of the city before and after the disaster: the left image shows Antakya in December 2022, while the right shows the same area in April 2024. The figure highlights both the physical impact of the earthquake and the subsequent demolition work required for the city's reconstruction.

To make matters worse, on April 11 2023, just a few months after the earthquakes, the Hatay region was struck by heavy rainfall, leading to severe flooding in areas already devastated by the seismic events. These floods not only exacerbated the existing humanitarian crisis but also further hindered recovery efforts. Floodwaters damaged temporary shelters, disrupted supply chains, and hindered access to essential services, thereby delaying reconstruction activities and prolonging the displacement of affected populations (ACAPS, 2023).
The combined impact of the earthquake and subsequent flooding makes this urban setting a relevant case for examining multi-hazard vulnerability during the intermediate recovery phase, enabling an urban-scale analysis of recovery needs and offering insight into how the recovery process consisting of a temporary environment can be improved to strengthen long-term resilience.

4.3. Localizing critical intermediate Infrastructure

As outlined in Section 4.2, the destruction in Antakya following the February 2023 earthquakes disrupted access to essential services. As made clear in the theoretical framework, the restoration of basic functionality during the intermediate recovery phase depends not only on the physical reconstruction of infrastructure, but also on the accessibility of critical locations such as emergency shelters, healthcare facilities, and markets. This section identifies and maps key infrastructure in Antakya required to meet the community's intermediate needs. For a detailed explanation of the georeferencing and processing used to map these locations, see Appendix A.

Shelter locations

The destruction of over 70% of residential structures has made temporary housing an important part of the recovery process. In the immediate aftermath of the earthquake, numerous formal and informal temporary shelters, primarily tents, were set up across Antakya to meet urgent housing needs. As conditions stabilized, more organized forms of temporary housing emerged, notably container units installed on the outskirts of the city where space permitted larger shelter camps.

Figure 4.3 shows the spatial distribution of these facilities, represented by green dots. A total of 34 shelter locations were identified based on data from Hatay Planning Center (n.d.). Their accessibility under post-disaster and flood scenarios is analyzed in the following sections.

Market locations

Markets play an important role in supporting local economic recovery after a disaster., as many commercial buildings were destroyed or became inaccessible. To facilitate economic activity, temporary market locations were established, often in the form of container units where people could restart their businesses. These markets provide essential goods and services to the community and offer a source of employment for many residents.

Figure 4.3 displays the market locations in Antakya, marked as orange dots. The market locations span both the outskirts and central areas of Antakya. According to data from Hatay Planning Center (n.d.), a total of 16 markets are set up.

Healthcare locations

After the earthquake, many regular healthcare facilities were damaged or became unusable. Therefore, container clinics were set up in the container camps where many displaced people were relocated (United Nations Office for the Coordination of Humanitarian Affairs (OCHA), 2023). These camps have since become important locations for accessing basic healthcare services. However, despite the presence of these container clinics, hospitals remain critical for providing advanced medical care and emergency treatments.

Figure 4.3 shows the locations of the hospitals in Antakya. While not all of these hospitals are located strictly within the defined area of interest, they have been included in the analysis due to their essential role in the region's healthcare system. The three hospitals that are operational during the intermediate recovery phase are marked as red dots (Hatay Planning Center, n.d.).

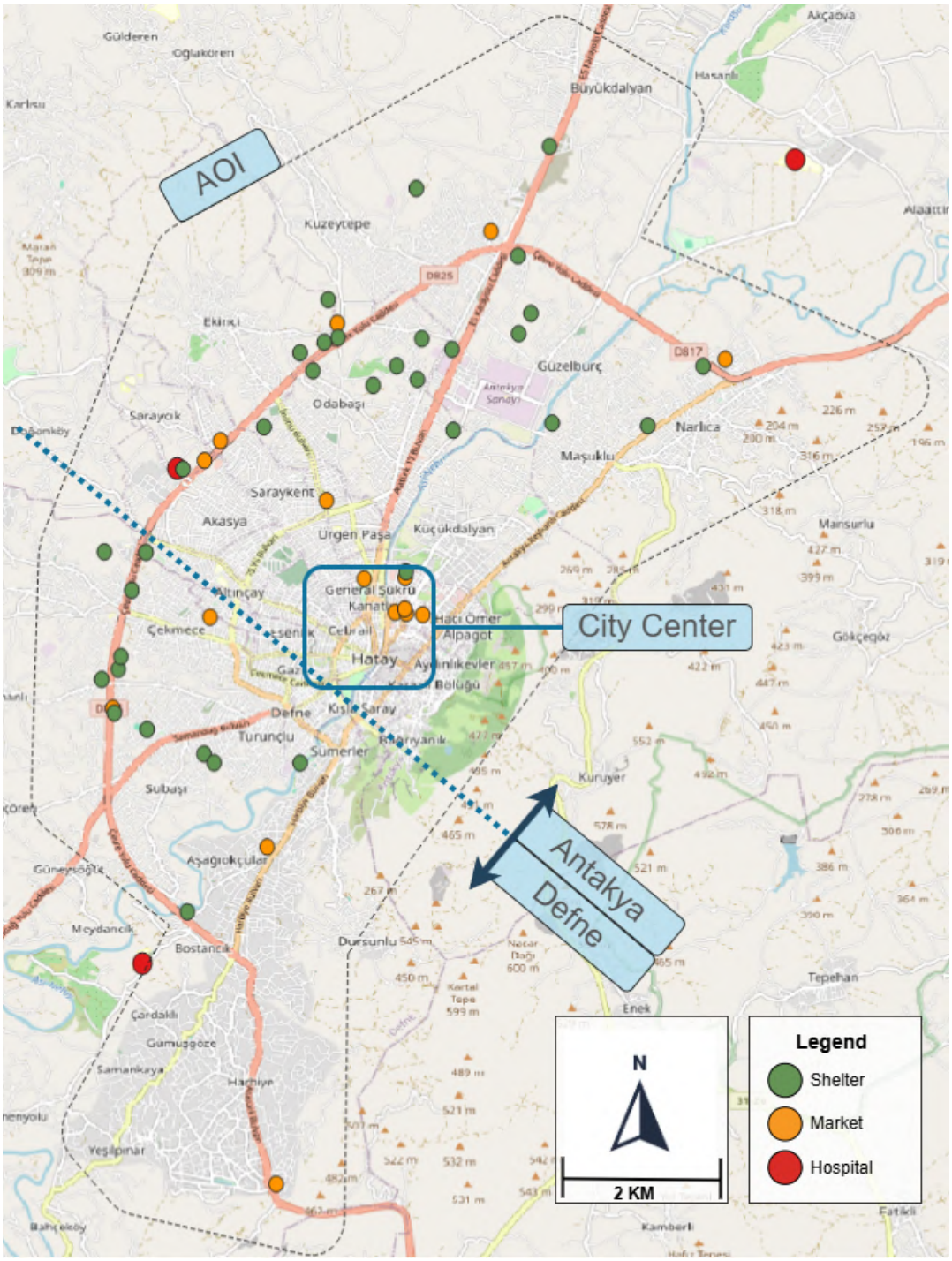

Figure 4.3: Locations of key amenities in Antakya's area of interest.
Green, orange, and red dots represent shelter, market, and hospital locations, respectively.

4.4. Flooding risks

In Türkiye, earthquakes are the most devastating natural hazard in terms of loss of life and damage to property. Floods, however, rank second overall and are the most destructive among climate-related disasters. Together, these hazards represent the most significant threats to the country's physical infrastructure, and economic and social systems (İrvem et al., 2024).

Flooding in urban areas can result from various causes, for example river overflow, coastal surges, or intense rainfall. In this research, the focus lies on pluvial flooding caused by heavy rainfall. Rainfall intensity is typically expressed in millimeters over a specific time period and is often analyzed using return periods, which indicate the statistical likelihood of a given rainfall event occurring (Grounds et al., 2017). The rainfall data used in this research are presented in Table 4.1, showing rainfall intensities in mm per six hours for return periods ranging from 25 to 100 years (Irvem & Topaloğlu, 2012).

The return periods and their corresponding rainfall intensities are used as input for the flood model to assess which areas within the Area of Interest are vulnerable to potential flooding. This enables a spatial analysis of flood risk, providing insights into how a secondary hazard may impact the community during the intermediate recovery period. Understanding flood exposure is therefore crucial not only for emergency response, but also for informing the spatial planning of temporary facilities and transport corridors during the recovery phase.

Table 4.1: Six-hour rainfall intensity (mm) for selected return periods in Antakya

	Return period (years)		
	25	**50**	**100**
Rainfall (mm)	30.5	34.5	39.0

4.5. Data availability

Table 4.2 summarizes the geospatial and attribute datasets used for network modeling and flood analysis in Antakya. These include shapefiles from Copernicus, road network data from OpenStreetMap, elevation and building footprints, and location data for shelters and amenities. The datasets were collected between November 2024 and March 2025 and reflect the most recent post-earthquake conditions.

Table 4.2: Overview of Data Sources and Collection Details

Data Description	**Datatype**	**Source**	**Collection Date**
Antakya Road System	Road network (OSMnx graph)	OpenStreetMap (2024)	November 14, 2024
Area of Interest	Shapefile	Copernicus	November 14, 2024
Road Damage Data	Shapefile	Copernicus	November 14, 2024
Built Environment Damage Data	Shapefile	Copernicus	November 14, 2024
Digital Elevation Model	DEM raster (30x30m)	Copernicus (2024)	February 10, 2025
Antakya Building Footprints	Building footprints shapefile	HDX (2025)	February 10, 2025
Shelter point data	KMZ file	AFAD (2024)	March 14, 2025
Amenity location data	PNG image	Hatay Planning Center (n.d.)	March 14, 2025

4.6. Model Output

4.6.1. Road Network Model with Integrated Attributes

Figure 4.4 shows the road network model of Antakya, corresponding to Step 1 of the modeling framework. The network was constructed using OpenStreetMap (OSM) data processed through OSMnx, resulting in a routable graph with over 10,000 nodes and more than 27,000 edges. With an average node degree of 2.8 and a standard deviation of 0.85, the network can be classified as dense and relatively homogeneous in terms of connectivity.

In preparation for hazard simulation, this baseline network was enriched with geospatial data on earthquake-induced road and building damage, as well as the mapped locations of temporary amenities such as shelters, hospitals, and markets (Step 2). The road segments in Figure 4.4 are color-coded based on their estimated level of accessibility, derived from earthquake-induced damage. Roads are classified into four disruption levels: severe (red), moderate (orange), minor (yellow), and no disruption (grey). This integrated model forms the foundation for analyzing hazard exposure and service accessibility under disrupted conditions.

4.6.2. Flood Scenario Representation

Figure 4.5 shows the simulated flooding pattern in Antakya under a Q100 rainfall scenario, corresponding to Step 3 of the modeling framework: identifying flood exposure zones within the Area of Interest. The simulation output was generated using the Arc-Malstrøm model and uses a Digital Elevation Model (DEM) with an original resolution of 30×30 meters, which was resampled to a 1×1 meter grid to align with finer-scale spatial layers such as building footprints. While this improves spatial detail for analysis and visualization, it does not enhance the vertical accuracy of the elevation data. Grid cells with modeled water depths greater than 0.5 meters are shown in blue.

To support interpretation of the results, OpenStreetMap (OSM) road data was manually overlaid in QGIS. This contextual layer is not part of the model output but provides spatial reference for assessing potential infrastructure exposure. The resulting flood layer serves as input for Step 4, where road segments are programmatically tagged using GeoPandas in Python, based on whether they intersect with flood extents under the Q25, Q50, and Q100 rainfall scenarios.

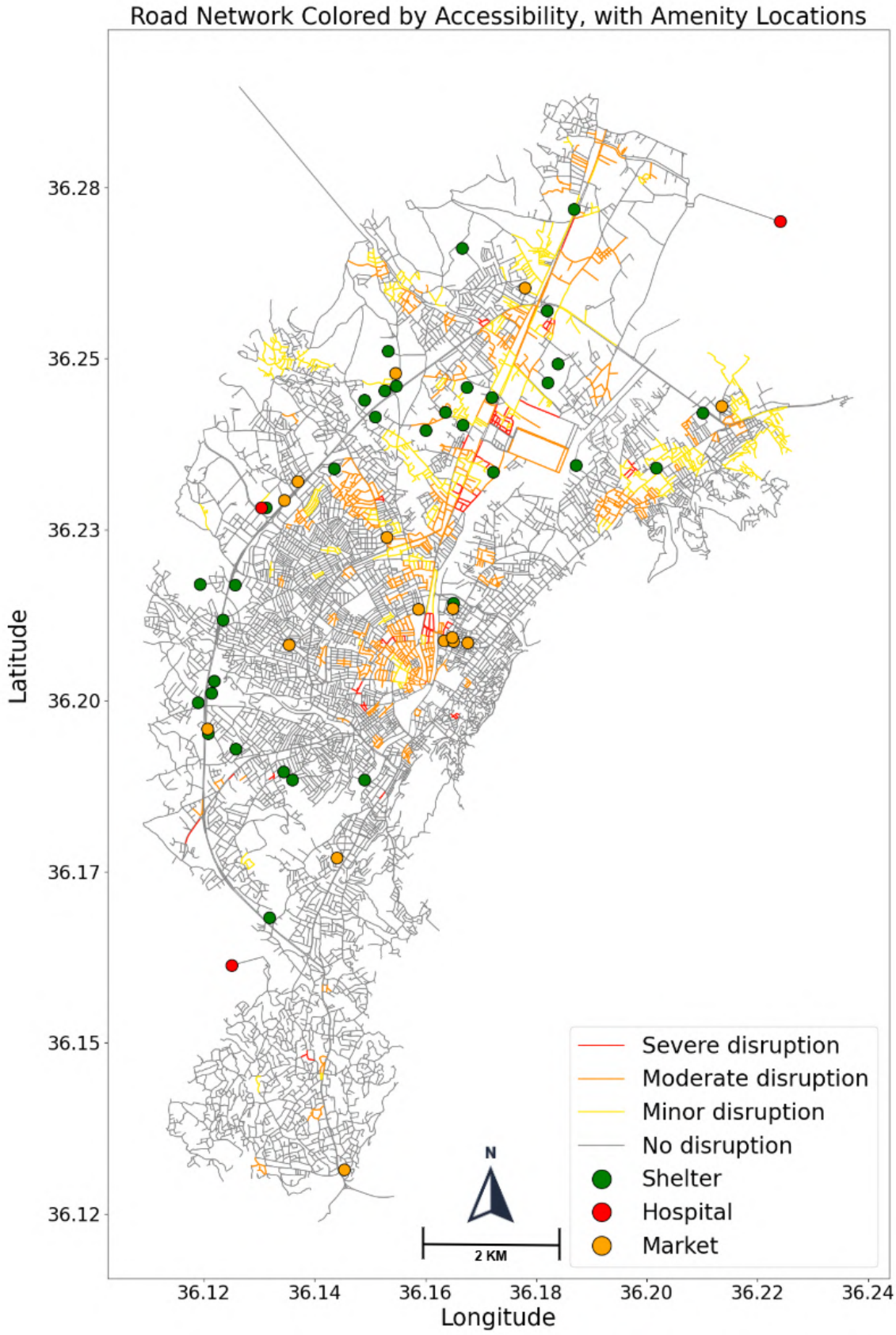

Figure 4.4: Plot of the Antakya road network.

Figure 4.5: Q100 Arc-Malstrøm flood model output of Antakya as visualized in QGIS. Flood depths > 0.5 m are shown in blue.

5

Results on Multi-Hazard Network Performance

This chapter presents the results of flooding model and the network-based analysis under multi-hazard conditions, using the three performance metrics: centrality, access to critical facilities, and travel delay. Each section presents how these metrics are affected by earthquake and flood scenarios, highlighting vulnerability, shifts in network structure, and implications for accessibility during the intermediate recovery phase.

5.1. Impact of Pluvial Flooding on Road Infrastructure

This section presents the effects of flooding on the road network. Output from the Arc-Malstrøm model has been spatially linked to road infrastructure, highlighting flooded segments in blue. Shelter and amenity locations are overlaid to indicate potential accessibility challenges. Figure 5.1 shows the Q100 scenario, with flooded roads and nearby critical services.
As shown in Table 5.1, differences across flood scenarios are minor; higher rainfall intensities only slightly increase the number of affected roads. However, many critical facilities are located near flood-prone roads, indicating a potential threat to service accessibility during heavy rainfall.

Given the limited variation between scenarios, only the Q100 results are shown here. Full outputs for Q25 and Q50 are included in Appendix B.

Table 5.1: Flooded roads per scenario based on 6-hour rainfall intensity (in mm).

Scenario (Return Period)	Rainfall (mm)	Flooded Roads	Total Roads	Flooded Percentage (%)
Flooded Q25	30.5	1374	27698	4.96
Flooded Q50	34.5	1460	27698	5.27
Flooded Q100	39.0	1576	27698	5.69

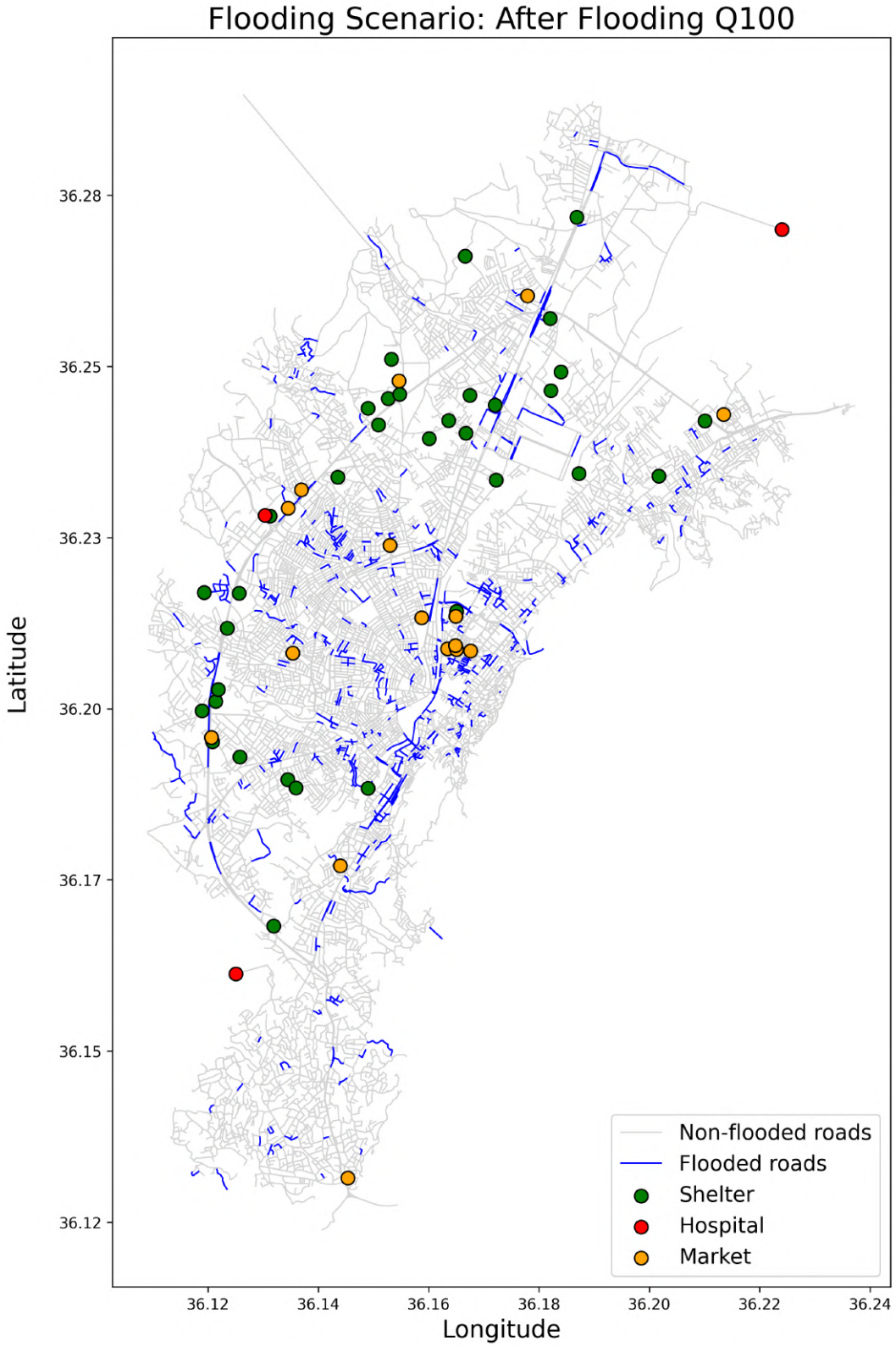

Figure 5.1: Flooding scenario Q100. Locations of shelters, hospitals, and markets overlaid on flooded and non-flooded road segments.

5.2. Edge Betweenness Centrality under Multi-Hazard Scenarios

This section analyzes changes in edge betweenness centrality under baseline (post-earthquake) and Q100 flood scenario. It first explores network-wide patterns, followed by an OD-based analysis of shelter-to-service routes. Finally, it compares network-wide and community-oriented perspectives to identify shifts in strategic connectivity. The results provide insights into which road segments become critical for maintaining access to essential services during the intermediate recovery phase and under multi-hazard impacts.

5.2.1. Network-Wide Centrality Distribution

General Exploration

To start a general exploration, Table 5.2 presents the normalized edge betweenness centrality values across percentile thresholds for each scenario. The results show that the majority of roads have low centrality scores, regardless of the scenario. The 25th and 50th percentiles remain low, indicating that most roads play a minor role in maintaining overall network connectivity. This suggests a network structure that is dependent on a relatively small set of critical links.

Under flooding scenarios, the spread of centrality values increases. Both the 99th percentile and maximum values rise under flood conditions, pointing to growing concentration of network load on fewer links. In the Q50 and Q100 scenarios, the maximum centrality increases even further while the 99th percentile slightly decreases, suggesting that network pressure becomes even more focused on a limited number of routes.

For example, the maximum centrality increases from 0.099 after the earthquake to 0.107 in Q25 and 0.120 in Q100. This indicates that under more severe forms of aggregative hazard, a few key road segments become increasingly critical by concentrating network load.

Table 5.2: Percentile thresholds of edge betweenness centrality per scenario, including the corresponding normalized values.

Percentile	After Earthquake	After Flooding Q25	After Flooding Q50	After Flooding Q100
Min	0.000000	0.000000	0.000000	0.000000
25%	0.000095	0.000096	0.000096	0.000097
50%	0.000290	0.000248	0.000250	0.000246
75%	0.001492	0.001285	0.001305	0.001294
90%	0.008160	0.006834	0.007103	0.007115
99%	0.048884	0.061511	0.057898	0.058762
Max	0.098854	0.107459	0.120140	0.120212

Network-wide Centrality Plots

Continuing on the general exploration, the maps in Figure 5.2 and Figure 5.3 visualize the edge betweenness centrality scores for the Antakya road network under different (multi-)hazard scenarios. The road segments are color-coded using a logarithmic color scale ranging from low centrality values in light gray to high centrality values in dark red, highlighting the relative importance of each road segment in terms of network connectivity. This logarithmic scale was chosen to better visualize the wide distribution of centrality values observed in Table 5.2, ensuring that differences between both low and high scores remain visually distinguishable.

Across all scenarios, the centrality plots confirms the outcomes shown in Table 5.2 and visualizes that the majority of road segments have low edge betweenness centrality values. In contrast, high centrality values are concentrated in a small subset of segments. This confirms the underlying network structure, with high centrality values generally following the city's main road infrastructure, while lower values align with local neighborhood streets.

When comparing the baseline scenario (post-earthquake) to the flood scenario, changes in the spatial distribution of centrality values can be observed. Several segments in the city center of Antakya and along the western ring road show a decrease in edge centrality or even become inactive under flooded conditions. In contrast, certain peripheral routes show increased centrality values, indicating a shift in shortest path usage across the network in response to flooding disruptions.

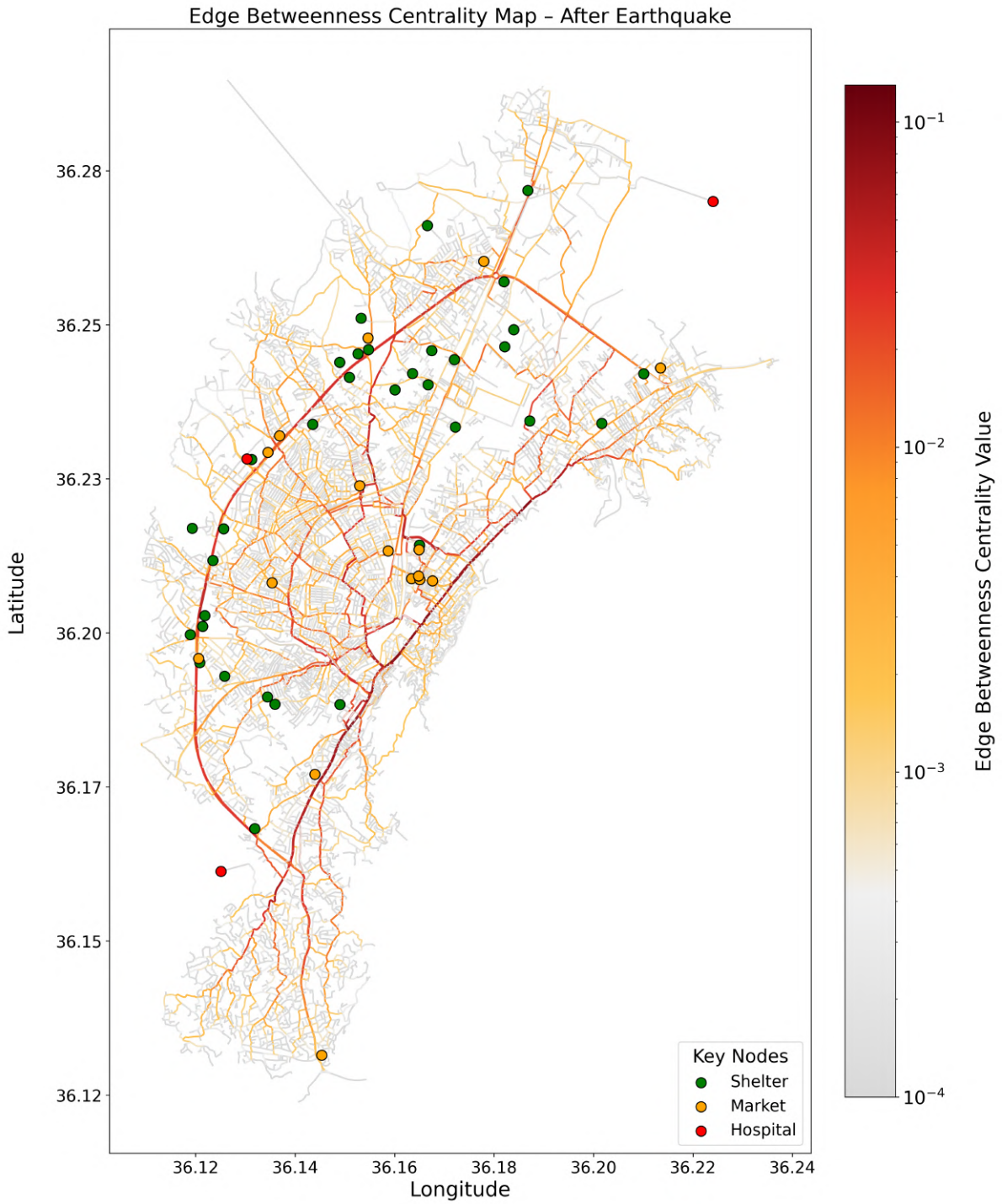

Figure 5.2: Edge betweenness centrality under the baseline scenario.

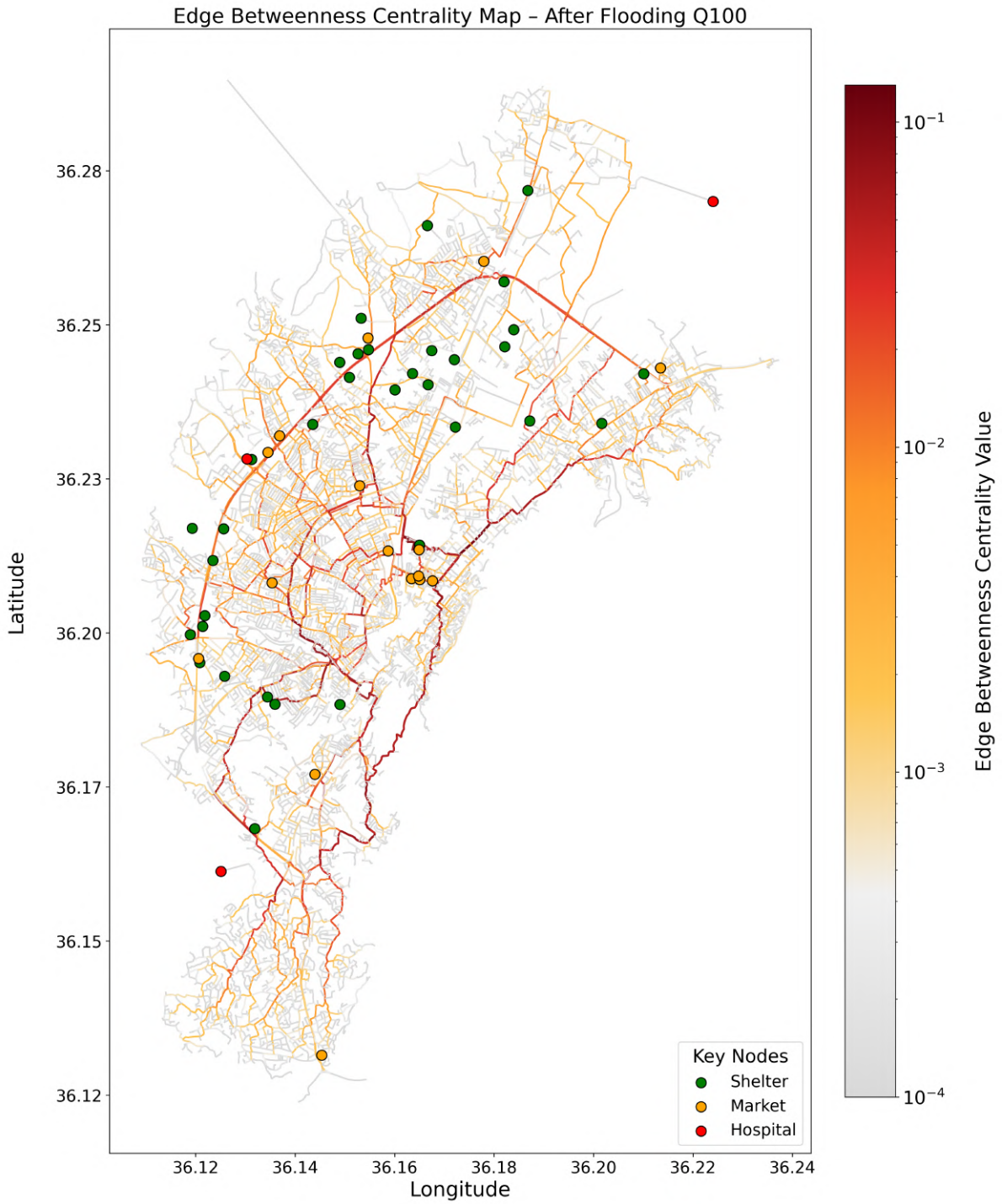

Figure 5.3: Edge betweenness centrality under the Q100 flood scenario.

5.2.2. Centrality of Shelter-to-Service Routes (OD-Based)

This section shifts the focus toward the affected population and their ability to reach essential services during the intermediate recovery phase under multi-hazard conditions. It centers on a subset of Origin-Destination (OD) nodes: shelters as origins, and hospitals and markets as destinations. For each OD pair, shortest paths are calculated and edge betweenness centrality is derived. Unlike the network-wide analysis, this approach highlights only the segments actively used to connect shelters to critical services, revealing key corridors essential for maintaining access during recovery.

The results are presented in Figures 5.4 and 5.5. A logarithmic color scale, ranging from grey to dark red, is applied. It is important to note that the absolute values are relatively low, which reflects the limited number of OD combinations in this focused subset. The key nodes are visualized for reference, aiding interpretation.

A number of distinct corridors emerge from the analysis. One example is the western section of the ring road, which acts as a critical funnel in the baseline, but becomes unused in the flooding scenarios. This aligns with earlier findings in the network-wide analysis, where the western ring road also stood out as a high-centrality corridor. The OD-based comparison confirms its dual importance; not only for general connectivity, but also for targeted access between shelters and services. Other key roads include those linking to the city center. While some of these remain accessible in the flood scenarios, others, particularly in the southern part of the city center, experience visible disruptions.

Compared to the baseline scenario, only minor shifts in OD-based centrality patterns are observed under the Q100 flood scenario. The same segments tend to be used across all intensities, and the overall spatial distribution of centrality remains unchanged. This suggests that while the flood scenarios introduce localized disruptions, they do not drastically alter the structural flow of OD-based travel routes in the network.

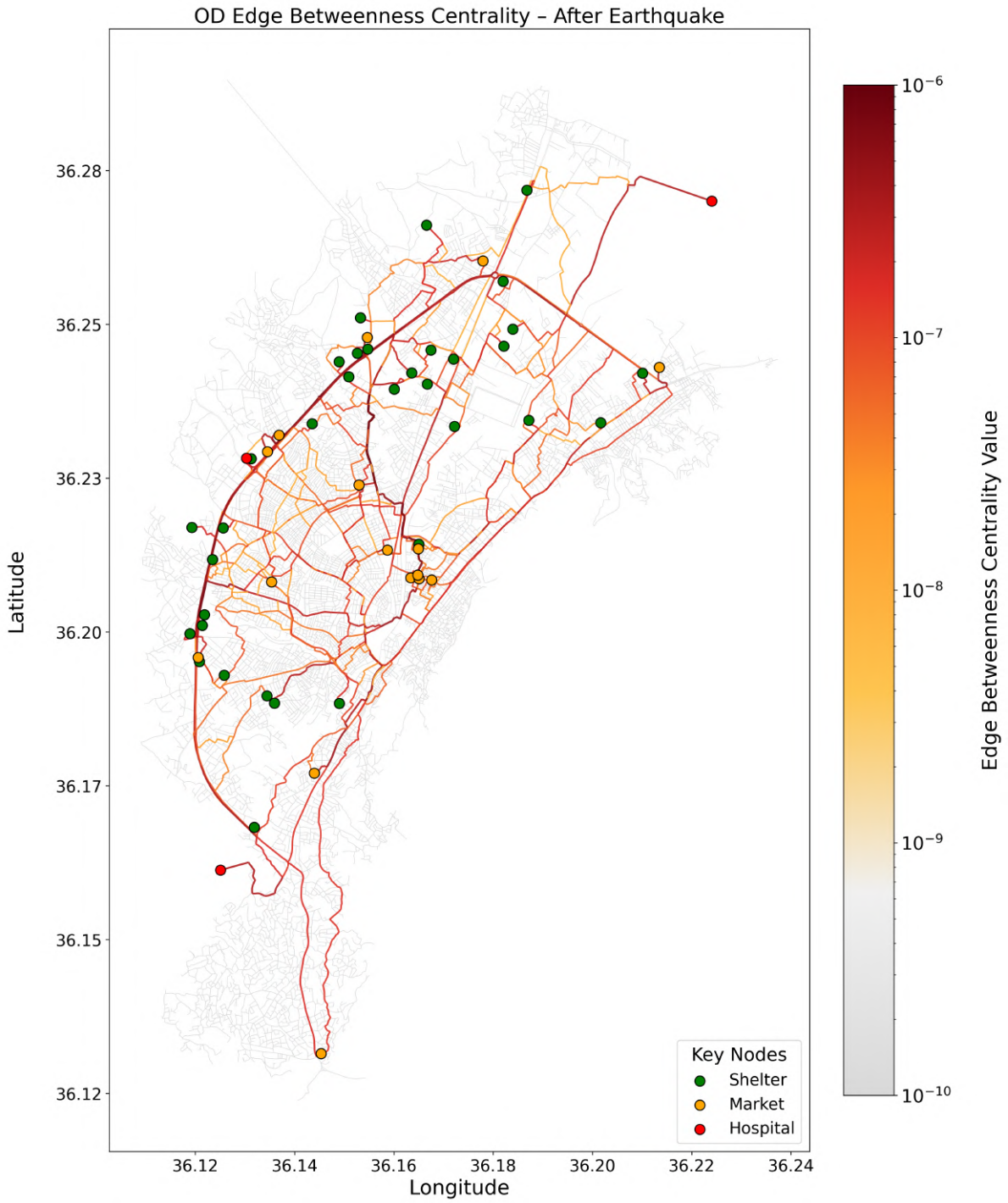

Figure 5.4: Origin–destination edge betweenness centrality under the baseline (post-earthquake) scenario.

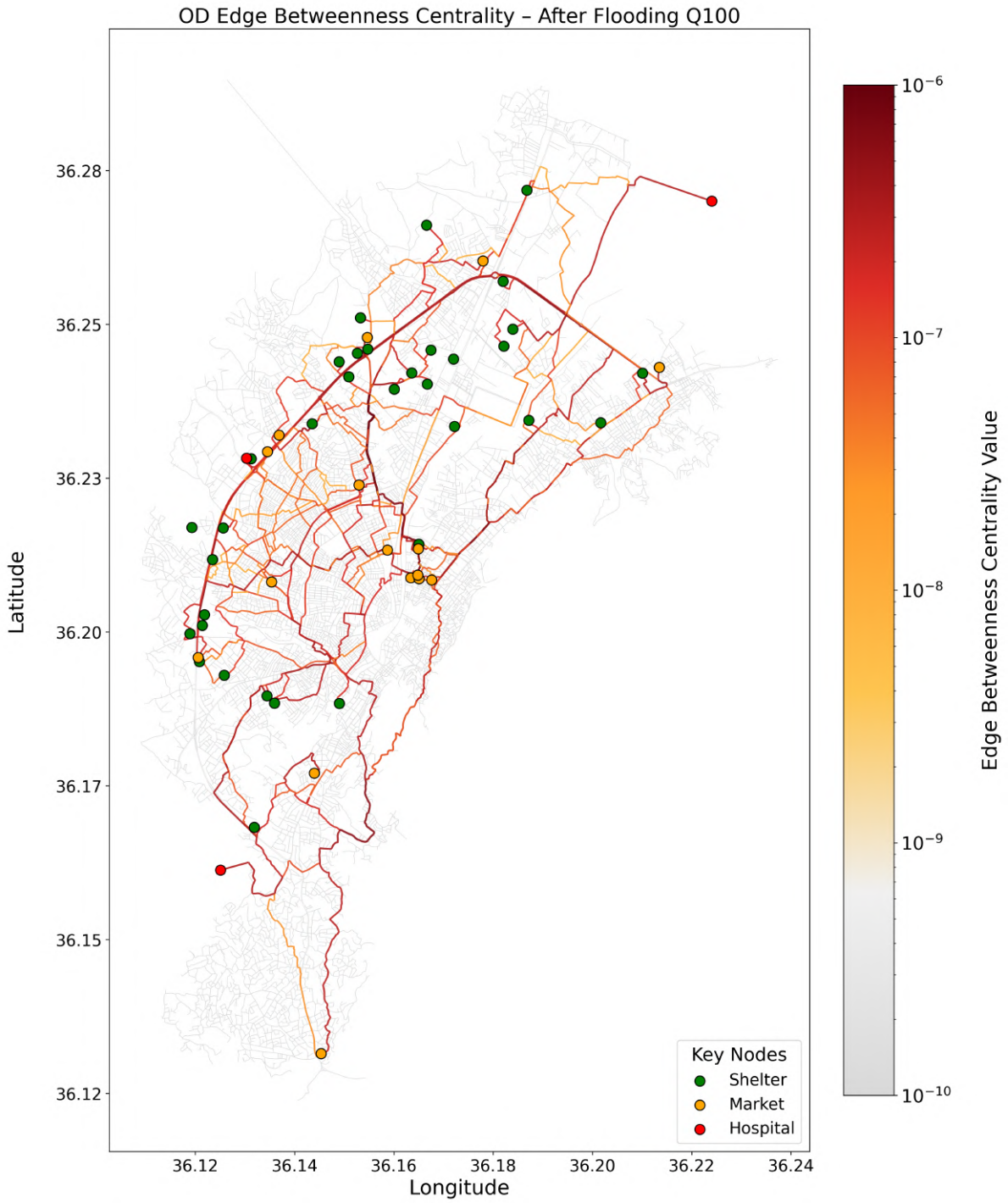

Figure 5.5: Origin–destination edge betweenness centrality under the Q100 flooding scenario.

5.2.3. Changes in Shelter-to-Service Route Centrality

This final part of the analysis narrows in on comparison of the community-oriented Shelter-to-Service (OD-Based) edge betweenness centrality, and compares the post-earthquake baseline with the Q100 flood scenario. To capture these changes, centrality values from the baseline are subtracted from those of each flood scenario. Due to the inherently low values of OD-based centrality, reflecting the limited number of shortest paths between key nodes, the resulting differences are also small, typically ranging from -7×10^{-7} to $+7 \times 10^{-7}$.

The results are presented in Figures 5.6. The observed differences indicate that flooding leads to a negative change in centrality along much of the ring road, particularly near several key nodes. While a few smaller parallel roads show slight increases, these changes are limited. This points to a possible loss of connectivity for certain origin-destination pairs, as some nodes may have become inaccessible under flooded conditions. In and around the city center, shifts in road usage again emerge, indicating changes in route selection. A relatively large increase is visible in the southern parts of the network, potentially reflecting compensatory rerouting away from more affected paths.

Top 30 Roads with Largest Decrease

Figure 5.7 visualizes the 30 road segments that experience the greatest decrease in Shelter-to-Service edge betweenness centrality following the Q100 flooding scenario. The plot is derived from the scenario comparison by ranking segments according to the negative change relative to the baseline (earthquake-only) condition.

The visualization highlights several corridors that serve a important role in maintaining functional connectivity for displaced populations. Notably, several segments in the city center, the main route toward Defne in the south, and the western ring road exhibit losses in centrality. These roads are structurally crucial for connecting shelters to critical services, and their disruption under flood conditions weakens the redundancy and efficiency of the network.

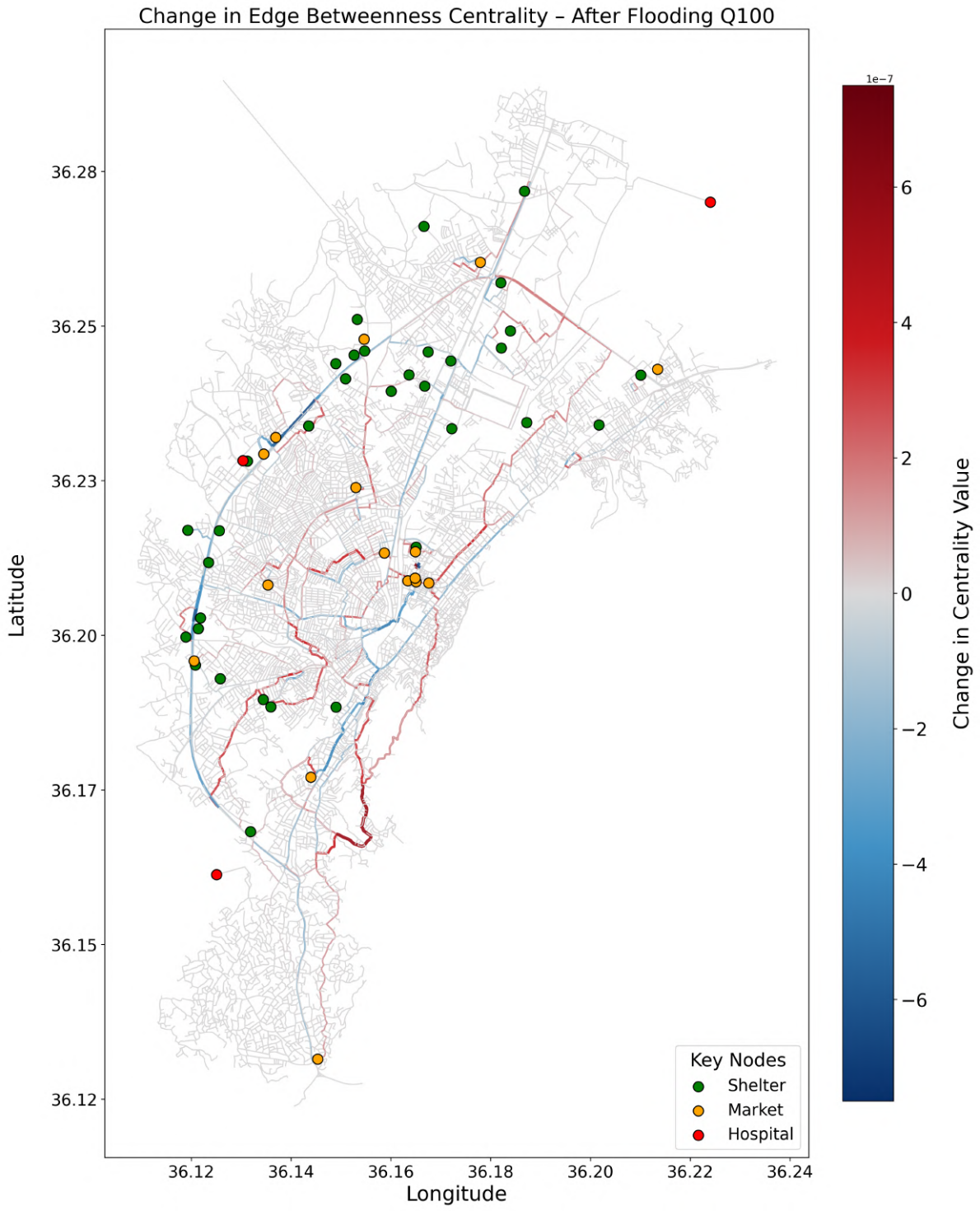

Figure 5.6: Change in Shelter-to-Service edge betweenness centrality between the Q100 flooding scenario and the baseline (post-earthquake) scenario.

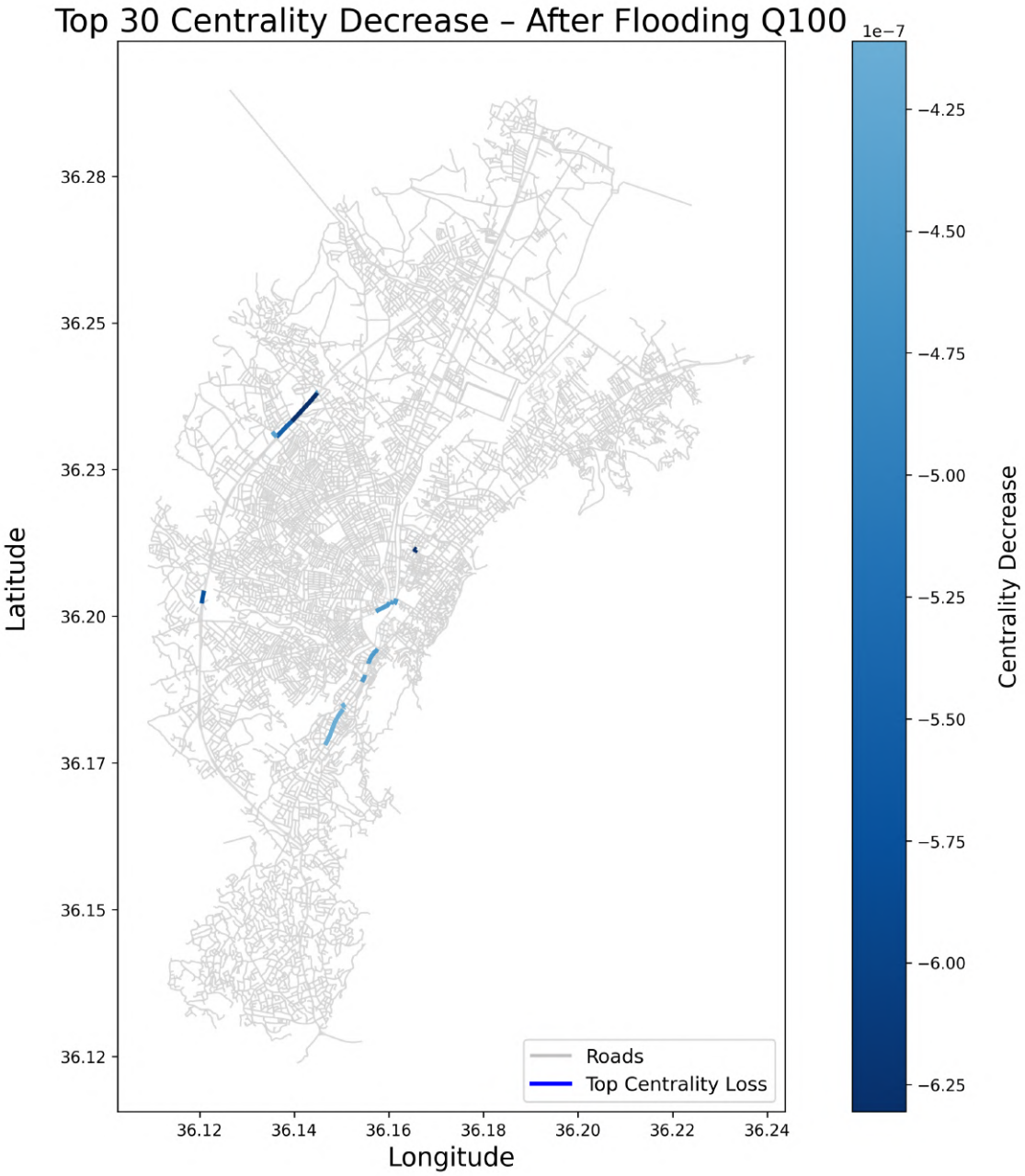

Figure 5.7: Top 30 road segments with the largest decrease in Shelter-to-Service edge betweenness centrality under the Q100 flooding scenario.

5.3. Access to Critical Services from Temporary Shelters

This section analyzes the accessibility from shelters to critical service nodes, namely hospitals and markets. Shortest-path distances were calculated for each origin-destination pair across the baseline and Q100 flooding scenario. The results enable the identification of vulnerable shelters, either due to complete network disconnection or substantial increases in travel distance to essential services.

5.3.1. Distribution of Shelter-to-Service Distances

The exploration of the accessibility results starts with the boxplot shown in Figure 5.8. This figure summarizes the distribution of travel distances from shelters to critical services under different hazard scenarios. For both hospitals and markets, a clear increase in travel distances is observed when comparing the earthquake-only baseline to the Q100 flood scenario. A general widening of the interquartile range is visible across scenarios, indicating that the variability in travel distances to essential amenities increases under flooding conditions. Additionally, a substantial number of outliers can be observed for hospital access, highlighting that certain shelter-to-amenity connections experience high travel distances under all conditions. This suggests that even a single, high-intensity flood scenario (Q100) can substantially disrupt network accessibility. Overall, these results demonstrate that flooding consistently reduces accessibility to both hospitals and markets.

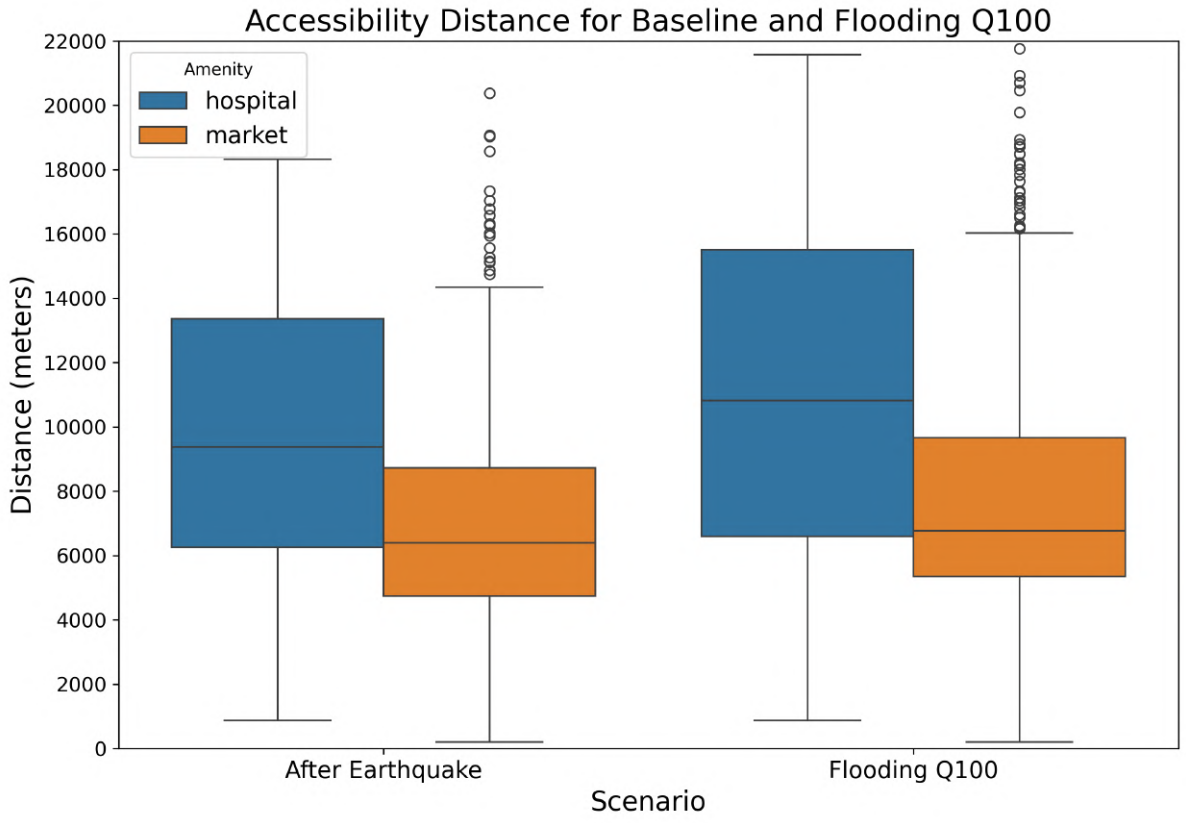

Figure 5.8: Accessibility distances to hospitals and markets under the Q100 flooding scenario.

Building on the first insights, Figures 5.9 and 5.10 present line histograms that further detail the distribution of shelter-to-amenity travel distances under the Q100 flood scenario. The x-axes represent travel distances in meters, grouped into bins of 1000 meters, while the y-axes show the number of origin-destination (OD) pairs falling within each distance bin. Markers are placed at the bin midpoints to enhance clarity. Cumulative lines are included to visualize the total number of OD-pairs reachable within a given distance. To ensure consistency, OD-pairs where the shelter lost access entirely due to flooding are excluded from this analysis.

For hospital accessibility, two major shifts emerge when comparing the baseline scenario to the flood scenario. Between roughly 5,000 and 15,000 meters, more hospitals are accessible in the baseline than under flood conditions. However, beyond 15,000 meters, the trend reverses, with the flood scenarios showing an increase in cumulative accessibility. This indicates that flooding forces shelter populations to travel longer distances to reach healthcare facilities.

In contrast, market accessibility remains relatively stable across both scenarios. Minor differences are visible, particularly within 5,000 meters, where slightly more markets are reachable in the baseline scenario. Flooding conditions shift some trips toward longer distances, resulting in a slightly flatter initial slope of the cumulative curves. Nonetheless, the overall impact on market access is less pronounced than for hospitals.

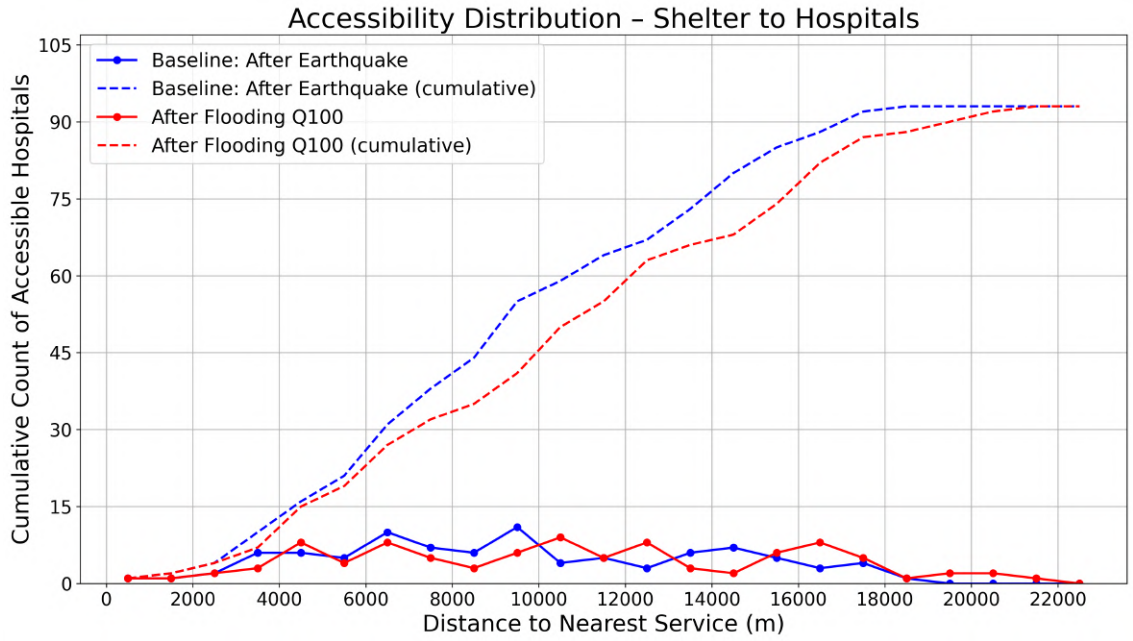

Figure 5.9: Distribution of shelter-to-hospital travel distances under the Q100 flood scenario. The X-axis shows distance bins of 1000 meters.

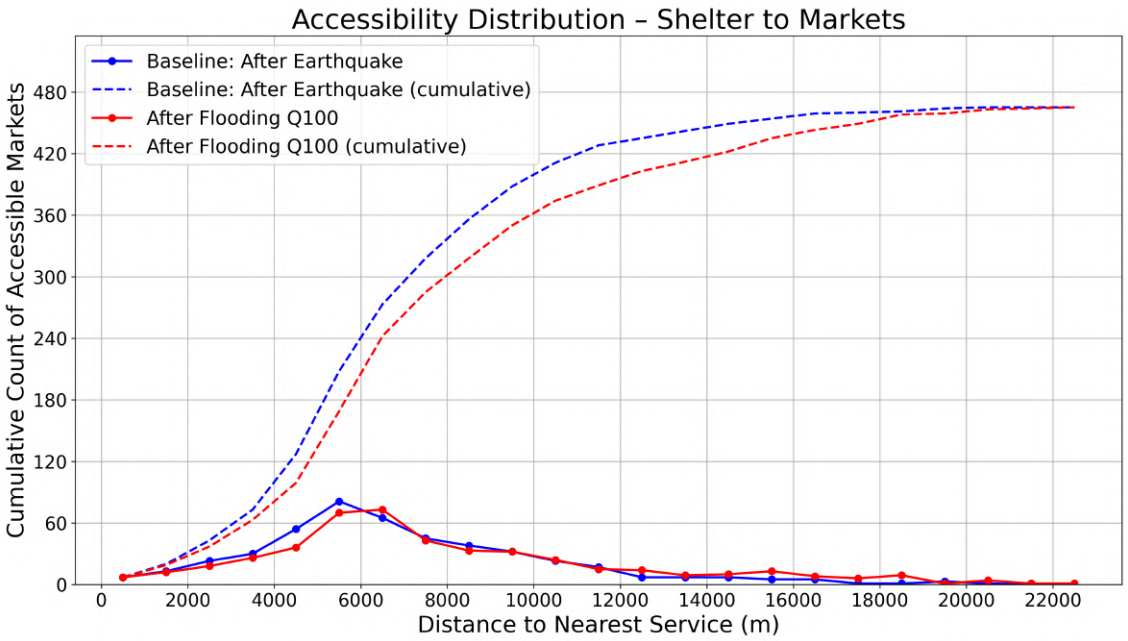

Figure 5.10: Distribution of shelter-to-market travel distances under the Q100 flood scenario. The X-axis shows distance bins of 1000 meters.

5.3.2. Accessibility Losses for Shelter–Amenity Routes

Figure 5.11 visualize the changes in shelter-to-amenity travel distances resulting from different flooding scenarios. Each cell represents a specific origin-destination (OD) pair between a shelter and an amenity (hospital or market). The color intensity indicates the magnitude of the increase in travel distance, with darker shades of red corresponding to greater increases. Cells marked with a cross (X) indicate OD pairs for which no viable route remains after flooding, meaning the location is disconnected from the network.

The accessibility difference map for the Q100 flooding scenario reveal several spatial patterns. Two shelters (3130 and 3148) become completely disconnected from the network, as no path could be found, resulting in a total loss of access to both hospitals and markets. Similarly, one market (3302) is fully isolated. The disconnection of these nodes highlights vulnerabilities within the network, demonstrating how flood events can further isolate already displaced communities and affect their access to essential services.

Across the network, both shelters and amenities experience increases in travel distance under flood conditions. While for many OD-pairs the change remains relatively moderate, several routes exhibit significant increases. Notably, certain markets, such as market 3302 and market 3301, and hospitals like hospital 3297, exhibit a significant decrease in accessibility. Similarly, multiple shelters display significant increases in travel distance, with shelter 3139 standing out. These patterns highlight that while flooding impacts the network broadly, specific origins and destinations are particularly vulnerable to severe disruptions.

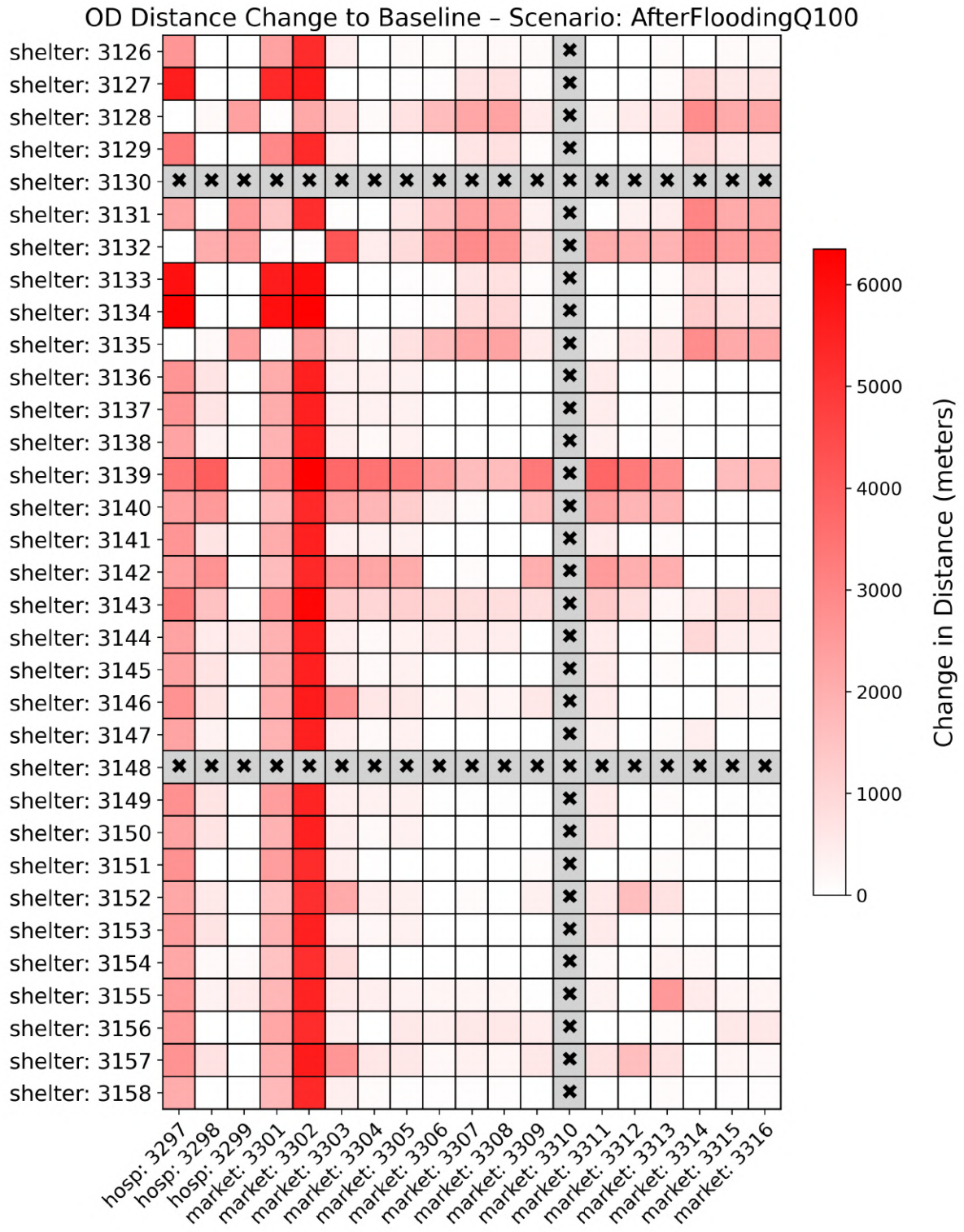

Figure 5.11: Change in shelter-to-amenity distances under the Q100 flooding scenario.

5.3.3. Spatial Distribution of Disconnected or Vulnerable Nodes

Following the identification of changes in accessibility at the OD-pair level, the spatial distribution of these effects across the road network is presented in Figure 5.12. This figure displays the locations of all shelters and amenities, with the top seven shelters and top three amenities from Figure 5.11 highlighted using star markers. Additionally, nodes that have become completely disconnected from the network are marked with crosses.

It is noteworthy that several of the disconnected nodes are situated along the western ring road of Antakya. This road had previously been identified as having a high betweenness centrality, highlighting its importance for the connectivity of the network. However, the disconnection of nodes along this corridor suggests that despite its structural significance, it is vulnerable to complete isolation during flooding.

Furthermore, many of the highlighted nodes experiencing the highest increases in travel distance are concentrated in the southern part of the city. This spatial pattern is consistent with earlier centrality-based vulnerability assessments, which indicated that this area was particularly sensitive to changes in network structure. The observed increases in travel distance confirm that accessibility in this part of Antakya is heavily impacted under the flood scenarios.

In addition, several disconnections and significant changes are observed in the northern part of the city. Although this was recognized to some extent in the earlier centrality analysis, it did not emerge as a particularly critical area at the time. However, the current accessibility results indicate that the northern sector is also substantially affected, revealing a larger-than-expected impact.

Cumulative accessibility Top N shelters

Figure 5.13a shows that, during the Q100 flood scenario, the cumulative number of reachable hospitals increases steadily with distance. All top shelters have access to at least one hospital within approximately 8000 meters. However, accessing additional hospitals requires substantially longer travel distances, with all distances to the second and third hospitals falling above 8500 meters up to 21000 meters. These distances largely lie within the fourth quartile or are classified as outliers, as also observed in Figure 5.8. This distribution indicates that although basic medical access is initially available, broader hospital accessibility requires significantly extended travel.

Figure 5.13b illustrates the cumulative accessibility of markets from the top seven shelters during the Q100 flood scenario. Compared to hospitals, the accessibility to markets shows greater variability across distance. Initially, very few markets are reachable within short distances. A sharp increase in the number of accessible markets occurs between approximately 8000 and 11000 meters, after which most shelters are able to reach the majority of available markets. This indicates that critical shelters are facing significant limitations in accessing basic supplies at short travel distances. These findings highlight an uneven spatial distribution of market accessibility, indicating that shelter populations are often reliant on a small subset of available amenities to meet their basic needs.

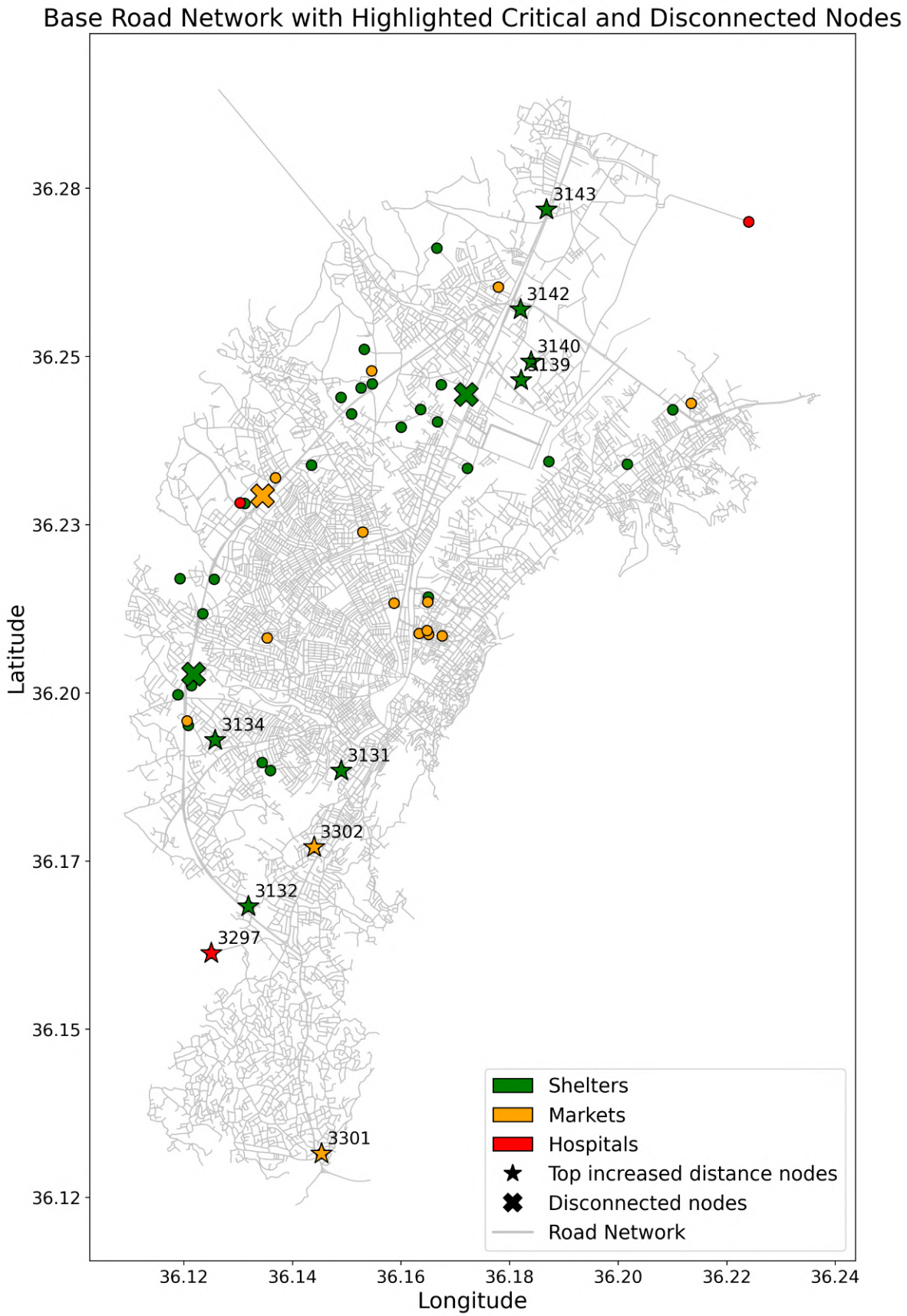

Figure 5.12: Highlighted nodes represent shelters, markets, hospitals with increased travel distance or disconnected under scenario Q100 Flooding.

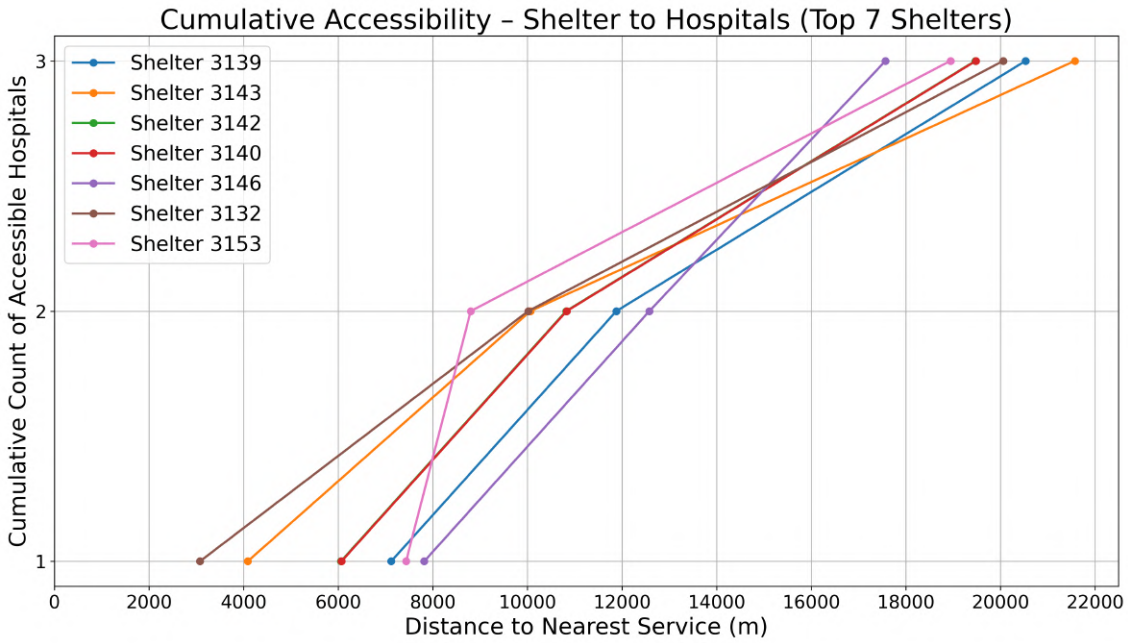

(a) Cumulative accessibility of top 7 shelters to hospitals.

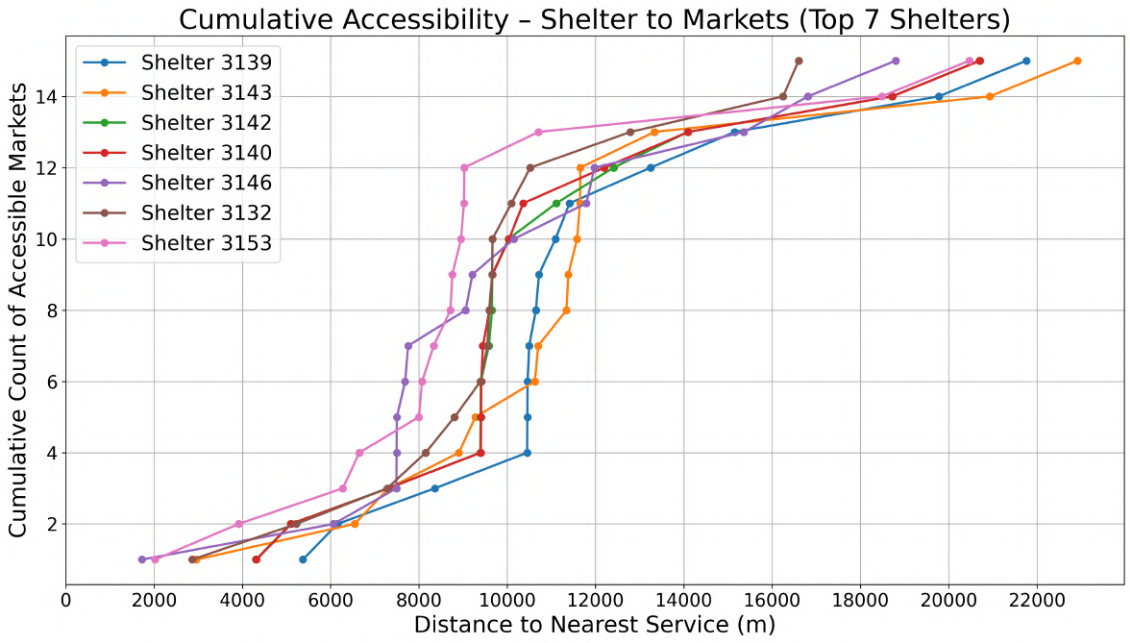

(b) Cumulative accessibility of top 7 shelters to markets.

Figure 5.13: Cumulative accessibility distributions for the top 7 shelters, showing the cumulative count of reachable hospitals (top) and markets (bottom) as a function of travel distance after flooding scenario Q100.

5.4. Disruption of Shelter Flows under Multi-Hazard Conditions

This final section investigates travel disruption by analyzing the flow from shelter locations to essential amenities. The total flow over the road network edges is determined based on the shelter capacities, measured by the number of containers established at each shelter site. This provides an indication of the potential traffic volume generated from each location. Using the resulting flow distribution, it is possible to identify which edges are likely to carry higher traffic volumes in the baseline scenario. The analysis is performed across all flooding scenarios to examine changes in flow patterns and to assess which critical edges, initially characterized by high traffic flow, may lose their functionality due to flooding impacts.

5.4.1. Baseline and Multi-Hazard Scenario Flow Distribution

To start this analysis, the edge flows within the study area are plotted. The results are presented in Figures 5.14 and 5.15, where a red color scale is used to represent traffic flow intensity, with darker red indicating higher flow. The spatial patterns in road usage largely resemble those observed in the OD-edge betweenness centrality analysis, as both measures are based on shortest route calculations. However, it is important to note that while betweenness centrality measures the number of shortest paths passing over an edge, the current analysis colors the edges based on actual traffic flow, resulting in different intensity distributions. Where the centrality analysis evaluates an edge based on its position within the network structure, the flow-based analysis reflects the actual expected use of the network.

In the baseline scenario, two road segments stand out with relatively high traffic flows: one located to the northwest of the city center and another along the adjacent ring road. Compared to the flooding scenarios, only the northwest segment near the center consistently maintains relatively high traffic flow, while flow across other segments becomes more dispersed due to flooding impacts. This redistribution of traffic flows is visible through the broader use of alternative routes in the flooding scenarios, as previously dominant routes lose accessibility and traffic is forced to reroute. Furthermore, there appears to be relatively little difference between the individual flooding scenarios, suggesting that increased rainfall intensity does not significantly alter the overall traffic distribution patterns.

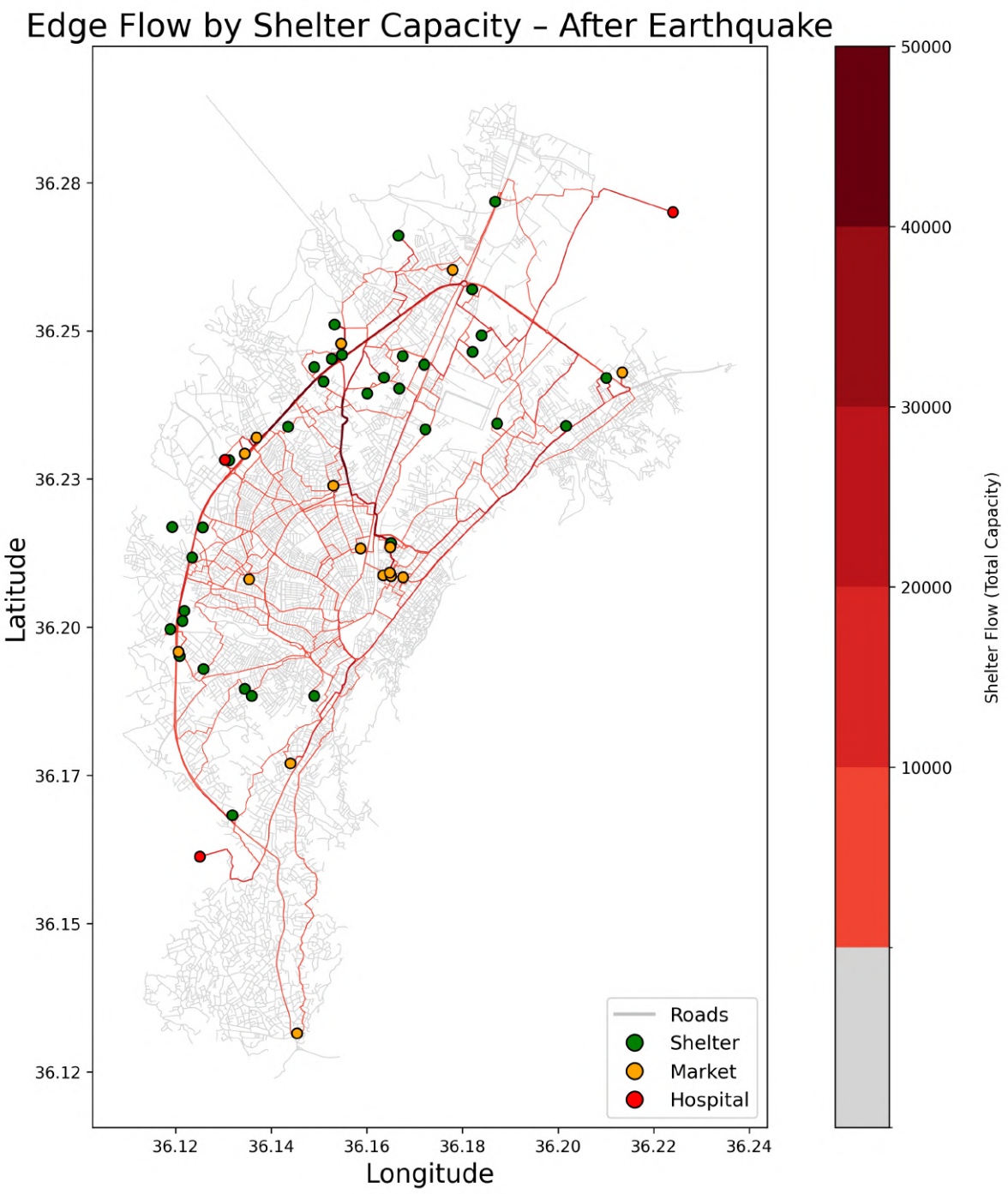

Figure 5.14: Shelter flows under the baseline (post-earthquake) scenario.

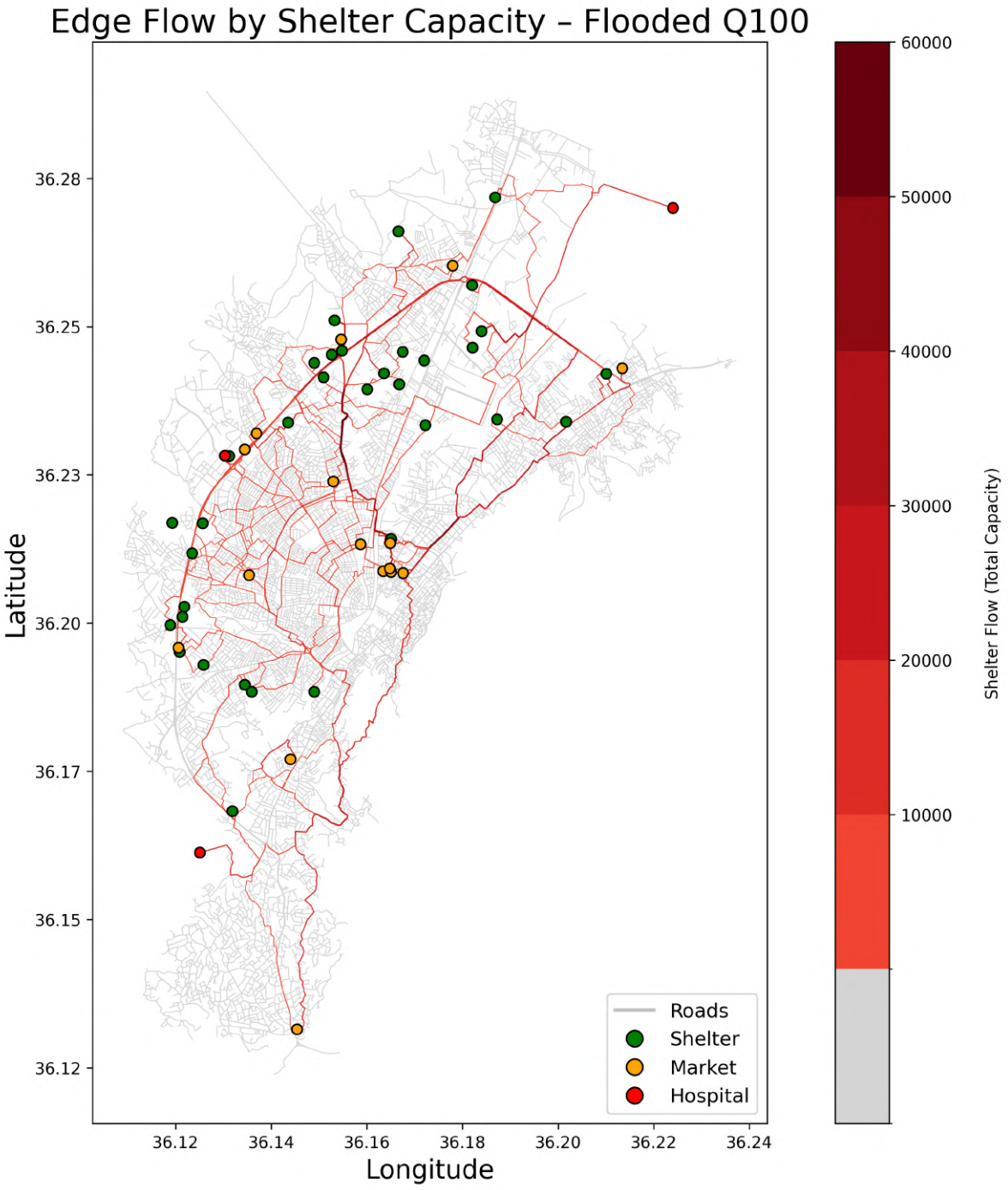

Figure 5.15: Shelter flows under the Q100 flooding scenario.

5.4.2. Flow Loss and Redistribution Due to Flooding

The next step in the analysis evaluates the travel disruption caused by flooding. To assess this, the differences in traffic flows between each flooding scenario and the baseline (post-earthquake) situation are calculated. By highlighting the roads where flow has changed, it becomes possible to identify which segments experience the greatest loss of functionality or are used more intensively due to rerouting.

The results are presented in Figure 5.16, showing the flow differences for the Q100 flooding scenario. In this map, red colors indicate a decrease in flow, often caused by road closures or reduced accessibility, while blue colors indicate an increase in flow as traffic is redistributed over alternative routes. It can be observed that flooding leads to both localized disruptions and broader rerouting effects across the network. Roads near flood-prone areas experience the most significant losses in flow, while surrounding corridors absorb part of the displaced traffic.

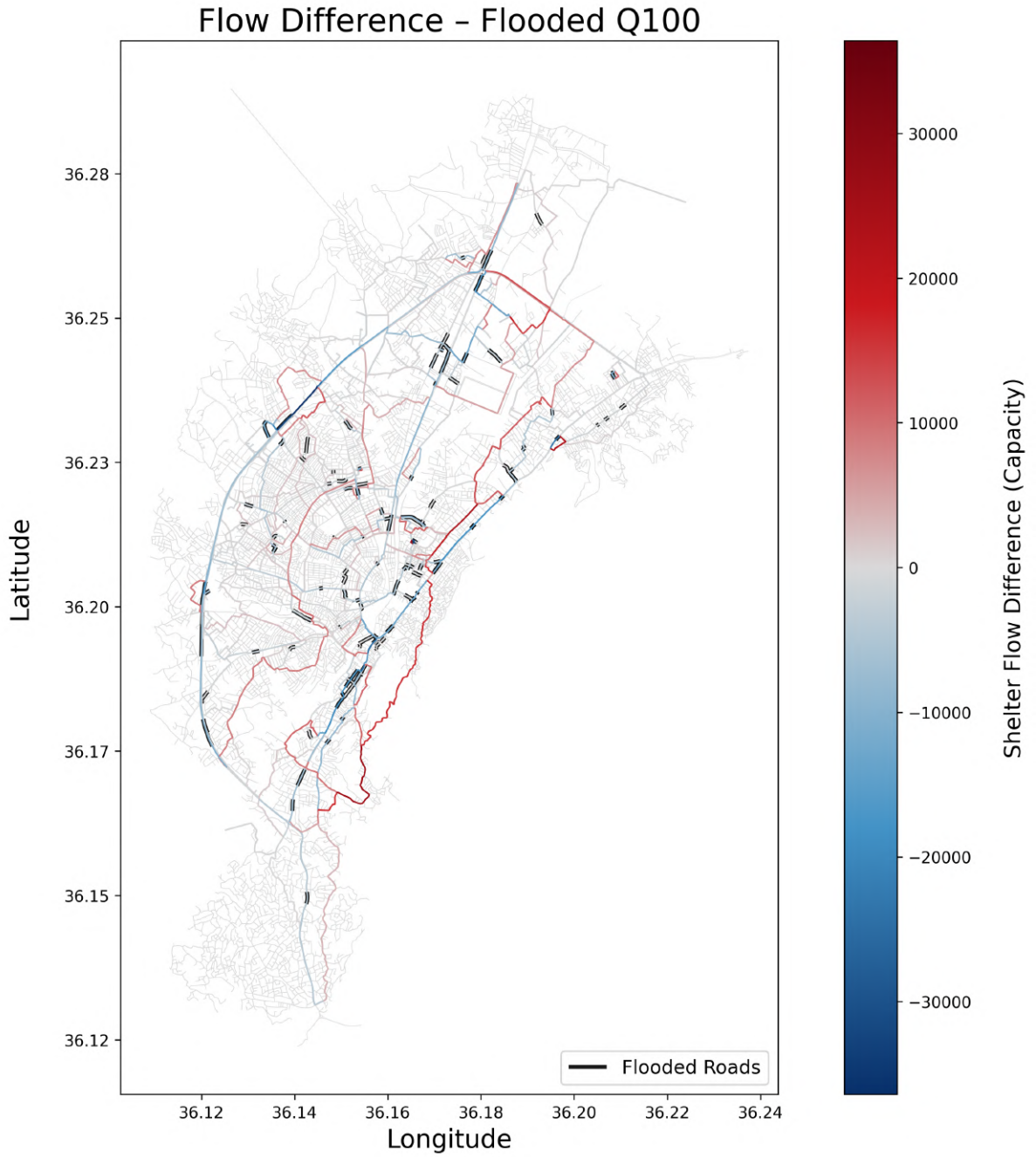

Figure 5.16: Shelter flow difference between the Q100 flooding scenario and the baseline. Blue indicates increased flow (use of alternative routes), and red indicates decreased flow (loss of accessibility).

Top N Flooded Road Q100 Scenario

To analyze which flooded roads contribute most to travel disruption, the impact of the top N flooded road segments under the Q100 scenario is evaluated. Figure 5.17 presents the cumulative travel disruption caused by the top N flooded roads. In the Q100 flooding scenario, a total of 1,576 road segments are flooded, as shown in Table 5.1.

The results reveal that the 30 most critical flooded roads already account for almost 50% of the total cumulative disruption, while the top 100 flooded roads account for 90%. A spatial overview of the top 30 highest-impact roads is provided in Figure 5.18. Interventions on these key segments could significantly reduce overall flow loss, thereby improving accessibility for displaced populations traveling from shelters to essential amenities.

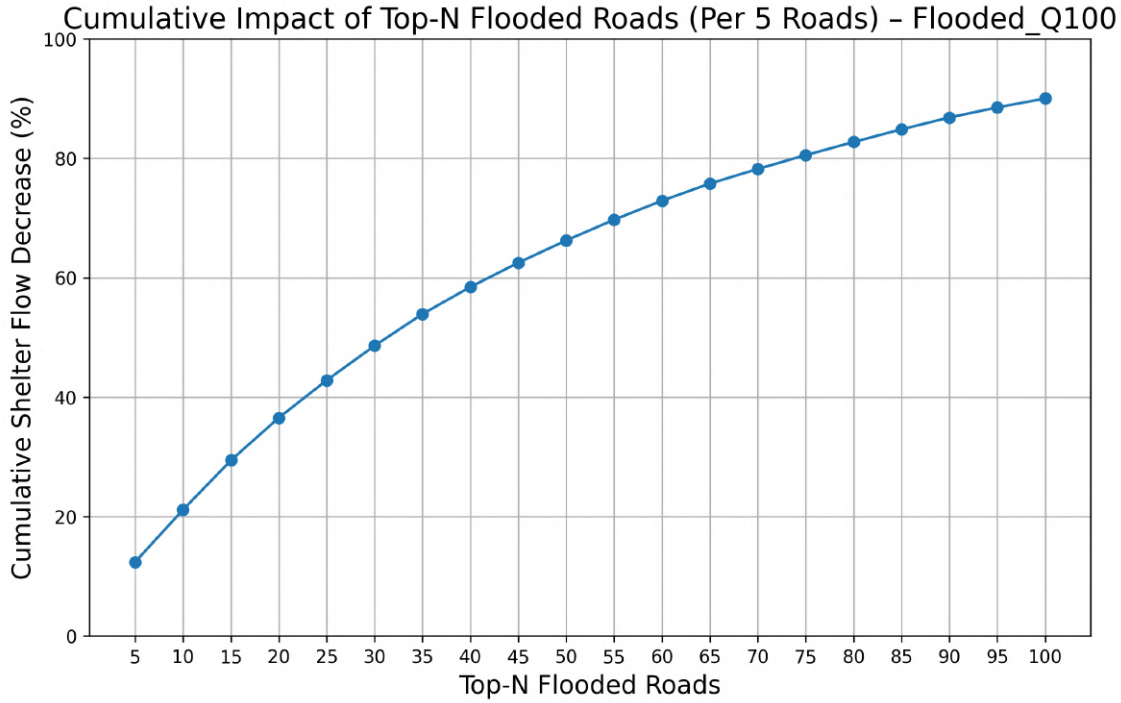

Figure 5.17: Cumulative contribution of the top-N flooded roads to the total shelter flow decrease. Each step represents a bin of five roads.

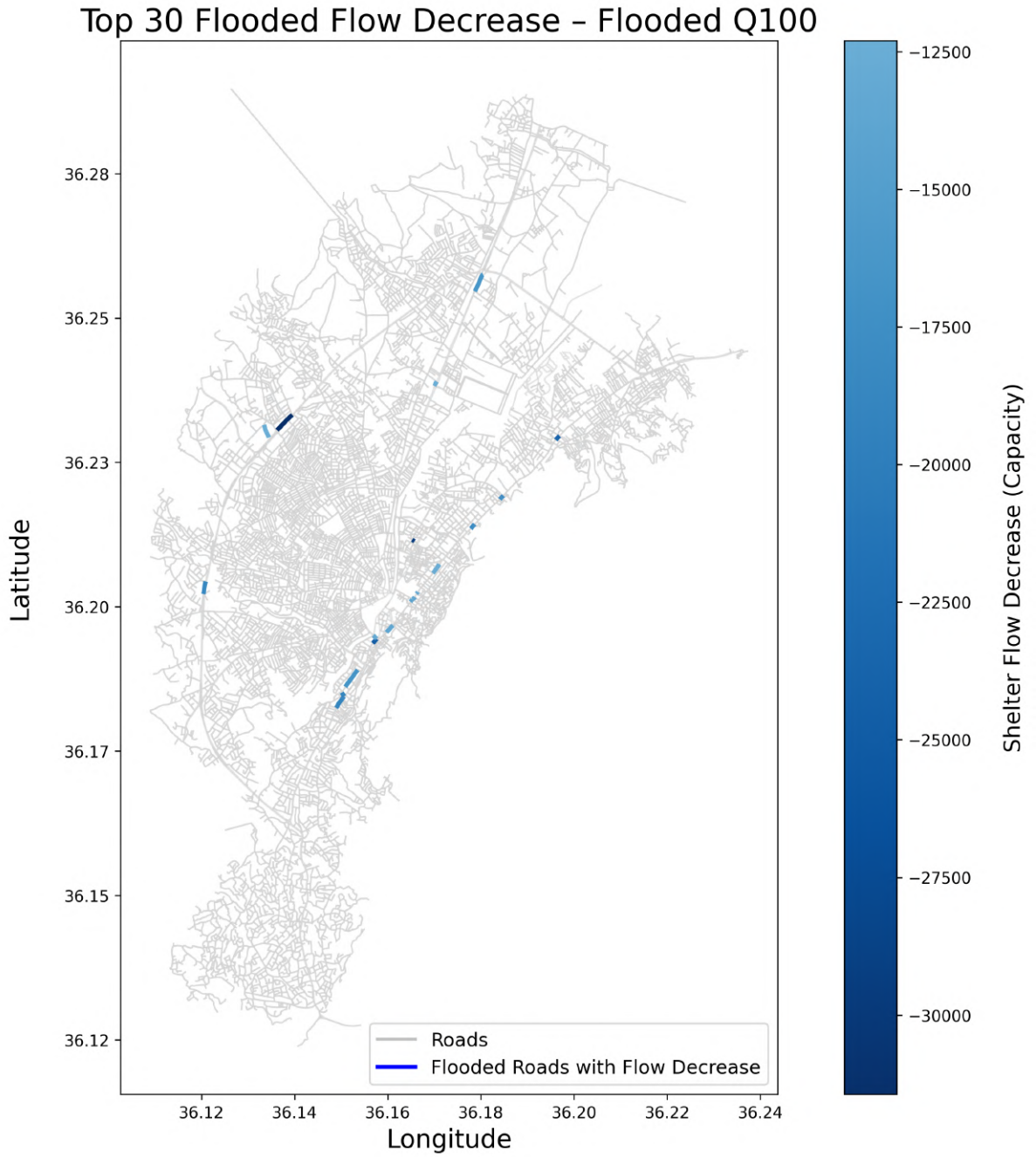

Figure 5.18: Top 30 flooded roads with the highest reduction in Travel Disruption for the Flooded Q100 scenario.

5.5. Summary of the Results

The results from the Antakya case study demonstrate that flooding during the medium-term recovery phase leads to substantial additional disruption of the transport network, beyond the damage caused by the earthquake itself. Although only about 5–6% of road segments become flooded, many of these are situated at structurally critical locations.

The edge betweenness centrality analysis highlights the western ring road, the corridor toward Defne, and the city center as key segments in terms of structural importance. These roads rank among the top segments under normal conditions, but lose their central role during the Q100 flood scenario, forcing many shortest paths to reroute.
Shelter flow results confirm the critical function of these same corridors. The main roads through the city center, toward Defne, the western ring road, and the northern axis carry large cumulative shelter capacities. Under flooding, these flows are rerouted to secondary streets, resulting in longer and more indirect routes across the network.

The accessibility analysis reinforces the spatial patterns found in the other metrics. In Defne, multiple shelters and nearby amenities experience sharp increases in travel distance under flood conditions, and in some cases, access is entirely lost. Similar disruptions occur along the western ring road and in the northern districts, where several key shelter-to-service connections are either severely degraded or completely disconnected. This alignment suggests that these areas not only serve structurally important roles but also contain vulnerable service clusters whose accessibility is particularly sensitive to network disruptions.

Together, the three performance metrics present a consistent yet layered picture of network vulnerability. While they each emphasize similar corridors, such as the western ring road, the route to Defne, and the northern sector, they capture different dimensions of disruption caused by flooding. Centrality points to structural importance, shelter flow reveals functional usage patterns, and accessibility reflects the extent to which access to critical services is compromised. The partial overlap between these metrics, but also noticeable differences, underlines the value of a multi-perspective approach: it enables a more comprehensive understanding of how flood-related disruptions propagate and where recovery planning should prioritize resilience investments.

6

Discussion and Limitations

6.1. Discussion

This research highlights the importance of adopting a multi-hazard perspective in transportation recovery planning. The results demonstrate that flooding substantially worsens network performance in systems already compromised by earthquake damage, particularly by reducing accessibility to critical services and rerouting shelter flows through less optimal corridors.

The betweenness centrality analysis reveals shifts in network reliance, with secondary roads gaining critical importance once primary corridors become disrupted by flooding. This finding aligns with resilience theory, emphasizing the importance of redundancy and robustness for maintaining functionality under disruptive conditions. However, the emergence of new critical links introduces additional vulnerabilities, suggesting that recovery strategies must anticipate and adapt to evolving risks rather than solely restoring pre-disaster conditions.

Results from the accessibility analysis reveal uneven spatial impacts. Communities characterized by limited initial connectivity experienced the most substantial losses in accessibility following flooding events. These findings corroborate existing literature highlighting the spatial inequality inherent to post-disaster recovery. Importantly, they underscore that network resilience is not purely structural, but inherently social: roads serving vulnerable populations require prioritization not only for repair but also for protection against future hazards.

The flow-based analysis further reinforces this point. By quantifying travel flows between shelters and critical services, the analysis identifies road segments supporting the highest movement volumes and, thus, most critical for recovery. Significant flow reductions observed in key corridors during flooding scenarios illustrate that localized flood impacts can lead to broader, network-wide consequences, particularly when baseline capacities are already compromised.

Moreover, the Antakya case study emphasizes how intermediate (mid-term) recovery phases remain particularly susceptible to compounded risks. While immediate emergency response may restore partial functionality, this transitional phase often lacks sufficient robustness against further disruptions. This supports recent literature advocating more adaptive, phase-specific recovery strategies. Unlike long-term reconstruction plans, which generally prioritize durability and sustained resilience, intermediate recovery efforts must effectively balance speed, flexibility, and hazard awareness.

Finally, the proposed modeling framework demonstrates how multi-hazard scenarios can be operationalized by integrating network theory and flood modeling. Although the applied approach involves simplifications, it delivers actionable insights and provides a methodological basis that can readily be extended to address additional hazard combinations (e.g., landslides, aftershocks, or heatwaves). Furthermore, this approach facilitates comparative analyses across different time frames or geographical contexts, enabling identification of both universal patterns and location-specific vulnerabilities.

6.2. Limitations

This study has several limitations that should be considered when interpreting its results. While the model provides valuable insights supporting resilient recovery planning, it relies on assumptions and simplifications inherent to any modeling approach. Although such abstractions are necessary for managing analytical complexity, their influence on outcomes must be recognized when drawing conclusions and making policy recommendations.

Earthquake and flood impacts are modeled using static input data, specifically, post-earthquake damage records and simulated flooding maps. Road accessibility after earthquakes is determined by damage categories translated into assumed accessibility scores. Although structured and transparent, this approach simplifies real-world damage patterns and omits localized variability. Similarly, the flood modeling assumes fully impermeable surfaces and lacks temporal dimensions, thus not accounting for dynamic processes such as changing water levels, infiltration, or drainage. These simplifications may result in over- or underestimations of flooding impacts, potentially misrepresenting accessibility losses.

Furthermore, the network model excludes certain functional road characteristics such as capacity, speed limits, and hierarchical road classifications. Shelter flows are represented as static proxies for actual mobility demand, and travel routes are determined based on shortest-path algorithms alone. Consequently, the analysis neglects real-world travel behavior, including route choice under uncertainty, congestion, and alternative route usage. These omissions limit the model's capacity to accurately reflect operational complexities within disrupted transportation systems.

Finally, the analysis focuses exclusively on static snapshots of the intermediate recovery phase, not capturing the inherently dynamic nature of post-disaster recovery. Infrastructure conditions,

accessibility requirements, and population needs typically evolve over time. Additionally, the model does not consider behavioral adaptations to disruptions, such as risk perception-driven route adjustments, reliance on informal transportation options, or responses to real-time information. These adaptive behaviors significantly influence actual community movement patterns and should be integrated into future research frameworks.

7

Conclusion & Policy Recommendations

Despite increasing recognition of the importance of resilient disaster recovery, the intermediate recovery phase remains vulnerable and insufficiently addressed in current research. Existing studies predominantly focus on either immediate emergency response or long-term reconstruction, often overlooking compounded impacts resulting from multi-hazard conditions during intermediate recovery periods. This research addressed this gap by examining how combined earthquake and flooding impacts affect transportation networks during mid-term recovery, guided by the following research question:

How can mid-term recovery be modeled to evaluate and enhance transportation network resilience under multi-hazard conditions in earthquake-affected communities?

Recovery plans that incorporate potential multi-hazard conditions aim to restore transportation networks and communities while accounting for additional vulnerabilities posed by subsequent disasters. Enhancing resilience requires that essential amenities and shelter sites remain functional and accessible throughout the recovery process. Achieving this calls for the explicit integration of multi-hazard risk assessments into recovery planning frameworks.

To support multi-hazard recovery planning, this research developed a modeling framework integrating network theory and flood analysis to assess transportation network performance during intermediate recovery phases. The framework was informed by an illustrative case study of Antakya, Türkiye, where severe earthquakes were followed by significant flooding in 2023. Utilizing graph theory, the tool simulates network disruption, evaluates accessibility to critical amenities, and incorporates flooding data to capture cascading impacts. Three performance metrics derived from this model directly support targeted interventions and informed decision-making during mid-term recovery.

The three performance metrics applied in this study were selected based on established measures

in the literature and provide complementary insights into network resilience under multi-hazard conditions. The first metric captures structural importance through edge betweenness centrality, identifying road segments that are critical for maintaining overall connectivity. These segments help prevent fragmentation and can be prioritized in recovery planning. The second assesses accessibility, measuring changes in shortest path distances between shelters and essential services such as hospitals and markets. This highlights areas where displaced populations are most at risk of losing access to critical amenities. The third metric captures the functional impact of flooding by overlaying shelter flow data with flood exposure, identifying which flooded road segments interrupt the highest volumes of movement. Shelter flow is computed by distributing the container capacity of each shelter across shortest-path routes to all service nodes, assigning proportional flow to each road segment based on its routing frequency. Reopening these key corridors would yield the greatest improvements in mobility and service accessibility. Together, these metrics offer a multi-dimensional perspective on both network-wide vulnerabilities and location-specific access constraints under multi-hazard conditions, supporting more targeted and informed decisions during the intermediate recovery phase.

Key Findings from the Antakya Case Study

The findings from the Türkiye case study reveal that flooding events further deteriorate network functionality in the mid-term recovery phase following an earthquake.

In the southern part of Antakya, particularly the Defne district, flooding renders the main access corridor impassable, as indicated by the network centrality analysis. This results in significant network fragmentation, forcing shortest paths to reroute via secondary roads. Although Defne contains relatively few shelters and amenities, the accessibility metric shows that those present experience the largest reductions in accessibility under flood conditions. Due to the low concentration of amenities and shelters, this vulnerability is less visible in the flow disruption metric. Nonetheless, the area's reliance on a small number of secondary access routes increases the risk of isolation for displaced populations.

In and around the city center, especially along the western ring road, where most shelters and amenities are located, flooding affects several main road segments. The flow disruption metric shows that this leads to a redistribution of shelter flows onto nearby secondary routes. While accessibility losses in terms of travel distance remain relatively modest, these disruptions still have a substantial impact on overall mobility patterns. Targeting recovery efforts at these key segments, particularly along the western corridor, would therefore offer considerable gains in accessibility and prevent major disruptions to the mobility of a large share of the affected population.

The results also highlight the corridor extending from the city center toward the northern part of Antakya as a highly critical section of the network. A shelter located along this route becomes completely disconnected under flooding conditions, according to the accessibility analysis. Flood simulations confirm that large portions of this corridor are inundated, rendering them unusable for shortest-path travel. In addition to this isolated shelter, several other nearby

amenities and shelters along the same corridor face the largest increases in travel distance across the study area. This spatial concentration of disruption highlights how localized flooding can cause large accessibility losses, particularly in areas with limited network redundancy.

Finally, the results demonstrate that an increase in flooding intensity (Q25, Q50, Q100 scenarios) does not necessarily lead to a proportional increase in the number of impacted road segments. Instead, specific corridors consistently emerge as critical across scenarios, emphasizing that vulnerability is highly spatially concentrated. This suggests that targeted recovery efforts focused on a limited number of key corridors could substantially improve community accessibility, regardless of the severity of the flooding.

Closing Perspective
This developed tool, combining road network and flood models with decision attributes, provides insights into the effects of additional flooding during the mid-term recovery phase. By capturing key elements of this recovery phase in the modeling process, the tool identifies vulnerable roads, shelters, and amenities, thereby supporting more resilient recovery planning and highlighting where interventions are needed to minimize cascading impacts. Integrating such multi-hazard insights into recovery efforts can help ensure that critical amenities and the transportation corridors connecting them remain accessible during future hazard events. This need is clearly illustrated by the observation that several shelter and market locations are currently situated in high flood-risk areas, exposing displaced populations to renewed disruptions during recovery.

7.1. Policy Recommendations

To enhance disaster recovery in urban areas, policymakers are advised to adopt an integrated, multi-hazard perspective, particularly during the mid-term recovery phase, when communities are most vulnerable to additional risks. The findings of this research illustrate how flood hazards, when layered on top of existing earthquake damage, can severely disrupt transportation access and affect already displaced populations from critical services.

A first step is to prioritize the protection and reinforcement of critical transportation corridors, and to establish redundant access routes for essential amenities. As demonstrated in the Antakya case study, the disruption of just a few key road segments, such as those along the western ring road or the Defne corridor, can result in major network fragmentation and loss of accessibility. Reinforcing these vulnerable segments and developing nearby secondary alternatives can greatly enhance system robustness and prevent isolation during multi-hazard events.

Furthermore, it is essential to strategically review the location of critical amenities, including shelters, hospitals, and markets, from a multi-hazard perspective. The analysis showed that several of the amenities in Antakya were placed in areas highly exposed to flooding, rendering them inaccessible. Strategic placement or protective measures are necessary to ensure that these amenities remain operational and reachable during compounding disasters.

Finally, recovery frameworks should be updated to integrate multi-hazard risk assessments into design standards. Instead of prioritizing infrastructure based solely on its pre-disaster functionality, restoration time, or resource availability, recovery planning should also integrate multi-hazard risk considerations to ensure long-term resilience. This forward-looking approach increases not only robustness and redundancy, but also the system's capacity for rapid and adaptive recovery.

By providing insights into critical corridors, amenity vulnerabilities, and hazard-exposed segments, the developed tool supports more informed decisions on protection of critical roads, strategic amenity placement, and multi-hazard resilient design. In doing so, the tool offers policymakers clear insights through its decision attributes, helping them to identify critical areas, understand the spatial dynamics of vulnerability, and make more informed recovery choices under multi-hazard conditions.

7.2. Scientific Contribution

This research addresses two key gaps in the field of disaster resilience: the limited attention to the intermediate recovery phase and the absence of multi-hazard perspectives in post-disaster infrastructure planning.

The first contribution lies in centering the intermediate recovery phase, a period between emergency response and long-term reconstruction that remains understudied. Although this phase is marked by heightened vulnerability and critical decisions, it is often overlooked in both academic and practical frameworks. This study develops a method specifically tailored to this phase, enabling analysis of transportation network performance when systems are partially restored but still exposed to risk. By doing so, it captures the distinct conditions and planning needs that characterize this transitional period.

The second contribution is the integration of a multi-hazard perspective into recovery modeling. Existing studies predominantly focus on single hazards, failing to account for how one disaster may compound the effects of another. This research incorporates both earthquake and flood impacts into a single framework, using a network-based approach to assess their combined influence on accessibility and mobility. This allows for more realistic modeling of cascading disruptions and highlights how secondary hazards can undermine recovery efforts.

Together, these contributions offer a modeling framework for analyzing urban transportation resilience under compound risk. The framework operationalizes recovery assessment beyond the immediate aftermath and provides tools for evaluating system performance when exposed to multiple hazards. This supports a shift toward more robust, scenario-informed recovery strategies, addressing critical blind spots in current resilience planning.

7.3. Future Research

This research developed a tool that integrates road network and flood modeling to support decision-making during mid-term recovery under multi-hazard conditions. While the tool provides useful insights, several directions for future research could help improve and extend its application.

To start, it could be interesting to explore how a tool like this can be used in practice. Investigating how decision attributes align with existing policy frameworks or disaster coordination structures would be valuable for translating technical results into real-world decisions. This line of research could help operationalize the tool in institutional settings and enhance its practical relevance for mid-term recovery planning.
Furthermore, the scope of the tool could be expanded. While it currently focuses primarily on socio-economic factors, future research could expand its scope by incorporating integrated socio-environmental data. This would allow decision-makers to consider both the social vulnerability of communities and the ecological sensitivity of areas exposed to hazard impacts, such as floodplains or erosion-prone zones.

Beyond tool development and application, future research could also address more fundamental aspects of multi-hazard recovery planning. For instance, studies could investigate how to optimize the prioritization of road repairs by incorporating multi-hazard vulnerability into decision-making. While current approaches often focus on factors such as repair time, resource availability, or pre-disaster importance, future research could examine whether including additional hazard risk leads to more resilient or effective recovery outcomes.
Another interesting direction is the incorporation of dynamic flow modeling under multi-hazard conditions. Displacement following a disaster significantly alters mobility patterns throughout the city. Capturing how these flows evolve over time could improve the understanding of shifting accessibility needs and provide a more realistic perspective on recovery dynamics.

References

ACAPS. (2023, May). Briefing note: Türkiye - earthquake and flooding impact in hatay province [Retrieved April 17, 2025]. https://reliefweb.int/report/turkiye/acaps-briefing-note-turkiye-earthquake-and-flooding-impact-hatay-province-02-may-2023

AFAD. (2023). TADAS. https://tadas.afad.gov.tr/map

AFAD. (2024). Republic of türkiye disaster and emergency management authority [Accessed: 27 May 2025].

Akram, S., Baloch, M. Y. J., Alrefaei, A. F., Almutairi, M. H., Idrees, M., & Al-Kubaisi, H. A. R. A. (2024). Interface between mental health and the earthquake: considering humanitarian endeavor. *Frontiers in Public Health*, *12*. https://doi.org/10.3389/fpubh.2024.1326407

Alisjahbana, I., Ceferino, L., & Kiremidjian, A. (2022). Prioritized reconstruction of healthcare facilities after earthquakes based on recovery of emergency services. *Risk Analysis*, *43*(9), 1763–1778. https://doi.org/10.1111/risa.14076

Alizadeh, H., Sharifi, A., & Damanbagh, S. (2024). Assessing Urban Resilience to Pandemics with a Hybrid Framework of Planning, Absorption, Recovery, and Adaptation Abilities: A Case Study of Ahvaz, Iran. *International Journal of Disaster Risk Reduction*, *108*, 104573. https://doi.org/10.1016/j.ijdrr.2024.104573

Almeida, L. S., Goerlandt, F., & Pelot, R. (2022). Trends and gaps in the literature of road network repair and restoration in the context of disaster response operations. *Socio-Economic Planning Sciences*, *84*, 101398. https://doi.org/10.1016/j.seps.2022.101398

Arcaya, M., Raker, E. J., & Waters, M. C. (2020). The Social Consequences of Disasters: individual and community change. *Annual Review of Sociology*, *46*(1), 671–691. https://doi.org/10.1146/annurev-soc-121919-054827

Aydin, N. Y., Duzgun, H. S., Heinimann, H. R., Wenzel, F., & Gnyawali, K. R. (2018). Framework for improving the resilience and recovery of transportation networks under geohazard risks. *International Journal of Disaster Risk Reduction*, *31*, 832–843. https://doi.org/10.1016/j.ijdrr.2018.07.022

Balstrøm, T., & Crawford, D. (2018). Arc-Malstrøm: A 1D hydrologic screening method for stormwater assessments based on geometric networks. *Computers & Geosciences*, *116*, 64–73. https://doi.org/10.1016/j.cageo.2018.04.010

Boakye, J., Guidotti, R., Gardoni, P., & Murphy, C. (2021). The role of transportation infrastructure on the impact of natural hazards on communities. *Reliability Engineering & System Safety*, *219*, 108184. https://doi.org/10.1016/j.ress.2021.108184

Bodenstein, M., & Scaramucci, M. (2025). On the gdp effects of severe physical hazards. *European Economic Review*, 105019. https://doi.org/10.1016/j.euroecorev.2025.105019

Borzenkova, O. (2023, April). Health Needs in Türkiye Remain High Two Months after the Earthquakes. https://www.iom.int/news/health-needs-turkiye-remain-high-two-months-after-earthquakes

Boyd, A., Hokanson, J., Johnson, L., Schwab, J., & Topping, K. (2014). Planning for post-disaster recovery: Next generation. *APA Planning Advisory Service Reports*, 1–197.

Brake, H. T., Dückers, M., De Vries, M., Van Duin, D., Rooze, M., & Spreeuwenberg, C. (2009). Early psychosocial interventions after disasters, terrorism, and other shocking events: Guideline development. *Nursing and Health Sciences*, *11*(4), 336–343. https://doi.org/10.1111/j.1442-2018.2009.00491.x

Bruneau, M., Chang, S. E., Eguchi, R. T., Lee, G. C., O'Rourke, T. D., Reinhorn, A. M., Shinozuka, M., Tierney, K., Wallace, W. A., & Von Winterfeldt, D. (2003). A framework to quantitatively assess and enhance the seismic resilience of communities. *Earthquake Spectra*, *19*(4), 733–752. https://doi.org/10.1193/1.1623497

Canterbury Earthquake Recovery Authority. (2012). *Recovery Strategy for Greater Christchurch Mahere Haumanutanga o Waitaha* (tech. rep.). https://www.greaterchristchurch.org.nz/assets/Documents/greaterchristchurch/recovery-strategy-for-greater-christchurch-Copy2.pdf

Çelik, M., Ergun, Ö., & Keskinocak, P. (2015). The Post-Disaster Debris Clearance problem under incomplete information. *Operations Research*, *63*(1), 65–85. https://doi.org/10.1287/opre.2014.1342

Chowdhury, J., Scarr, S., & Arranz, A. (2023). How search and rescue teams pull survivors from the rubble after earthquakes. https://www.reuters.com/graphics/EARTHQUAKE-RESCUE/mopajqojmva/

Cluster, G. S. (2021). *Disaster Shelter Projects 9th Edition Case Study A.17 / Indonesia 2021 / Earthquake* (tech. rep.). https://shelterprojects.org/shelterprojects9/A.17-Indonesia-SP9.pdf

Contreras, D. (2016). Fuzzy boundaries between Post-Disaster phases: the case of L'Aquila, Italy. *International Journal of Disaster Risk Science*, *7*(3), 277–292. https://doi.org/10.1007/s13753-016-0095-4

Copernicus. (2024). Copernicus GLO-30 Digital Elevation Model. https://portal.opentopography.org/raster?opentopoID=OTSDEM.032021.4326.3

Dahiphale, D. (2023). Mapreduce for graphs processing: New big data algorithm for 2-edge connected components and future ideas. https://doi.org/10.36227/techrxiv.21802102

Davidson, H. (2025). Tibet earthquake: rescuers search for survivors after powerful quake kills 126. https://www.theguardian.com/world/2025/jan/08/tibet-earthquake-rescuers-search-for-survivors-shigatse

De Ruiter, M. C., Couasnon, A., Van Den Homberg, M. J. C., Daniell, J. E., Gill, J. C., & Ward, P. J. (2020). Why we can no longer ignore consecutive disasters. *Earth s Future*, *8*(3). https://doi.org/10.1029/2019ef001425

Demiroz, F., & Haase, T. W. (2018). The concept of resilience: a bibliometric analysis of the emergency and disaster management literature. *Local Government Studies*, *45*(3), 308–327. https://doi.org/10.1080/03003930.2018.1541796

Di Ludovico, D., D'Ovidio, G., & Santilli, D. (2019). Post-earthquake reconstruction as an opportunity for a sustainable reorganisation of transport and urban structure. *Cities*, *96*, 102447. https://doi.org/10.1016/j.cities.2019.102447

Drakes, O., & Tate, E. (2022). Social vulnerability in a multi-hazard context: a systematic review. *Environmental Research Letters*, *17*(3), 033001. https://doi.org/10.1088/1748-9326/ac5140

Faturechi, R., & Miller-Hooks, E. (2014). Measuring the Performance of Transportation Infrastructure Systems in Disasters: A Comprehensive review. *Journal of Infrastructure Systems*, *21*(1). https://doi.org/10.1061/(asce)is.1943-555x.0000212

Federal Emergency Management Agency (FEMA). (2023, September). National Disaster Recovery Framework. https://www.fema.gov/emergency-managers/national-preparedness/frameworks/recovery

Graveline, M.-H., & Germain, D. (2022). Disaster Risk Resilience: conceptual evolution, key issues, and opportunities. *International Journal of Disaster Risk Science*, *13*(3), 330–341. https://doi.org/10.1007/s13753-022-00419-0

Grounds, M. A., LeClerc, J. E., & Joslyn, S. (2017). Expressing Flood Likelihood: Return Period versus Probability. *Weather Climate and Society*, *10*(1), 5–17. https://doi.org/10.1175/wcas-d-16-0107.1

Hakami, A., Kumar, A., Shim, S., & Nahleh, Y. (2013). Application of soft systems methodology in solving disaster emergency logistics problems. *World Academy of Science, Engineering and Technology International Journal of Industrial Science and Engineering*, *7*, 786–790.

Hassan, E. M., & Mahmoud, H. (2020). An integrated socio-technical approach for post-earthquake recovery of interdependent healthcare system. *Reliability Engineering & System Safety*, *201*, 106953. https://doi.org/10.1016/j.ress.2020.106953

Hatay Planning Center. (n.d.). Planlama Merkezi [Retrieved April 14, 2025]. https://hatayplanlamamerkezi.com/tr-TR/projects/plan/1

HDX. (2025, February). Turkey Buildings (OpenStreetMap Export) | Humanitarian Dataset | HDX. https://data.humdata.org/dataset/hotosm_tur_buildings

Hernantes, J., Rich, E., Laugé, A., Labaka, L., & Sarriegi, J. M. (2013). Learning before the storm: Modeling multiple stakeholder activities in support of crisis management, a practical case. *Technological Forecasting and Social Change*, *80*(9), 1742–1755. https://doi.org/10.1016/j.techfore.2013.01.002

Hosseini, S., Barker, K., & Ramirez-Marquez, J. E. (2015). A review of definitions and measures of system resilience. *Reliability Engineering and System Safety*, *145*, 47–61. https://doi.org/10.1016/j.ress.2015.08.006

Huq, M. E., Sarker, M. N. I., Prasad, R., Kormoker, T., Hossain, M. A., Rahman, M. M., & Al Dughairi, A. A. (2021). Resilience for disaster management: Opportunities and challenges. In G. M. M. Alam, M. O. Erdiaw-Kwasie, G. J. Nagy, & W. Leal Filho (Eds.), *Climate vulnerability and resilience in the global south: Human adaptations for sustainable futures* (pp. 425–442). Springer International Publishing. https://doi.org/10.1007/978-3-030-77259-8_22

Ingram, J. C., Franco, G., Rio, C. R.-D., & Khazai, B. (2006). Post-disaster recovery dilemmas: challenges in balancing short-term and long-term needs for vulnerability reduction. *Environmental Science & Policy*, *9*(7-8), 607–613. https://doi.org/10.1016/j.envsci.2006.07.006

Irvem, A., & Topaloğlu, F. (2012). Identification of flood risk area in the orontes river basin, turkey, using multi-criteria decision analyses.

İrvem, A., Dağ, İ., & Özbuldu, M. (2024). Flood analysis using the hec-ras software for antakya altınçay creek. *Mustafa Kemal University Journal of Agricultural Sciences*, *29*(3), 912–924. https://doi.org/10.37908/mkutbd.1507564

Iskandar, R., Tfaily, B. A., Cornou, C., Bard, P.-Y., Guillier, B., Harb, J., Lacroix, P., Adjizian-Gérard, J., Beck, E., Dugdale, J., Salameh, C., Saliba, N., & Zaarour, R. (2023). Estimating urban seismic damages and debris from building-level simulations: application to the city of Beirut, Lebanon. *Bulletin of Earthquake Engineering*, *21*(13), 5949–5990. https://doi.org/10.1007/s10518-023-01768-x

Jha, A. K. (2010, January). *Safer homes, stronger communities*. World Bank Publications.

Joyal, B. (2019, March). How to fix an earthquake in four days - Alaska Business Magazine. https://www.akbizmag.com/industry/construction/how-to-fix-an-earthquake-in-four-days/

Khazai, B., Anhorn, J., & Burton, C. G. (2018). Resilience Performance Scorecard: Measuring urban disaster resilience at multiple levels of geography with case study application to Lalitpur, Nepal. *International Journal of Disaster Risk Reduction*, *31*, 604–616. https://doi.org/10.1016/j.ijdrr.2018.06.012

Kovacevic, B. T. (n.d.). Turkey earthquake: How do search and rescue teams save people? https://www.bbc.com/news/world-64569943

Kramer, M., Terheiden, K., & Wieprecht, S. (2016). Safety criteria for the trafficability of inundated roads in urban floodings. *International Journal of Disaster Risk Reduction*, *17*, 77–84. https://doi.org/10.1016/j.ijdrr.2016.04.003

Laino, E., & Iglesias, G. (2024). Multi-hazard assessment of climate-related hazards for European coastal cities. *Journal of Environmental Management*, *357*, 120787. https://doi.org/10.1016/j.jenvman.2024.120787

Lee, R., White, C. J., Adnan, M. S. G., Douglas, J., Mahecha, M. D., O'Loughlin, F. E., Patelli, E., Ramos, A. M., Roberts, M. J., Martius, O., Tubaldi, E., Van Den Hurk, B., Ward, P. J., & Zscheischler, J. (2023). Reclassifying historical disasters: From single to multi-hazards. *The Science of The Total Environment*, *912*, 169120. https://doi.org/10.1016/j.scitotenv.2023.169120

Leobons, C. M., Campos, V. B. G., & De Mello Bandeira, R. A. (2019). Assessing Urban Transportation Systems Resilience: A Proposal of Indicators. *Transportation research procedia*, *37*, 322–329. https://doi.org/10.1016/j.trpro.2018.12.199

Li, S., Ma, Z., & Teo, K. L. (2020). A new model for road network repair after natural disasters: Integrating logistics support scheduling with repair crew scheduling and routing

activities. *Computers & Industrial Engineering*, *145*, 106506. https://doi.org/10.1016/j.cie.2020.106506

Linkov, I., & Kott, A. (2018, May). *Fundamental Concepts of Cyber Resilience: Introduction and Overview*. https://doi.org/10.1007/978-3-319-77492-3_1

MacDonald, C., Davies, B., Johnston, D. M., Paton, D., Malinen, S., Näswall, K., Kuntz, J., & Stevenson, J. R. (2015, January). *A framework for exploring the role of business in community recovery following disasters*.

McGee, M. (2018). Post-earthquake road repairs are almost complete - but they're only temporary. https://www.adn.com/alaska-news/2018/12/11/post-earthquake-road-repairs-are-almost-complete-but-theyre-only-temporary/

Meyers, T. (2021, December). Three years after a massive earthquake, restoring health care in Indonesia. https://www.directrelief.org/2021/11/three-years-after-a-massive-earthquake-restoring-health-care-in-indonesia/

Ministry of Civil Defence & Emergency Management. (2005, February). *Resilient New Zealand: A Aotearoa manahau - Focus on Recovery: A Holistic Framework for Recovery in New Zealand* (tech. rep.). https://www.civildefence.govt.nz/assets/Uploads/documents/publications/guidelines/information-series/is-05-05-focus-on-recovery.pdf

Nain, A., Jain, D., Gupta, S., & Kumar, A. (2023). Improving first responders' effectiveness in Post-Disaster scenarios through a hybrid framework for damage assessment and prioritization. *Global Journal of Flexible Systems Management*, *24*(3), 409–437. https://doi.org/10.1007/s40171-023-00346-z

Newman, M. E. J. (2003). The structure and function of complex networks. *SIAM Review*, *45*(2), 167–256. https://doi.org/10.1137/s003614450342480

Nishino, T., Tanaka, T., & Hokugo, A. (2012). An evaluation method for the urban post-earthquake fire risk considering multiple scenarios of fire spread and evacuation. *Fire Safety Journal*, *54*, 167–180. https://doi.org/10.1016/j.firesaf.2012.06.002

OCHA. (2023a, March). Türkiye earthquakes recovery and reconstruction assessment - Türkiye. https://reliefweb.int/report/turkiye/turkiye-earthquakes-recovery-and-reconstruction-assessment

OCHA. (2023b, April). Türkiye Earthquakes Situation Report IV (04.04.2023) - Türkiye. https://reliefweb.int/report/turkiye/turkiye-earthquakes-situation-report-iv-04042023

OpenStreetMap. (2024). Openstreetmap [Accessed: 14 November 2024].

Pal, S. C., Saha, A., Chowdhuri, I., Ruidas, D., Chakrabortty, R., Roy, P., & Shit, M. (2022). Earthquake hotspot and coldspot: Where, why and how? *Geosystems and Geoenvironment*, *2*(1), 100130. https://doi.org/10.1016/j.geogeo.2022.100130

Pan, S., Yan, H., He, J., & He, Z. (2021). Vulnerability and resilience of transportation systems: A recent literature review. *Physica A Statistical Mechanics and its Applications*, *581*, 126235. https://doi.org/10.1016/j.physa.2021.126235

Perrucci, D., & Baroud, H. (2020). A review of temporary housing management modeling: Trends in design strategies, optimization models, and decision-making methods. *Sustainability*, *12*, 10388. https://doi.org/10.3390/su122410388

Platt, S., Brown, D., & Hughes, M. (2016). Measuring resilience and recovery. *International Journal of Disaster Risk Reduction*, *19*, 447–460. https://doi.org/10.1016/j.ijdrr.2016.05.006

Platt, S., Gautam, D., & Rupakhety, R. (2020). Speed and quality of recovery after the Gorkha Earthquake 2015 Nepal. *International Journal of Disaster Risk Reduction*, *50*, 101689. https://doi.org/10.1016/j.ijdrr.2020.101689

Rezapour, S., Naderi, N., Tajik, N., & Rezapourbehnagh, S. (2018). Optimal deployment of emergency resources in sudden onset disasters. *International Journal of Production Economics*, *204*, 365–382. https://doi.org/10.1016/j.ijpe.2018.08.014

Smith, G. P., & Wenger, D. (2007, January). *Sustainable Disaster recovery: Operationalizing an existing agenda*. https://doi.org/10.1007/978-0-387-32353-4\{_}14

Testa, A. C., Furtado, M. N., & Alipour, A. (2015). Resilience of Coastal Transportation Networks Faced with Extreme Climatic Events. *Transportation Research Record Journal of the Transportation Research Board*, *2532*(1), 29–36. https://doi.org/10.3141/2532-04

The National Academy of Sciences. (2012). *Disaster resilience: A national imperative*. The National Academies Press. https://doi.org/10.17226/13457

TU Delft. (n.d.). MSC EPA. https://www.tudelft.nl/en/student/faculties/tpm-student-portal/education/master/msc-epa

United Nations. (2015, September). *Transforming our world: the 2030 Agenda for Sustainable Development* (tech. rep.). https://documents.un.org/doc/undoc/gen/n15/291/89/pdf/n1529189.pdf?token=exP5O3VFkmCQRzcTZw&fe=true

United Nations Development Programme (UNDP). (2008, February). *UNDP policy on early recovery* (tech. rep.).

United Nations Development Programme (UNDP). (2023, August). Six months after the earthquakes in Türkiye. https://www.undp.org/turkiye/publications/Six-months-after-the-earthquakes-in-Turkiye

United Nations Office for the Coordination of Humanitarian Affairs (OCHA). (2023). Türkiye: Earthquake response 2023 – hatay humanitarian snapshot (08 june 2023) [Retrieved April 16, 2025]. https://reliefweb.int/report/turkiye/turkiye-earthquake-response-2023-hatay-humanitarian-snapshot-08-june-2023

Ward, P. J., Daniell, J., Duncan, M., Dunne, A., Hananel, C., Hochrainer-Stigler, S., Tijssen, A., Torresan, S., Ciurean, R., Gill, J. C., Sillmann, J., Couasnon, A., Koks, E., Padrón-Fumero, N., Tatman, S., Lund, M. T., Adesiyun, A., Aerts, J. C. J. H., Alabaster, A., . . . De Ruiter, M. C. (2022). Invited perspectives: A research agenda towards disaster risk management pathways in multi-(hazard-)risk assessment. *Natural hazards and earth system sciences*, *22*(4), 1487–1497. https://doi.org/10.5194/nhess-22-1487-2022

World Health Organisation. (2024, December). Dealing with the psychological aftershocks of the Türkiye earthquakes: why mental health and psychosocial support are so desperately needed. https://www.who.int/europe/news-room/09-03-2023-dealing-with-the-psychological-aftershocks-of-the-t-rkiye-earthquakes--why-mental-health-and-psychosocial-support-are-so-desperately-needed

World Health Organization. (2024). Ensuring continuity of essential health services post-earthquake in West Nepal. https://www.who.int/nepal/news/detail/16-04-2024-ensuring-continuity-of-essential-health-services-post-earthquake-in-west-nepal

Wu, Y., & Chen, S. (2023). Traffic resilience modeling for post-earthquake emergency medical response and planning considering disrupted infrastructure and dislocated residents. *International Journal of Disaster Risk Reduction*, *93*, 103754. https://doi.org/10.1016/j.ijdrr.2023.103754

Xie, W., Rose, A., Li, S., He, J., Li, N., & Ali, T. (2018). Dynamic Economic Resilience and Economic Recovery from Disasters: A Quantitative Assessment. *Risk Analysis*, *38*(6), 1306–1318. https://doi.org/10.1111/risa.12948

Yu, Y.-C., & Gardoni, P. (2021). Predicting road blockage due to building damage following earthquakes. *Reliability Engineering & System Safety*, *219*, 108220. https://doi.org/10.1016/j.ress.2021.108220

Zamanifar, M., & Hartmann, T. (2021). Decision attributes for disaster recovery planning of transportation networks; A case study. *Transportation Research Part D Transport and Environment*, *93*, 102771. https://doi.org/10.1016/j.trd.2021.102771

Zeil, P. (2014). Myths and realities about the recovery of L'Aquila after the earthquake. *International Journal of Disaster Risk Reduction*, *8*, 125–142. https://doi.org/10.1016/j.ijdrr.2014.02.001

Zscheischler, J., Martius, O., Westra, S., Bevacqua, E., Raymond, C., Horton, R. M., Van Den Hurk, B., AghaKouchak, A., Jézéquel, A., Mahecha, M. D., Maraun, D., Ramos, A. M., Ridder, N. N., Thiery, W., & Vignotto, E. (2020). A typology of compound weather and climate events. *Nature Reviews Earth & Environment*, *1*(7), 333–347. https://doi.org/10.1038/s43017-020-0060-z

A

Mapping Shelter and Amenity Locations

This appendix describes the process used to map and georeference the shelter and amenity locations, in preparation for their integration into the urban network model. It outlines the methods applied in QGIS to spatially align the images with real-world coordinates and to extract point locations for further analysis.

A.1. Mapping Shelter locations

The shelter locations used in this research were obtained from KMZ files provided by N.Y. Aydin. These KMZ files were imported into QGIS to spatially map the shelters within the Area of Interest (AOI). A spatial filter was applied to select only the shelters located within the AOI boundaries. The filtered points were then merged into a single GeoPackage (GPKG) file for further analysis.

The imported KMZ data, visualized in Figure A.1, displays the shelter locations as points on an OpenStreetMap background. Shelter locations were represented as points without exact addresses, suitable for spatial selection.

While the shelter locations themselves were already accurately mapped, the associated shelter capacity information was not correctly imported. To address this, the KMZ files were loaded into Google Earth, where the shelter capacities were manually extracted and added to the attribute table in QGIS. The final dataset allowed for analysis using the shelter location and capacity during the intermediate recovery phase.

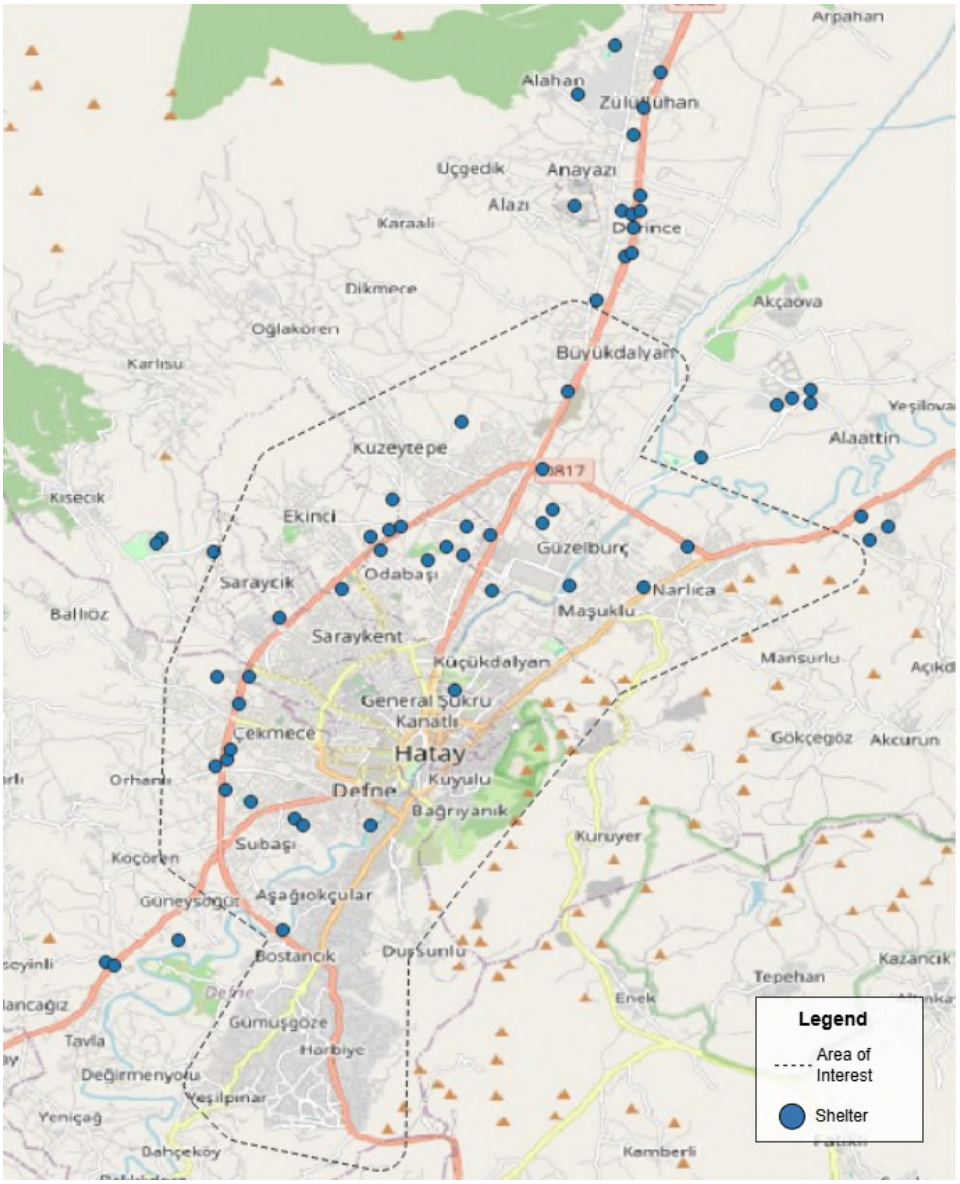

Figure A.1: Visualization of shelter locations imported from KMZ on an OpenStreetMap background in QGIS.

A.2. Georeferencing and Mapping Amenity locations

Figure A.2 shows the images used for this process, obtained from Hatay Planning Center (n.d.). Panel (a) displays the coordinated marketplace locations within Antakya and Defne after the 2023 earthquake, while panel (b) shows the health facilities active during the same period.

The images were first imported into QGIS, after which a georeferencing process was performed. Known geographic coordinates were assigned to several recognizable landmarks visible on both the images and the base maps. A minimum of four ground control points (GCPs) were selected per image to ensure accurate spatial alignment, using a polynomial transformation method. The georeferencing was conducted within the WGS 84 coordinate reference system (EPSG:4326).

After georeferencing, a new point layer was created in QGIS. The amenity locations were manually digitized by placing points at the corresponding positions visible on the georeferenced images. These points were then saved as a shapefile, enabling their use in the network accessibility and recovery analysis.

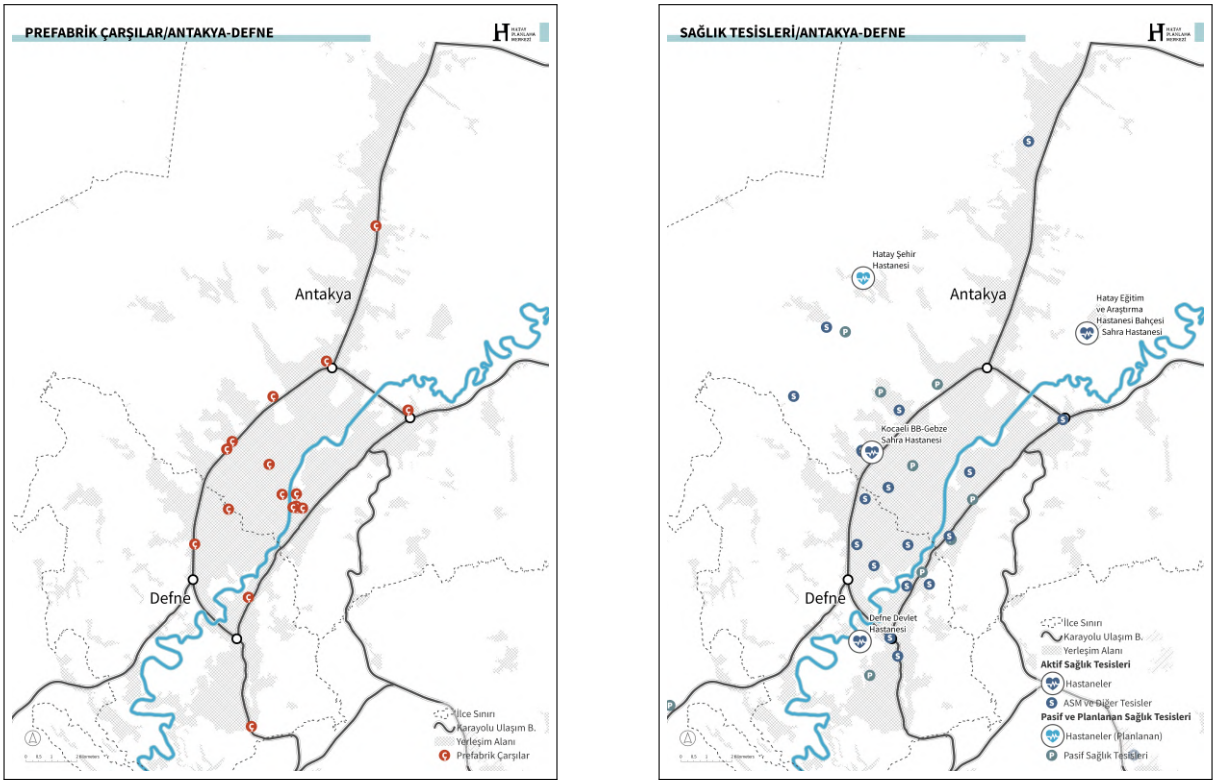

(a) Locations of the coordinated marketplaces within Antakya & Defne after the 2023 earthquake.

(b) Locations of the health facilities within Antakya & Defne after the 2023 earthquake.

Figure A.2: Images for georeferencing and mapping of critical amenities in QGIS (Hatay Planning Center, n.d.).

B

Results Q25 and Q50 Flooding Scenario

This appendix presents the results of the Q25 and Q50 flood scenarios for the core components of the three network performance metrics: edge betweenness centrality, accessibility to critical services, and shelter-based flow patterns. These outputs provide a reference for comparison with the main analysis in Chapter 5, which focused on the baseline and Q100 scenarios. The figures included here allow for an initial assessment of how varying flood intensities affect the structure and function of the transport network. However, more in-depth analyses, such as OD-based centrality shifts, quantified accessibility losses, and critical link identification, are reserved for the Q100 scenario and are discussed in the main text.

Arc-Malstrøm Flood Results

The maps in Figure B.1 and B.2 show the flooded road segments under the Q25 and Q50 scenarios, along with the locations of shelters and essential services. Although only a small share of the total road network becomes inundated, the flooded segments often intersect with critical areas, including corridors near shelters and essential service points.

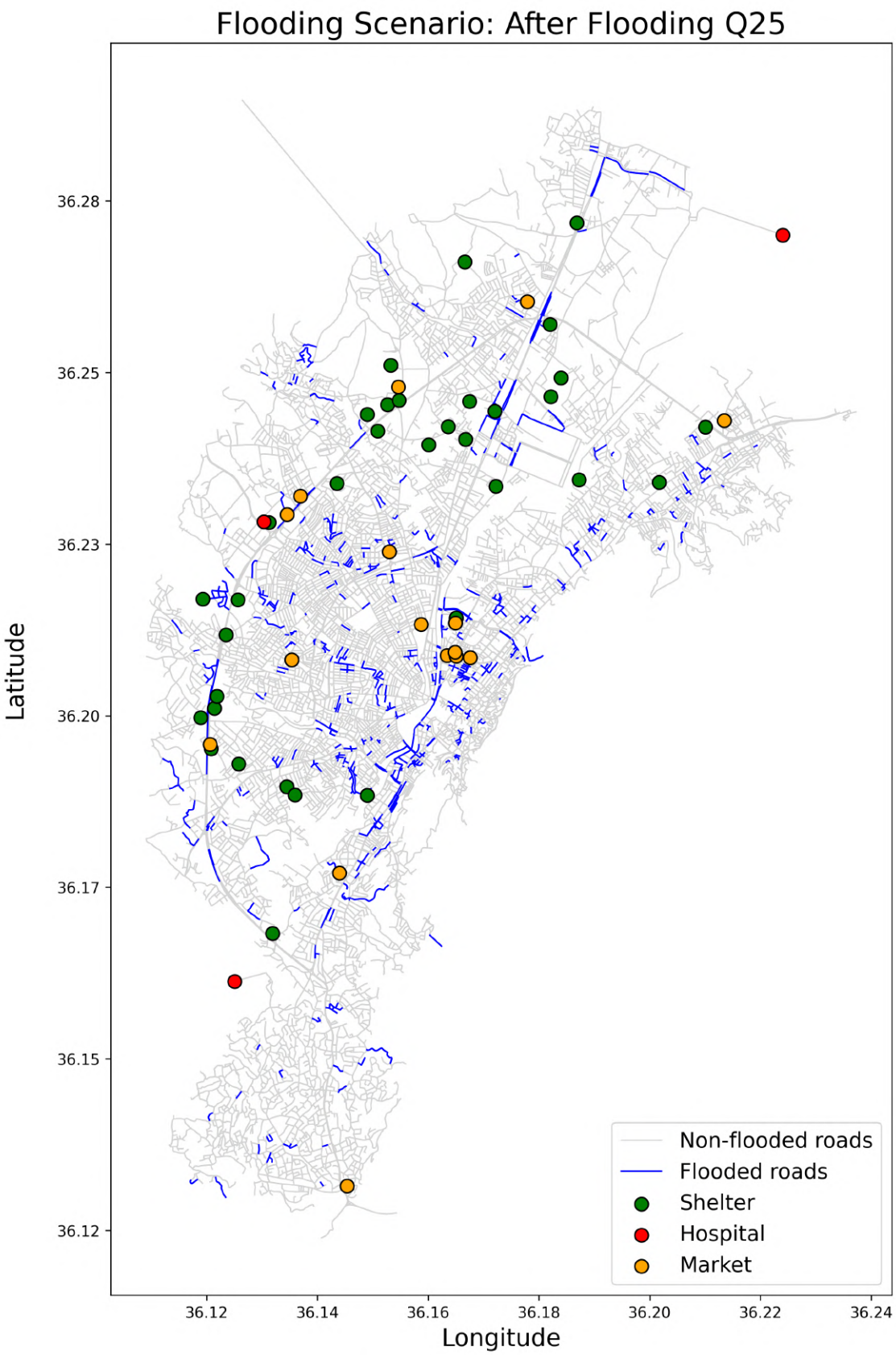

Figure B.1: Flooded road segments and key service locations under the Q25 flood scenario.

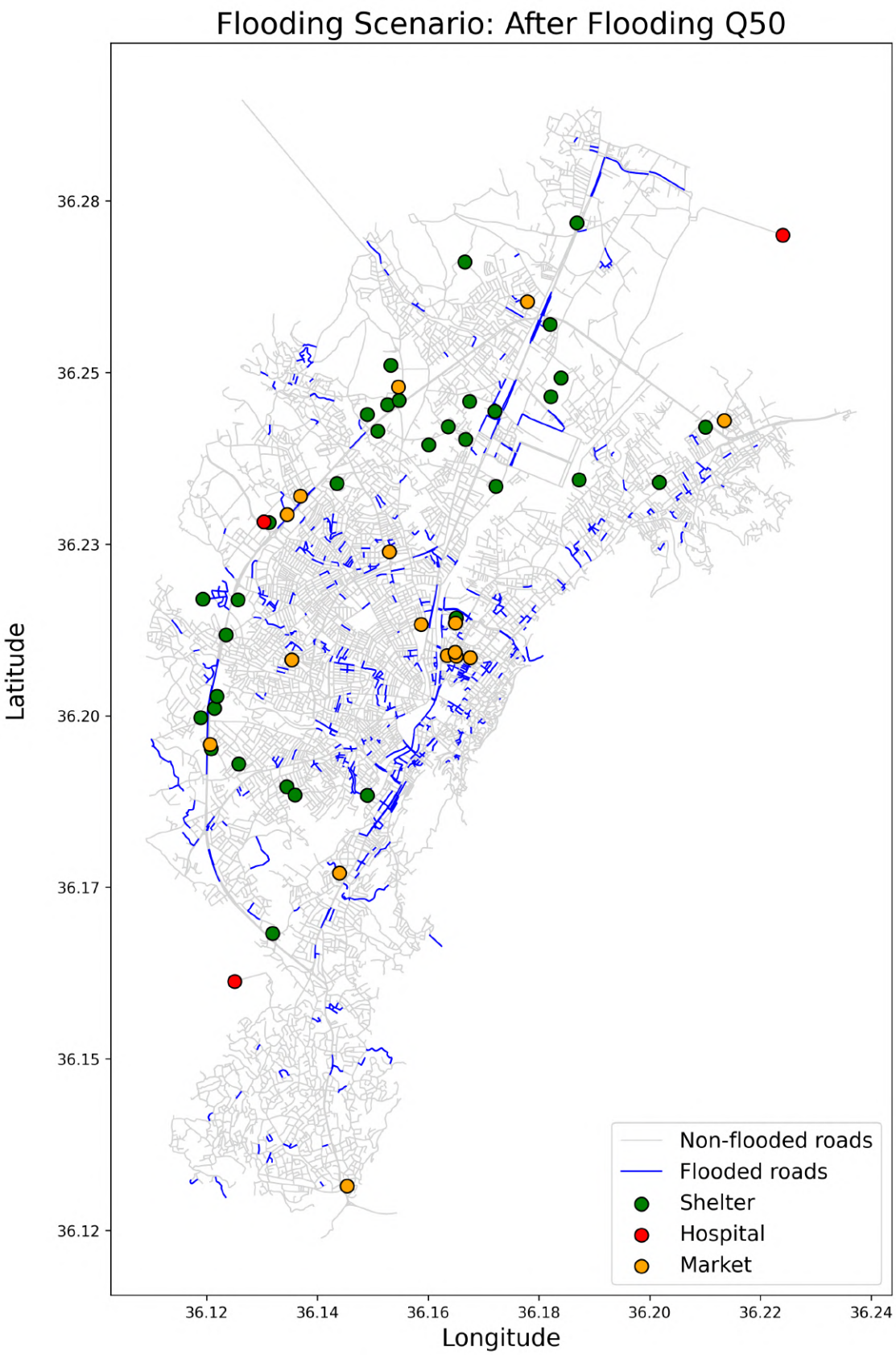

Figure B.2: Flooded road segments and key service locations under the Q50 flood scenario.

Edge Betweenness Centrality

Edge Betweenness Centrality Maps Flooding Q25 and Q50 - Network Wide

The visualizations B.3 and B.4 identify which road segments are most frequently used in shortest paths across the entire network. The Q25 and Q50 scenarios reveal how flood-induced disruptions affect structural importance

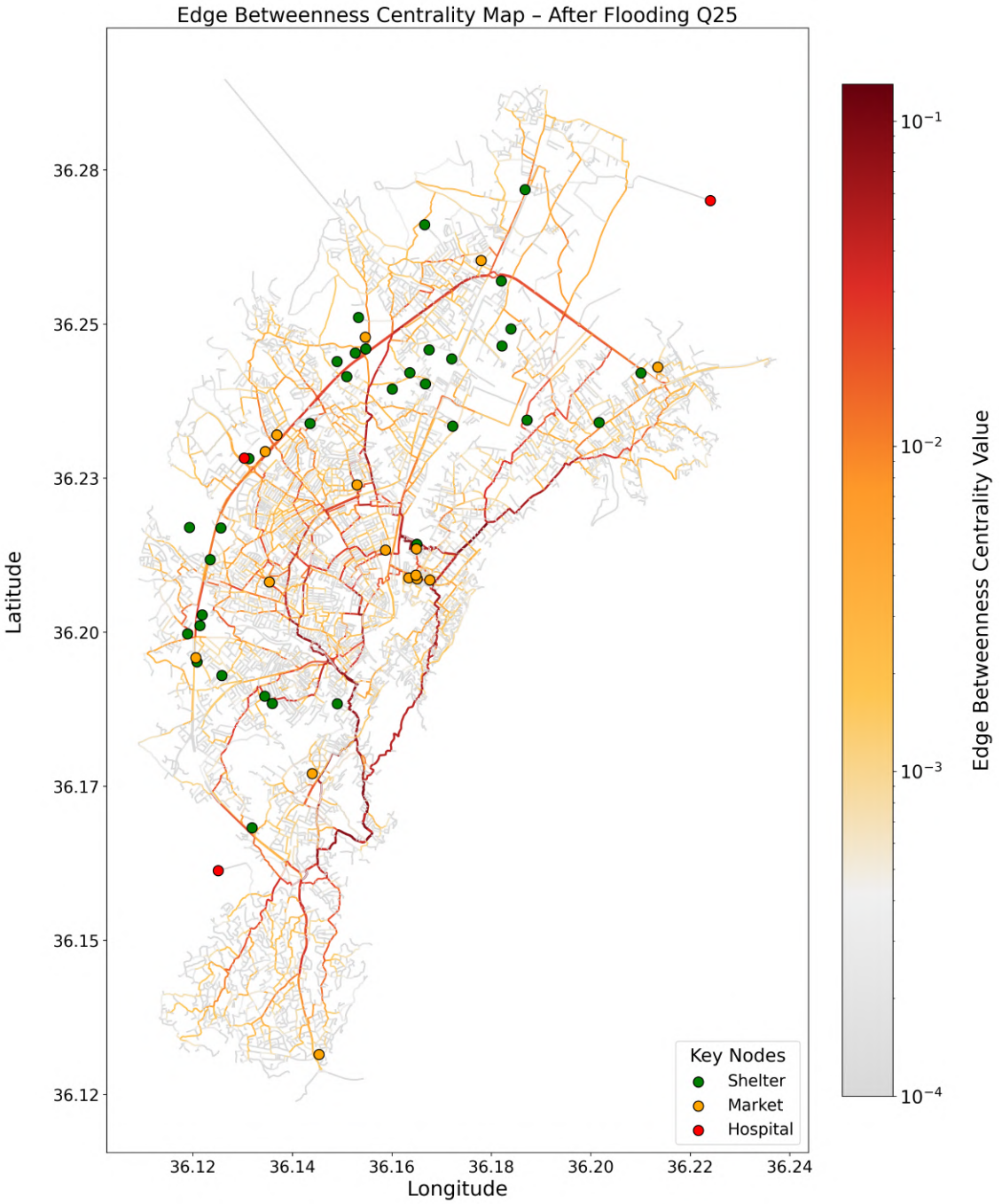

Figure B.3: Edge betweenness centrality map under the Flooded Q25 scenario.

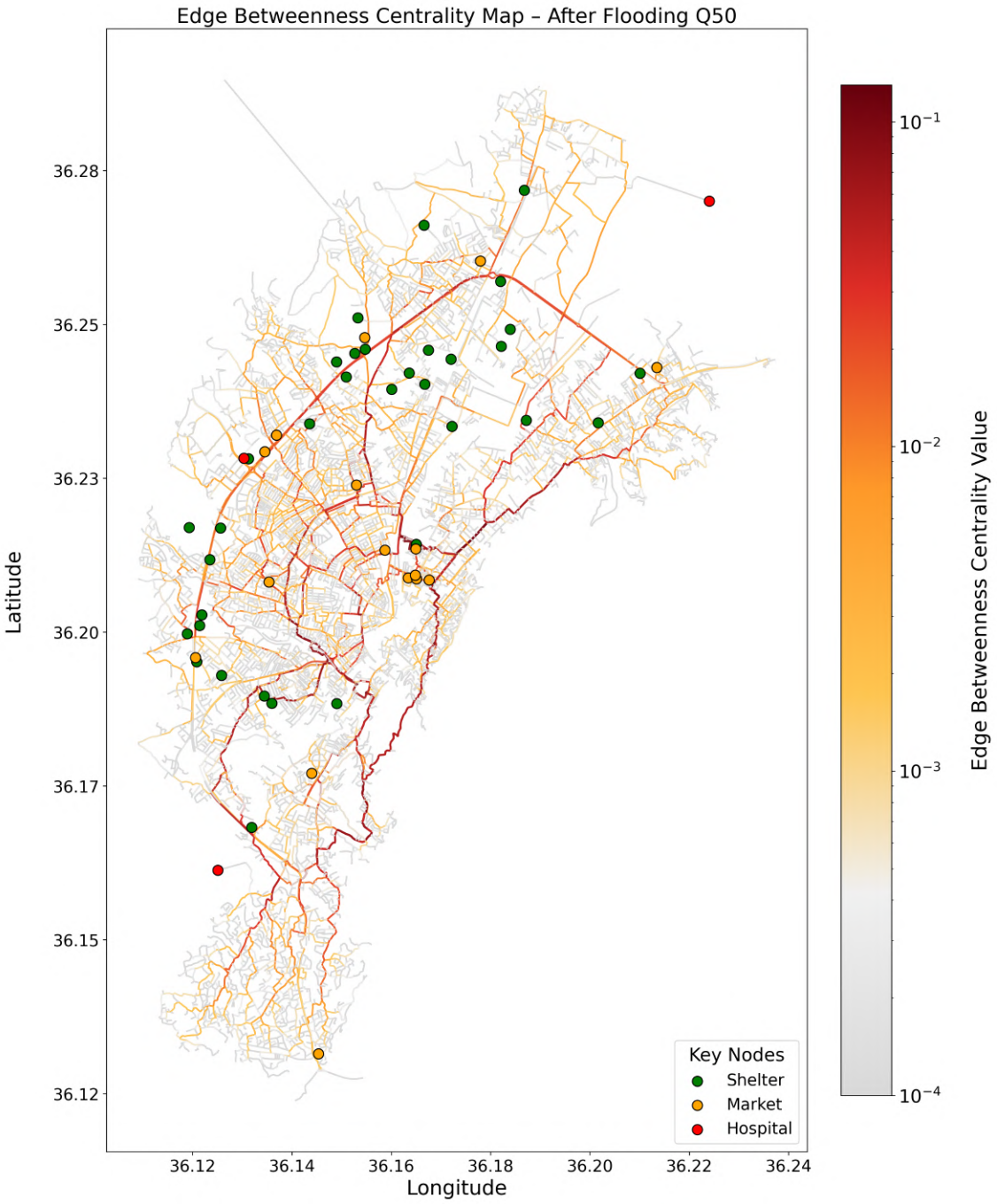

Figure B.4: Edge betweenness centrality map under the Flooded Q50 scenario.

Edge Betweenness Centrality Maps Flooding Q25 and Q50 - Shelter-Amenity Subset

The visualizations B.5 and B.6 identify which road segments are most frequently used in shortest paths across the subset of the network. The Q25 and Q50 scenarios reveal how flood-induced disruptions affect structural importance

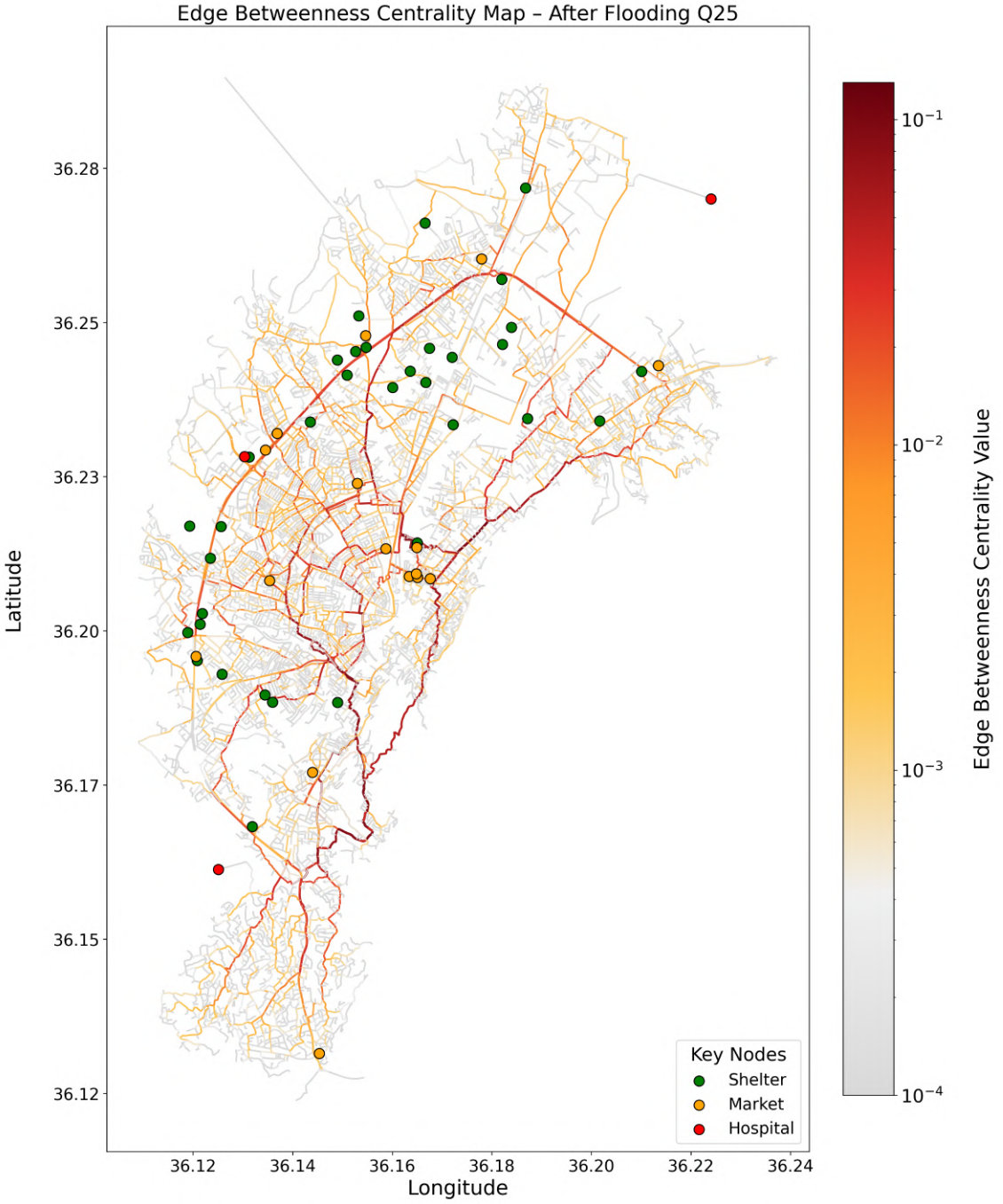

Figure B.5: OD-based edge betweenness centrality map under the Flooded Q25 scenario.

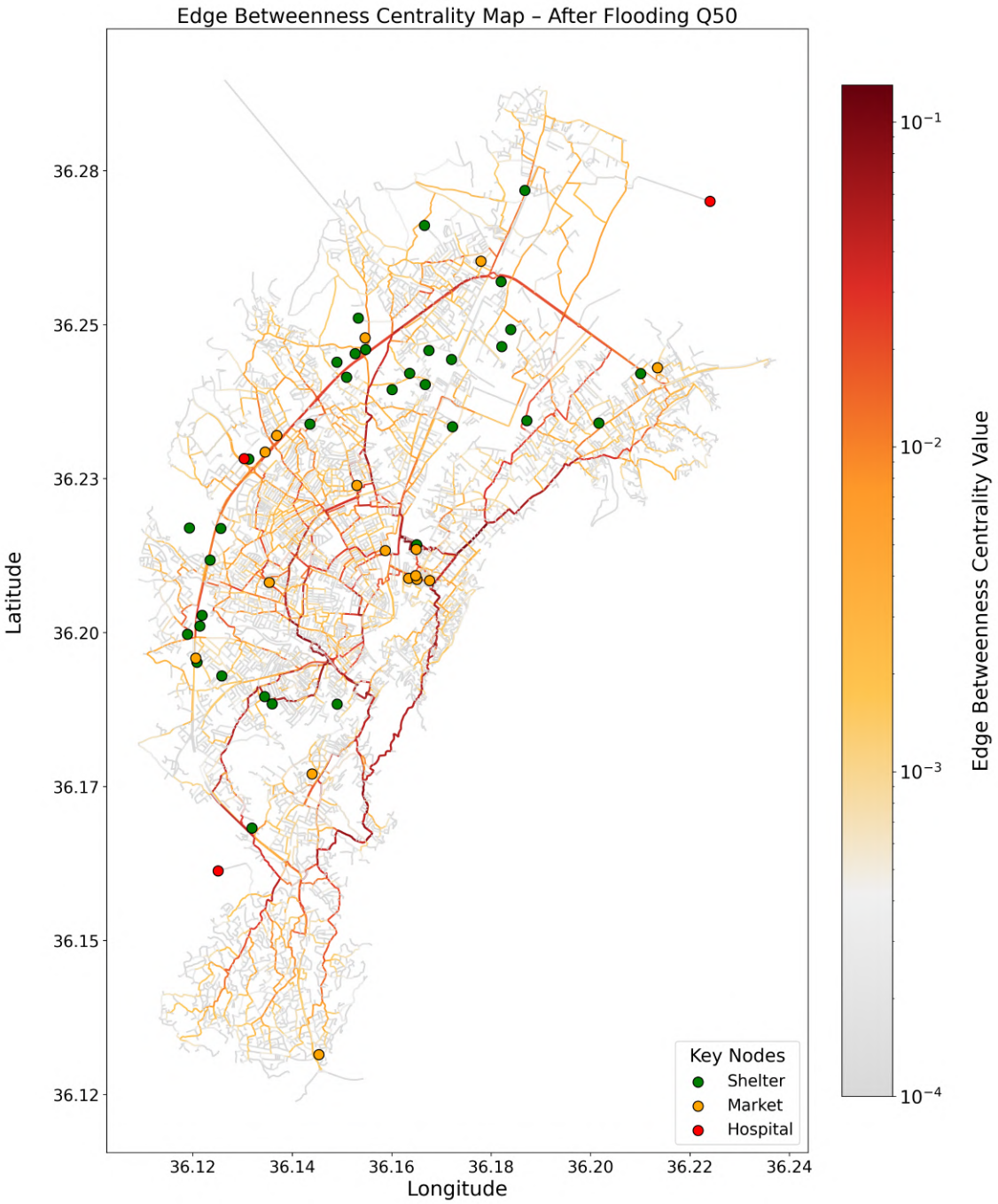

Figure B.6: OD-based edge betweenness centrality map under the Flooded Q50 scenario.

Access to Critical Services

The figures B.7 and B.8 show how access to hospitals and markets from shelter locations is affected under different flood scenarios. The color intensity indicates the increase in travel distance compared to the baseline earthquake scenario, while the black crosses represent disconnected origin-destination pairs.

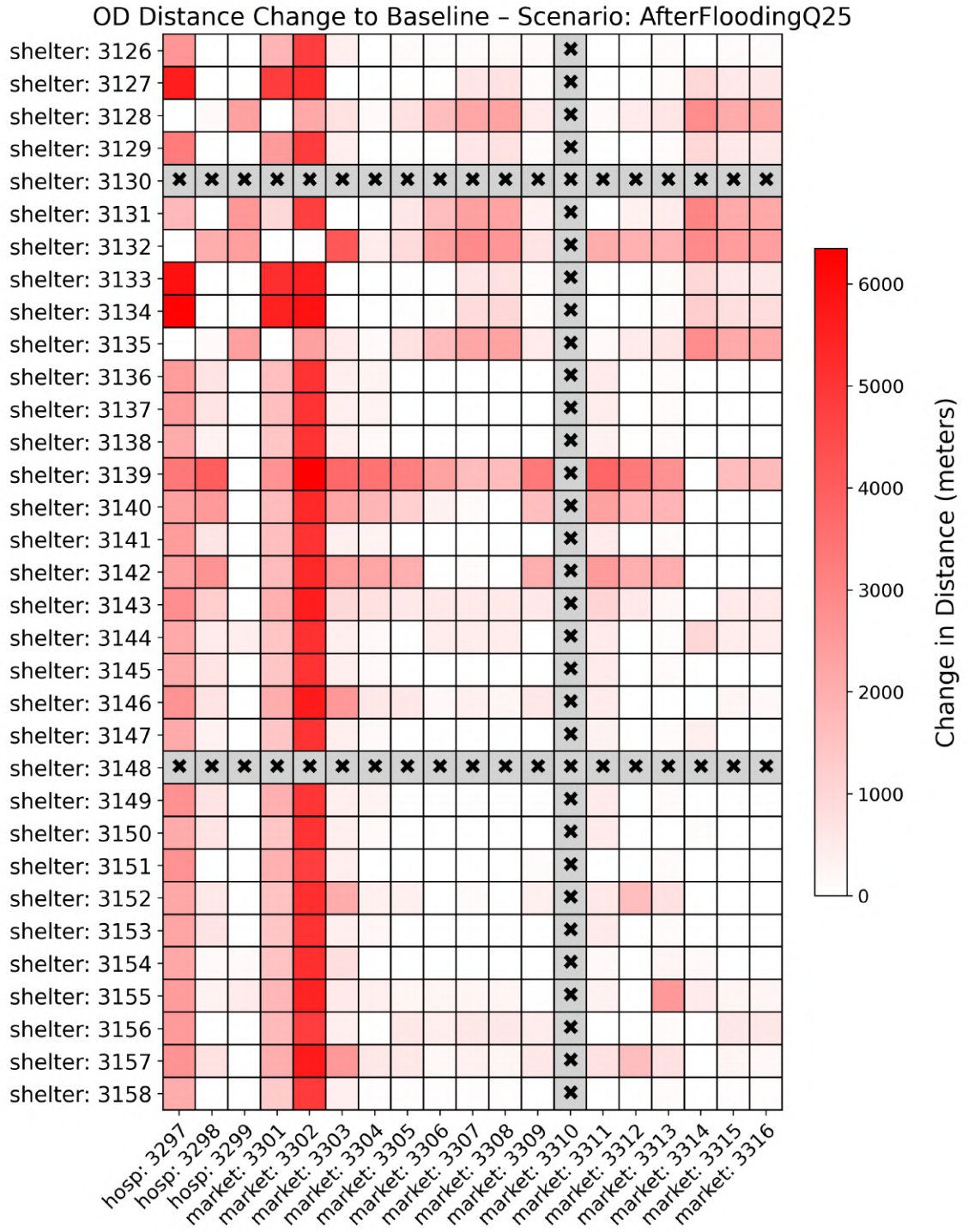

Figure B.7: Change in OD travel distance compared to baseline for the Q25 flood scenario.

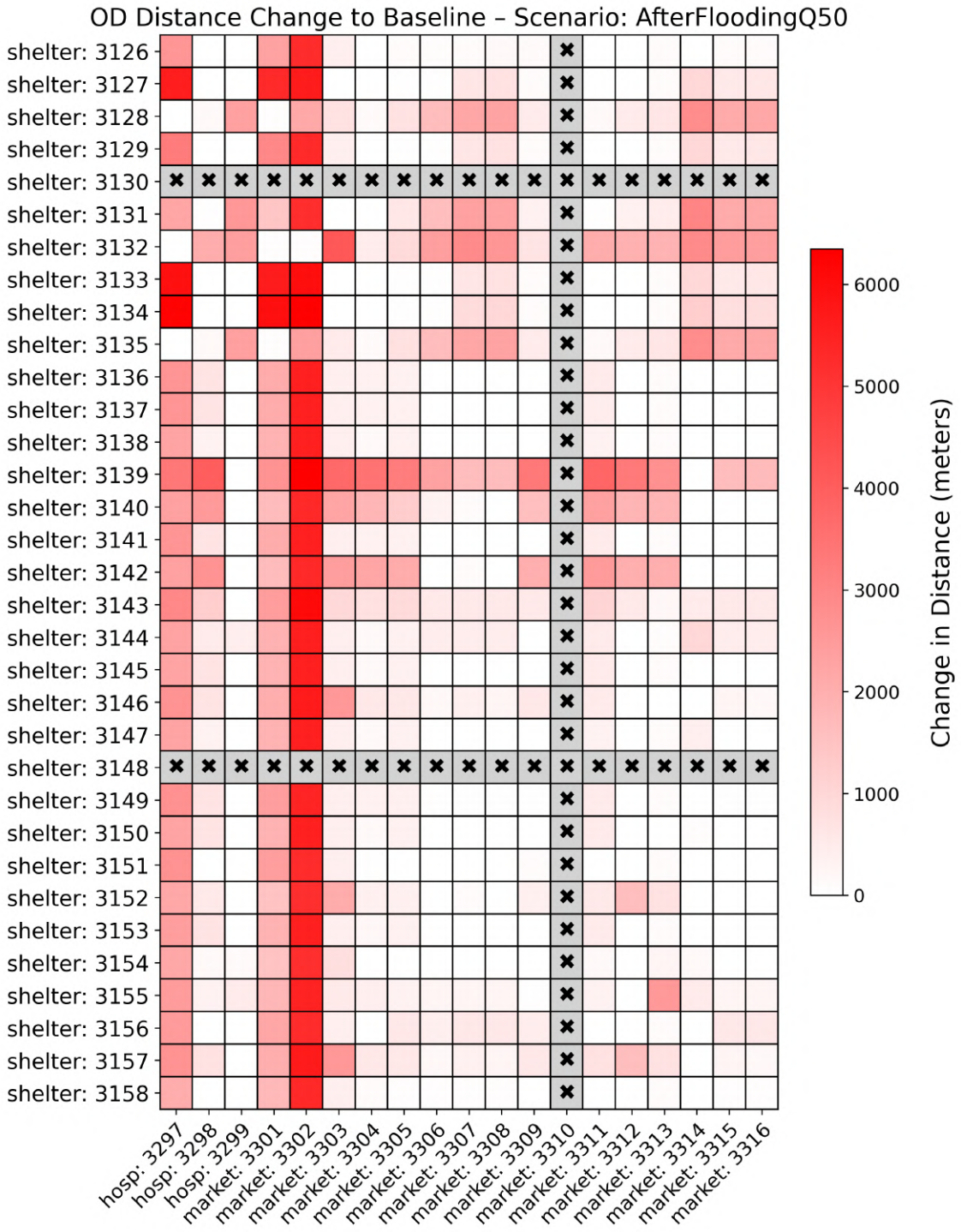

Figure B.8: Change in OD travel distance compared to baseline for the Q50 flood scenario.

Disruption of Shelter Flows

The maps B.9 and B.10 visualize estimated shelter-related travel demand across the road network, based on shelter capacity and shortest path routing to essential services. The flow values reflect the cumulative capacity of shelters that would utilize each road segment.

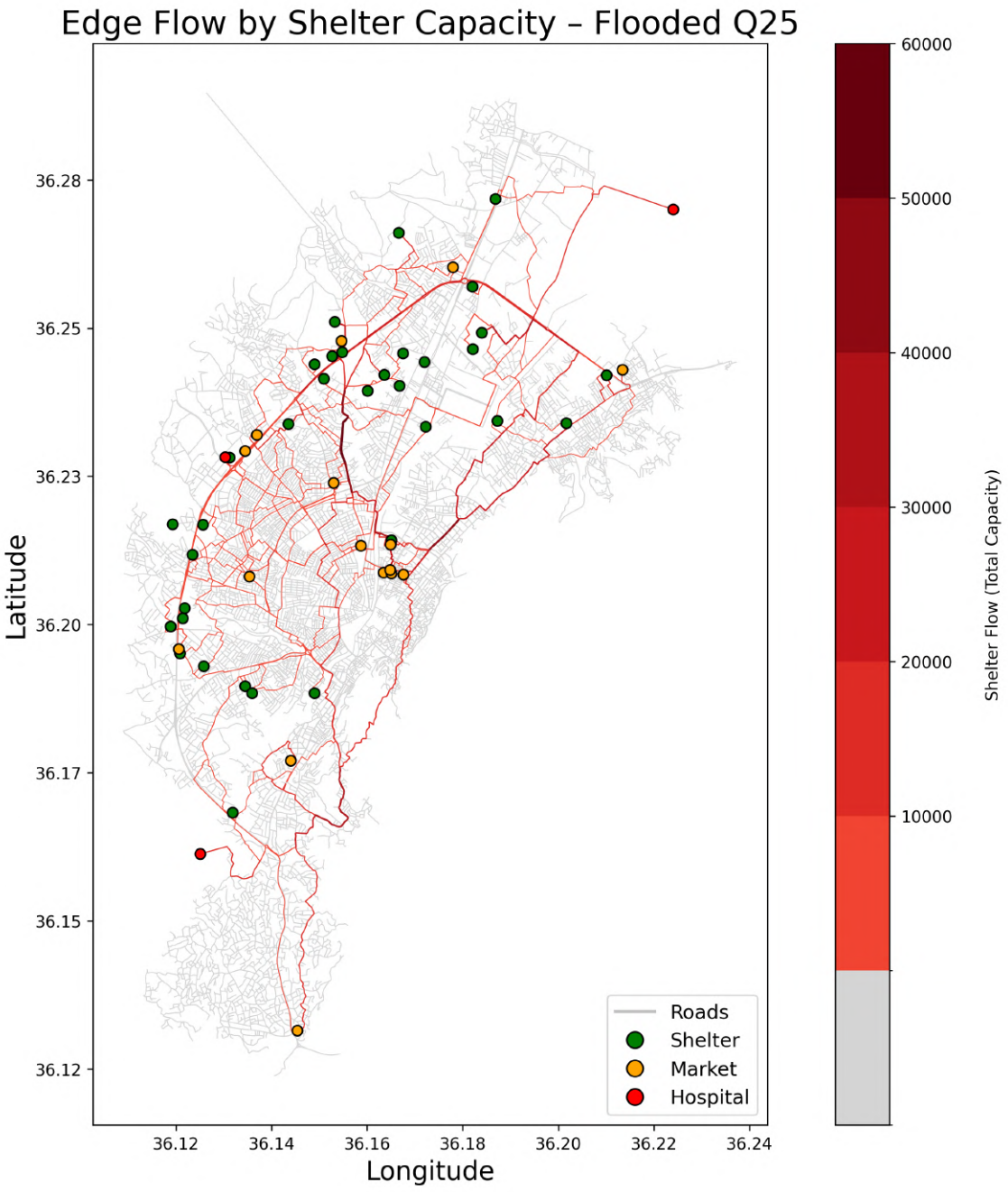

Figure B.9: Edge-level shelter flow under the Q25 flood scenario.

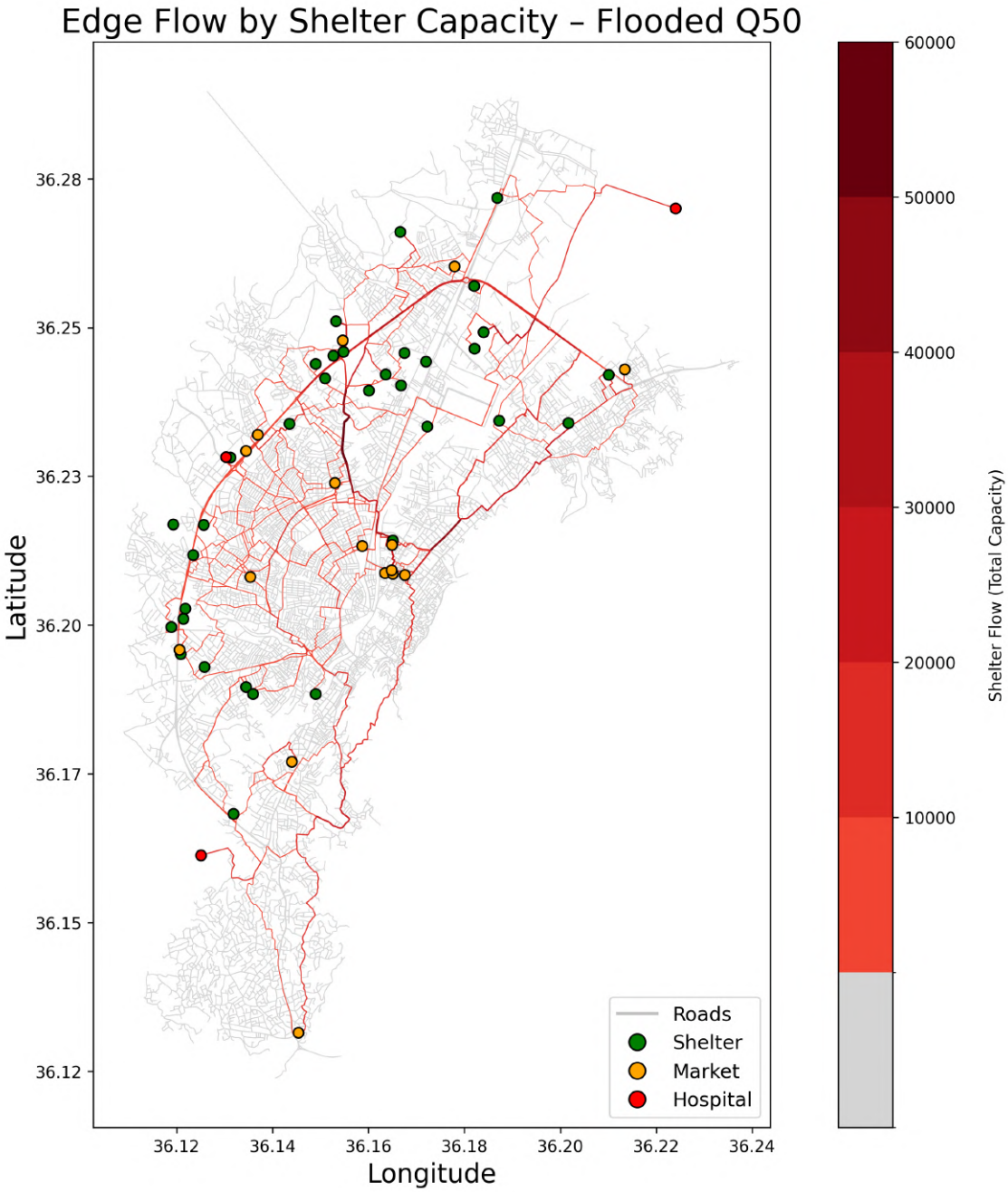

Figure B.10: Edge-level shelter flow under the Q50 flood scenario.